Giant Magnetoresistance Electric Guitar Pickup

A Major Qualifying Project Report
submitted to the Faculty of
WORCESTER POLYTECHNIC INSTITUTE
in partial fulfilment of the requirements for the
Degree of Bachelor of Science in
Electrical and Computer Engineering

By:
Caroline Atteya
Dan Campbell
Kaung Myat San Oo
João Mauricio Vasconcelos

Submitted to:

Professor Stephen Bitar
Worcester Polytechnic Institute

March 25, 2016

Table of Contents

List of Figures

List of Tables

Acknowledgements

The GMR Major Qualifying Project team would like to thank... Prof. Bitar for his expertise and guidance throughout the project, Mr. William Appleyard for his help with milling, soldering, and other construction regarding the housing case for the GMR pickup, Joseph St.Germain for his help with the 3D printing of the GMR pickup fixture, OSH Park for their help with troubleshooting the GMR pickup PCB, and NVE for providing tolerances for the shield resistor values within the GMR sensor package.

Abstract

Giant Magnetoresistance (GMR) is the phenomenon of thin film metallic materials changing their resistances up to 50% in magnetic fields resulting in improved sensitivity when compared to existing Hall Effect devices. This project explores using GMR in a guitar pickup application comparable to inductive and Hall Effect types. A GMR-based prototype was designed, constructed and tested on the basis of sensitivity, bandwidth, signal-to-noise ratio, and power consumption. Results show that GMR is a viable alternative to both inductive and Hall Effect pickups with improved performance in several areas.

Executive Summary

In the early 1900's the world started to become accustomed to the benefits of electronics with things such as radios, refrigerators and household appliances. As time marched forward, more and more common objects embraced the benefits of these electronic inventions. One such object, or specifically an instrument, was the guitar. Played for hundreds of years along with other similar stringed instruments, the guitar had always relied on the acoustic properties of its body to produce its rich sound. Then, in 1931 the first electric guitar pickup was invented that would allow guitars to compete with the brass instruments of the popular "big bands". Throughout the 1900's the electric guitar would gain popularity with musicians, eventually shaping the course of the music industry forever.

These electric guitars no longer needed to have the large hollow body that acoustic guitars required to amplify sound. Instead, these guitars were based around the inductive pickup. These pickups utilized the phenomenon known as Faraday's law of induction which attributes the voltage around a closed loop is equal to the magnetic flux enclosed by the circuit. Around a single loop, this voltage is very small and not suitable for a guitar pickup. However, Faraday saw that adding N loops together with the same magnetic flux through each simply adds the voltage from each loop to create a larger voltage across all coils. In the inductive pickup, there are typically six magnets, one for each string, placed under the strings with very fine wire wrapped hundreds of times around the magnets to create a sufficient voltage. The pickup is then able to sense the changing magnetic field caused by the string vibrations and converts that to an electric signal that is then amplified.

As technology advanced, new methods for sensing magnetic fields were developed with one of the more popular ones being the Hall Effect. The Hall Effect is simply the creation of a

voltage across a conductor caused by the deflection of charges due to a magnetic field. This voltage is perpendicular to the primary current that supplies the electrons for deflection.

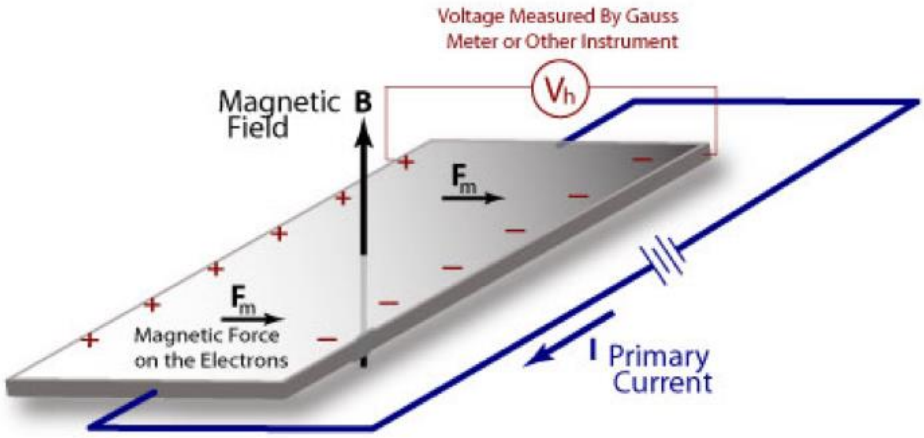

Figure 1: Hall Effect sensor theory of operation (Source: NDT Resource Center)

The Hall Effect sensor has become a popular choice for many sensing applications that require contactless sensing such as gear tooth detection and proximity sensing. There have also been a handful of attempts to create Hall Effect guitar pickups using these sensors. However, the inductive pickup remains the preferred choice for many musicians today.

In 1988, scientists discovered the phenomenon known as Giant Magnetoresistance, or GMR. Previously, magnetoresistance was limited to very small values; around ~5% changes in resistance. These scientists, however, discovered that in thin film magnetic materials, the GMR effect showed changes in resistance up to 50% when in the presence of a magnetic field. This discovery made way for sensors that show high sensitivity.

The goal of this project is to investigate these GMR sensors within the framework of a guitar pickup application. The process included research into the theoretical background of the GMR effect and how it operates, a comparison of existing pickup technology, the design of a GMR pickup and Hall Effect comparison pickup, and the testing and comparison of each.

The GMR pickup consisted of six major blocks including the sensor. They include the buffered AC bridge, instrumentation amplifier, summing amplifier and two low pass filters. The first block, the GMR sensor, was a Wheatstone bridge with two GMR elements. The GMR elements were on opposite sides so that as the resistance changed in each element, one would pull an output voltage higher while the other element pulled an output voltage lower and vice-versa. The main issue with the sensor is that, with the biasing magnet in place, there was a DC offset of around 200mV that needed to be removed before amplification. This was accomplished with the buffered AC bridge which successfully eliminate the DC bias without a direct bias path to the circuit ground.

With the DC bias removed, the remaining signal from the sensor was then amplified using a INA118PB instrumentation amplifier from Texas Instruments. The amplifier was set to a gain of 1001 by using a gain resistor of 50Ω, calculated using the gain equation $G = 1 + \frac{50k\Omega}{R_G}$. This In-Amp showed favorable noise characteristics along with a low power draw for this battery application.

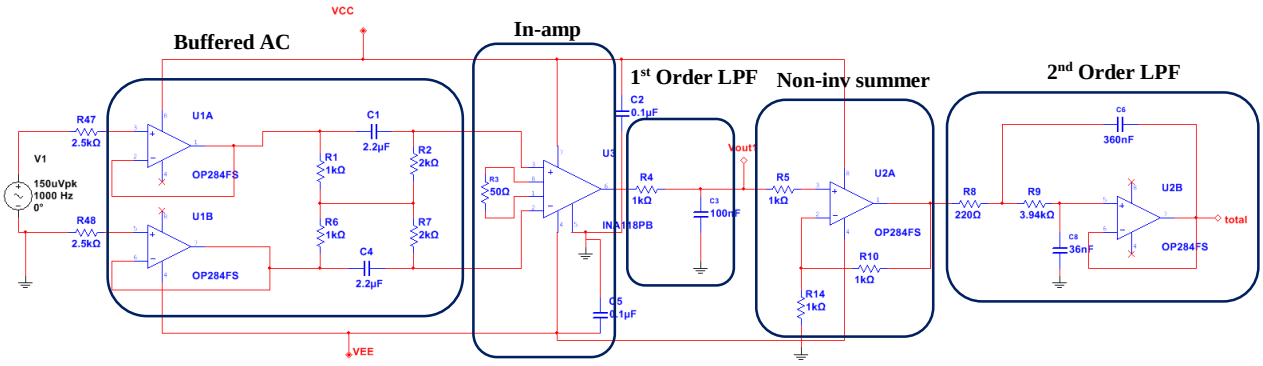

Figure 2: GMR pickup signal conditioning circuit for one string

The In-Amp was followed by a first order lowpass filter with a cutoff frequency of 1.6kHz to remove frequencies beyond the range of the guitar notes and their harmonics. The lowpass filter was the last stage on each individual string before it was fed into the summing amplifier which

used a non-inverting configuration to sum the signals from the six strings to form the full waveform. The summed waveform was then sent through a second order low pass Sallen-Key filter to further attenuate frequencies above the required range for the guitar.

With the GMR pickup constructed, a Hall Effect pickup was also created to compare the sensors. The Hall Effect pickup was constructed using simpler circuitry which consisted of an active bandpass filter and a summing amplifier. The original design also consisted of a notch filter but was removed from the final design due to PCB issues.

The final designs were then tested to evaluate their performance on the basis of sensitivity, bandwidth, signal-to-noise ratio, and power consumption. From the figures below, the signal size and shape can be seen alongside a spectral analysis for each signal from the pickups.

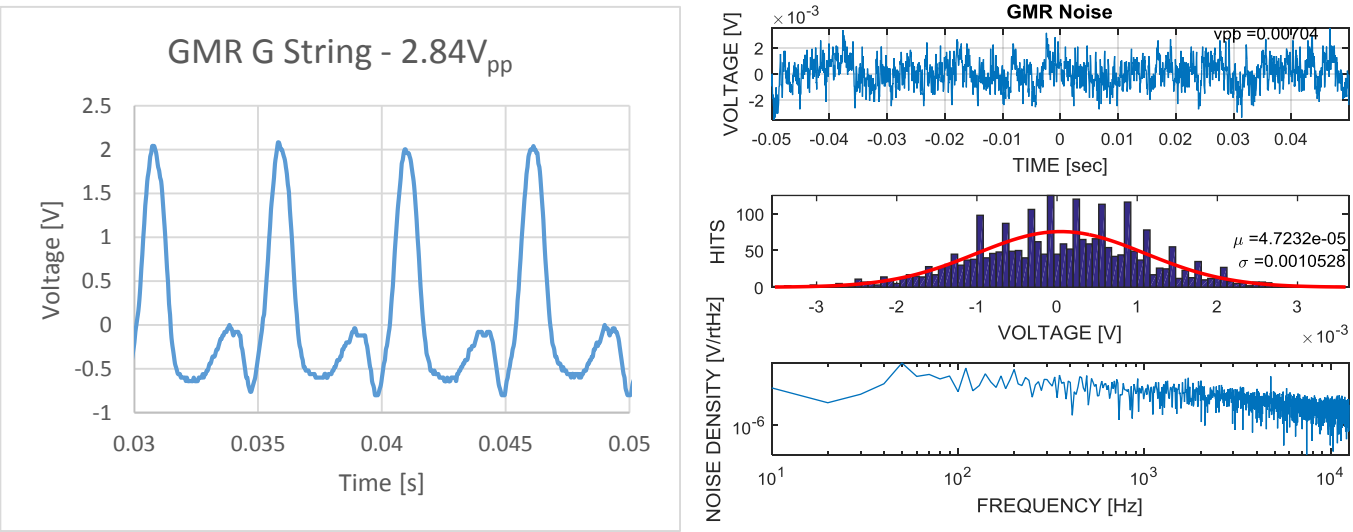

Figure 3: GMR pickup signal and noise

From the testing that was performed, the GMR pickup performed well compared to an existing inductive pickup while the Hall Effect pickup had much more noise in the frequency band of the guitar. The spectral analysis of the noise showed that the nose was roughly ten times greater in density (V/rtHz) when compared to the other pickups. This increased noise resulted in

a pickup that could not perform on the same level as the GMR and inductive pickups and showed that the Hall Effect sensor generates, or picks up more noise than a GMR sensor.

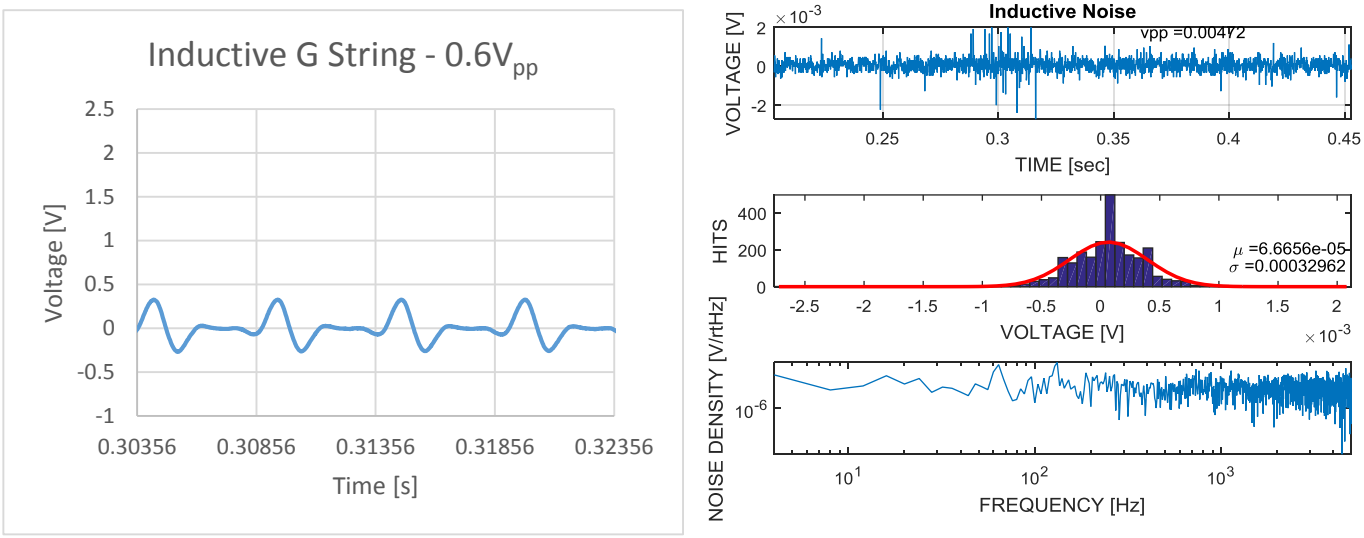

Figure 5: Inductive pickup signal and noise

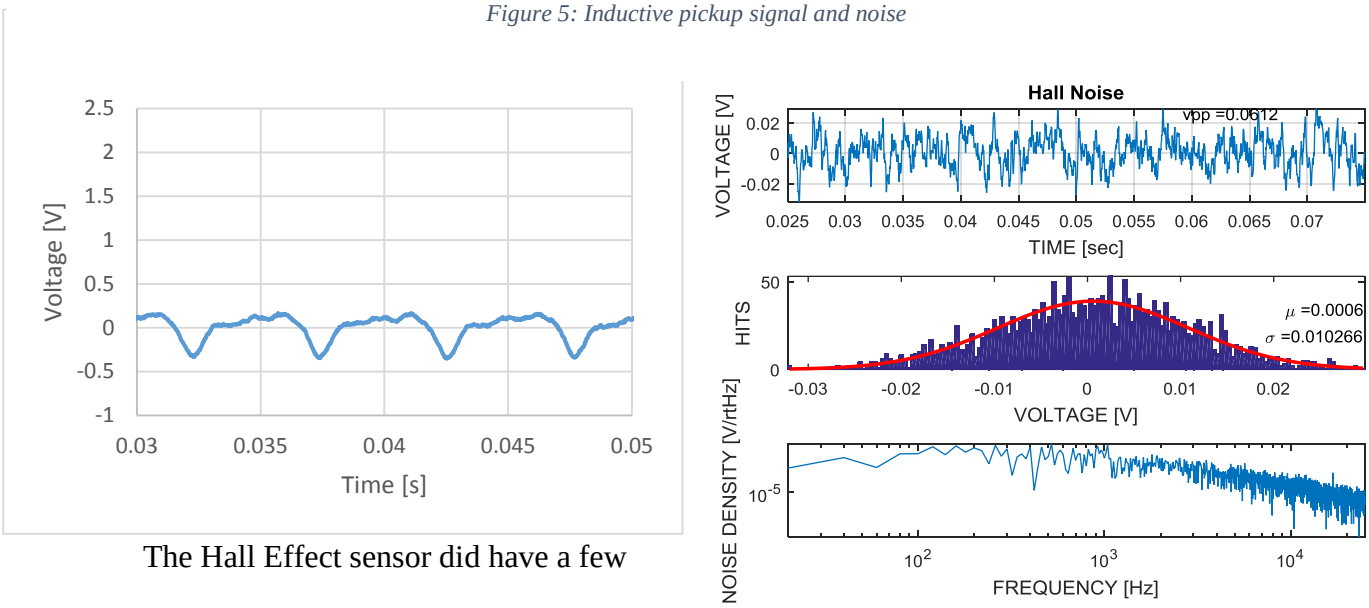

The Hall Effect sensor did have a few

Figure 4: Hall pickup signal and noise

minor advantages over the GMR sensor however. One was that the axis of sensitivity for the Hall Effect sensor was perpendicular to the face of the surface mount component, as opposed to the GMR where the axis of sensitivity was along the face of the surface mount component. This

made it much easier to design a PCB for the Hall Effect sensor because the board could lay flat on the guitar body without board area being a concern. Meanwhile, the GMR board needed to be short enough to be able to fit beneath the strings while standing vertically.

The other strength of the Hall Effect sensor, or perhaps a drawback of the GMR sensor, was that the GMR sensor had a sharp lowpass filtering behavior at very low frequencies, around 300Hz. This lowpass filter greatly attenuated the amplitude of the higher frequencies of the guitar and distorted the sound a small amount. This effect was not mentioned in a datasheet and a reason for the filtering was not discovered during testing.

Overall, the Hall Effect sensor may be popular for a wide range of applications, but for the guitar pickup application the sensor picked up too much noise to be a viable option with the given circuitry and selected sensor. The GMR pickup, however, performed very well in comparison to the inductive pickup and showed similar SNR values and noise spectrums.

Introduction

People have been playing stringed instruments, such as a guitar, for hundreds or perhaps thousands of years. For much of this time, these instruments relied on the acoustic properties of the instruments itself to produce the correct sound. Then, instruments and music went through a revolution with the invention of the electric guitar in the 1930's. The basic principle behind these electric guitars is electromagnetic induction in which a changing magnetic field through a loop of wire "induces" a current in said wire. This phenomenon gave rise to the inductive pickup which has remained the standard for electric guitars to this day. Since the creation of the inductive pickup, active pickups (requiring power), have been designed that allow for on guitar amplification, filtering and EQ. These active pickups have been made with different technologies including adapting inductive coils, and the Hall Effect. As new magnetic sensor technology is created and develops, they will likely be utilized in guitar technology. In recent years, Giant Magnetoresistance has been growing in popularity and has made brief appearances in the guitar pickup world.

The Giant Magnetoresistance (GMR) effect, discovered in 1988 is a phenomenon that occurs in thin film materials where the material's resistance changes when exposed to a magnetic field. Previously, magnetoresistive effects had shown changes up to approximately 5%; however, GMR materials exhibit changes in resistance up to 50%. This effect was shown in a variety of thin film materials and its large change in resistance gives rise to its name "Giant" Magnetoresistance.

This paper outlines the design and testing of a new guitar pickup designed around these GMR sensors as well as the design of a Hall Effect pickup to compare the GMR pickup with. The pickup design incorporated various buffering and filtering techniques to achieve a good pickup.

The ultimate goal of creating a GMR pickup is show the viability of the sensor technology while creating a pickup that is capable of replicating the sound qualities of a passive pickup.

Background

This section of the paper introduces the theory behind magnetic sensing. Different magnetic sensing technologies including electromagnetic induction, the Hall Effect and Giant Magnetoresistance are discussed and compared to each other.

Introduction to Magnetic Sensing

In order to understand how guitar pickups are designed, it is important to understand the underlying theories of magnetic sensing. Magnetic sensing is a sensing method that utilizes the deep interconnection between magnetic and electric phenomena to allow for non-invasive measurement for a wide range of circuit applications. These magnetic sensors make use of various phenomena from physics and material science to offer a variety of measurement ranges, sensitivities, and physical sizes. This section will cover a few of the current technologies and their various applications.

Current Technologies

Modern magnetic sensors make use of one of two methodologies, vector magnetometers and scalar magnetometers. A majority of commercially available sensors are vector magnetometers. As the names imply, vector magnetometers measure the magnetic field in both direction and magnitude by reacting to changes in the vector components of the field. On the other hand, scalar magnetometers are only capable of measuring the magnitude of a magnetic field vector. Both forms of magnetometers have benefits and drawbacks that make each fit into their own niche for certain applications. Some of the magnetic sensing technologies that utilize these

two methodologies are shown below along with their respective sensitivities. In this particular figure, GMN and E are the values of geomagnetic noise (0.1nT), interference produced by the Earth, and the Earth's magnetic field (25-60μT) respectively.

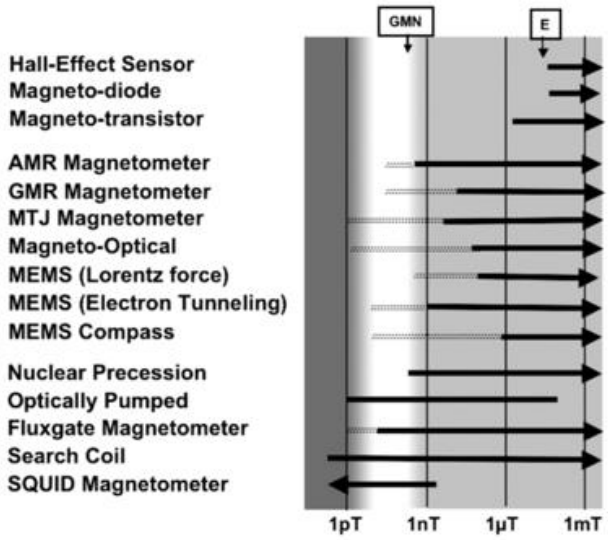

Figure 6: Magnetic Sensing Sensitivities, (Source: Magnetic Fields and their Applications, Lenz and Edelstein)

Electromagnetic Induction

One of the first and simplest methods of detecting disturbances in a magnetic field is through electromagnetic induction. Discovered in 1831 by Michael Faraday, electromagnetic induction is the generation of a voltage across a conductor by exposing it to a time varying magnetic field (Ulaby, 2006). The dependence on a time varying magnetic field is a major reason why alternating current became the standard for large scale power applications. Induction allowed for the creation of electrical generators, induction motors, transformers and many other important creations.

The basic theory of electromagnetic induction is that the induced electromotive force in any closed circuit is equal to the rate of change of the magnetic flux enclosed by the circuit (Jordan & Balmain, 1968). Mathematically, it is described as:

$$\varepsilon = -\frac{d\phi_B}{dt} \quad (1)$$

where E is the electromotive force and Φ_B is the magnetic flux. This theory is key to detecting the vibration of ferromagnetic objects, such as guitar strings. For many applications, the voltage produced by a single closed loop of conductor is not large enough. However, one of the fascinating characteristics of electromagnetic induction is that the electromotive force is proportional to both the magnetic flux as well as the number of turns in a coil of wire. This occurs because each turn of a coil can be treated as discrete loops. For N turns the total electromotive force is equal to $d\Phi_{B1}/dt + d\Phi_{B2}/dt + ... + d\Phi_{BN}/dt$ which is equivalent to:

$$\varepsilon = -N\frac{d\phi_B}{dt} \quad (2)$$

Hall Effect

Another common way for magnetic sensing is using Hall Effect sensors. In order to know how this sensor works, it is important to understand how the magnetic field interacts with electric charges. One of the crucial characteristics of the magnetic field is its perpendicular nature around a moving charge. When an electric charge moves in the presence of a magnetic field, it is acted upon by a magnetic force known as the Lorentz Force. The perpendicular relationship of the magnetic field, moving charge (or current), and the force follows the so called "Right Hand Rule". In order to quantify the Lorentz force, it can be calculated via the equation

$$F = q\,[E + v\,x\,B] \quad (3)$$

where q is the charge of an electron, E is the electric field vector along the wire, v is the velocity vector of the moving charge, and B is the magnetic field vector.

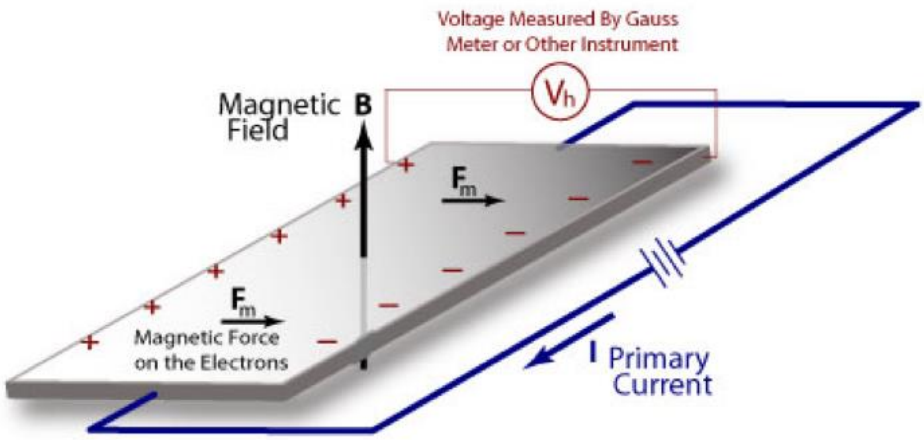

Figure 7: Hall Effect Demonstration, (Source: NDT Resource Center)

The Lorentz force causes the negatively charged electrons to deflect to one side of the conductor and positive charges deflect to the other side. The deflection of charges generates a separation of charge with a greater concentration of negative charges on one side of the conductor and positive charges on the other. This created separation of charge gives rise to an electric field across the conductor, which correlates to a proportional voltage, known as the Hall voltage, perpendicular to the current. This creation of the Hall voltage, which is expressed below mathematically, across a piece of conductor is known as the Hall Effect, where t corresponds to thickness of the conductor, I is the current perpendicular to the Hall voltage, B is the magnetic flux density and R_H is the Hall Effect coefficient.

$$V_H = R_H \left(\frac{I}{t} \times B\right) \tag{4}$$

Giant Magnetoresistance (GMR)

Giant magnetoresistive sensors are the most novel tool for magnetic sensing. The fundamental idea behind the GMR effect is that electrons alter their trajectory when moving through a magnetic field. Thus, metals (especially magnetic metals) experience a change in their

resistance when they are placed in a magnetic field. The resistance of a metal with current flowing parallel to the applied magnetic field is different from the resistance of one with current perpendicular to the magnetic field. This difference is referred to as the magnetoresistive effect. For many metals, this difference in resistance is on the order of 5% but in 1988, Baibich and other researchers observed changes in resistance as much as 50% at low temperatures when a magnetic field (approximately 20kG) was applied to Fe/Cr multilayer ultrathin films. This enormous magnetoresistive effect was then found to occur in a number of multilayer ultrathin magnetic film systems and was labelled "giant magnetoresistance" effect. (White, 1992)

There are two conditions that must be met for the Giant Magnetoresistance effect to appear:

1. There must be some way to change the relative orientations of the magnetizations in adjacent magnetic metal layers.
2. The thickness of the films involved must be less, preferably a fraction, of the mean free path of an electron in the multilayer array. (White, 1992)

Heuristic Model of the Giant Magnetoresistive Effect

The magnetic layers of a GMR sensor are made of ferromagnetic materials. There are only three elements that are ferromagnetic: Iron (Fe), Cobalt (Co) and Nickel (Ni). Ferromagnetic materials exhibit a special phenomenon called hysteresis where all electrons readily align their spins with each other in response to an external magnetic field. This alignment tends to persist after the magnetic field is removed. In reality, not all electrons align in the same orientation but a difference in density between the "spin up" electrons and the "spin down" electrons is created and so the material becomes magnetized. This difference in density also creates a difference in conductivities for the different spin states. The observed difference in electrical conductivities is

often called “spin dependent transport” or “spin polarized current” which represents the foundation for Giant Magnetoresistive Sensors. (Reig, Cardoso de Freitas, & Mukhopadhyay, 2013)

The idea of spin-polarized current is based on the following: the resistance to the flow of electrons in a metal is determined by the scattering processes to which the electrons are subject. If the scattering processes is strong and effective, the mean free path for an electron is small and the resistance of current path is large. On the other hand, if the scattering process is weak, this leads to a long mean free path and a low resistance for the current path. (White, 1992)

The scattering processes are demonstrated in the figure below:

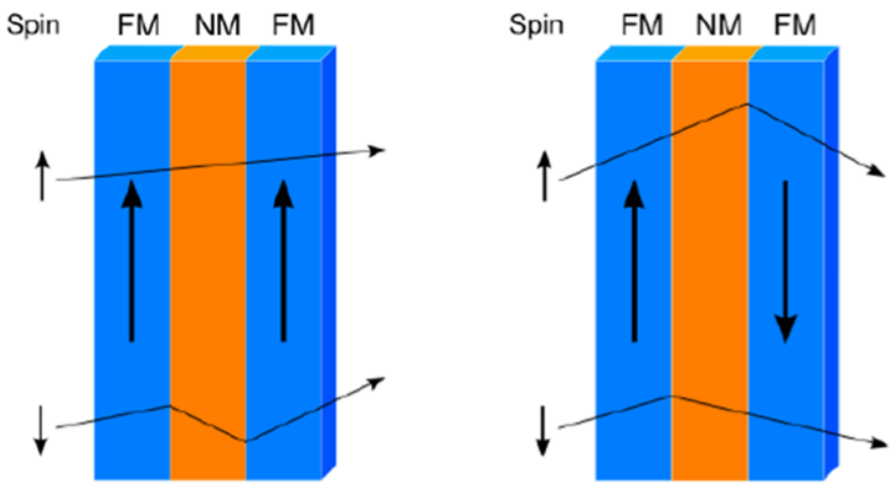

Figure 8: Heuristic Model for the GMR Effect (Source: Giant Magnetoresistance (GMR) Sensors (Vol. 6))

In Figure 3, the image on the left represents a multilayer magnetic film array with parallel magnetizations. When an electron with an “up-spin” is moving through the first ferromagnetic layer, the electron won’t be scattered much since the layer has the same magnetic orientation as the electron. Passing through the non-magnetic layer, the electron will not be affected since the layer does not have an overall magnetic orientation. Finally, the electron will pass through the second ferromagnetic layer where scattering is also very weak. This results in an overall long free

mean path for the “up-spin” electron as demonstrated in the figure which causes a lower resistance for the current path.

On the other hand, when a “down-spin” electron is passing through the ferromagnetic layer with an upward magnetic orientation, the projectile of the electron changes (electron is strongly scattered). Thus, when the electron exits the ferromagnetic layer and enters the non-magnetic layer, the electron returns back to its “natural” projectile path and so it’s free mean path is interrupted. The electron’s projectile path changes once more when the electron enters the second ferromagnetic layer. Consequently, the free mean path for the “spin-down” electrons end up being short and so the resistance of the current path is larger.

Alternatively, the image on the right represents a multilayer magnetic film array with antiparallel magnetizations. In this structure, electrons with both orientations are scattered equally. The “up-spin” electron is scattered strongly at the ferromagnetic layer with a downwards magnetic orientation and is barely scattered at the layer with similar magnetization. An opposite scattering process happens with the “down-spin” electrons. This results in the same mean free path for both electron spins and so the same resistance for the current paths.

Parallel Configuration

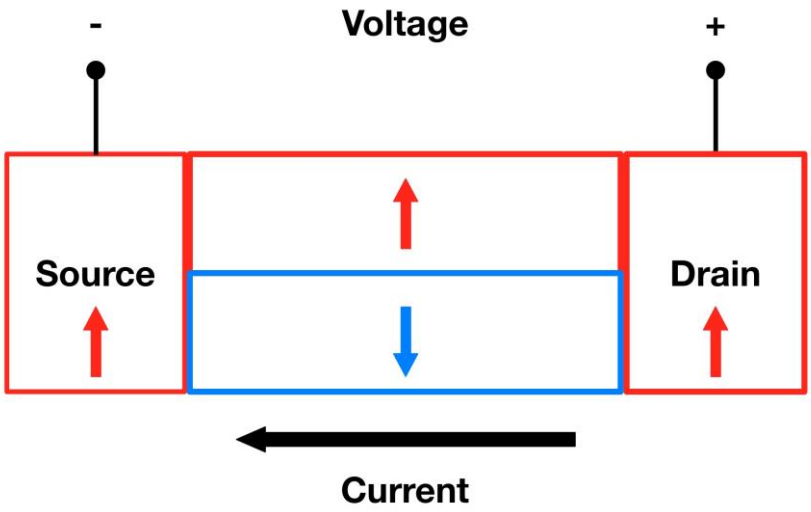

Figure 9: Parallel Configuration for GMR Multilayer

Figure 9 demonstrates the structure of a GMR element with magnetic layers of parallel configurations. The source and the drain are made of ferromagnetic materials. In this case, the source and the drain have parallel magnetic orientations. The non-magnetic layer in between is modelled as two channels of electrons: a channel of "up-spin" electrons and a channel of "down-spin" electrons. The two channels have no overall magnetic orientation. Considering the mean free path for each electron spin discussed earlier, the resistances at layer interfaces and of the non-magnetic layer are modelled in the schematic below:

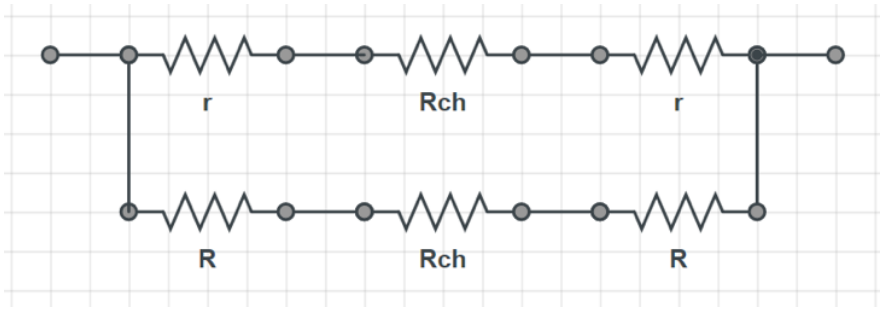

Figure 10: Schematic for Parallel Inter-layer Resistances

From Figure 10, we can represent the resistance for the parallel configuration in the following equation:

$$R_P = \frac{2rR}{r+R} \tag{5}$$

Anti-parallel Configuration

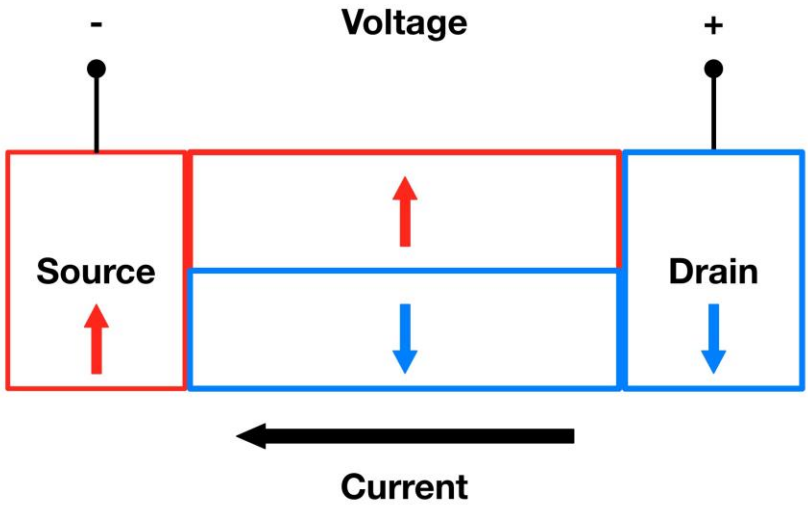

Figure 11: Anti-Parallel Configuration for GMR Multilayer

Figure 11 demonstrates the structure of a GMR element with magnetic layers of antiparallel configurations. In this case, the source and the drain have antiparallel magnetic orientations. The non-magnetic layer in between is modelled as two channels of electrons: a channel of "up-spin" electrons and a channel of "down-spin" electrons. The two channels have no overall magnetic orientation. Considering the mean free path for each electron spin discussed earlier, the resistances at layer interfaces and of the non-magnetic layer are modelled in the schematic below:

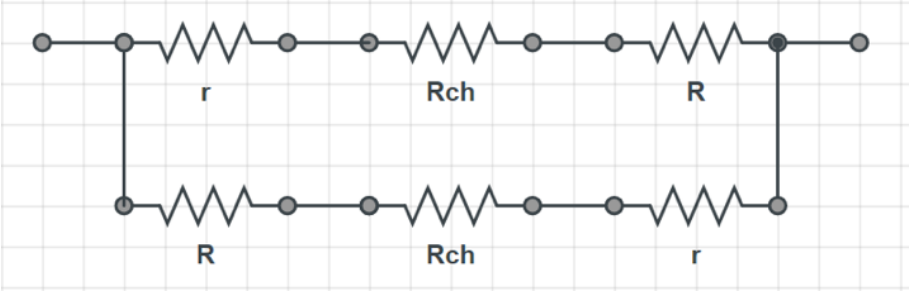

Figure 12: Schematic for Anti-parallel Inter-layer Resistances

From Figure 12, we can represent the resistance for the parallel configuration in the following equation:

$$R_{AP} = \frac{R + r}{2} \tag{6}$$

The cause of this giant variation of the resistance between the parallel and antiparallel configurations is attributed to the scattering of the electrons at the layer interfaces. (Reig, Cubells-Beltran, & Muñoz, 2009)

Basic GMR Structures

The images below represent the most common configurations for a GMR device and the characteristics of each structure. The structures are compared in terms of how the much resistance of each structure could change with the change in magnetic field.

1. **Multilayer**

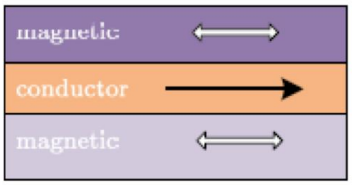

Magnetic Films: 4-6nm

Conductor Layer: 3-5nm

MR Levels: 4%-9%

Applications: Bioelectronics, Angle Detectors

2. **Spin Valve**

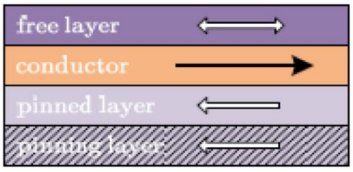

Same as Multilayer Structure + Pinning Layer

MR Levels: 4%-20%

Applications: Hard Disk Drives

3. **Magnetic Tunnel Junction**

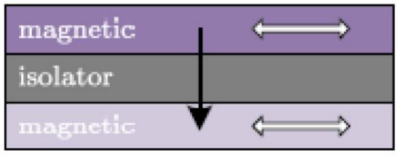

Same as Spin Valve but has an isolator layer instead of a conductor layer

MR Levels > 40% (have reached 200%)

Applications: MRAM, Angle Measurement

4. **Granular Alloy**

Figure 13: GMR Structures, (Source: Magnetic Field Sensors Based on Giant Magnetoresistance)

Guitar Pickup Technologies

This section discusses different technologies used for electric guitar pickup application starting with the popular traditional inductive pickups.

Inductive Guitar Pickups

In the early 20th century, electronics and other electrical equipment became increasingly more useful to the average family. Electronic transducers, such as the radio, were coming about in an era of technological innovations in the United States. This wave of innovative thoughts and ideas spurred the creation of many inventions. From penicillin to the jukebox to the liquid-fueled rocket, there was a technological revolution in many industries.

The music industry underwent a similar technological development. Starting in the 1920's transducers were used to pick up the vibrations from stringed instruments. It started with the viola and string bass in 1924 and, then, Hawaiian guitars and Spanish guitars in the mid 1930's. After World War II, two companies dominated the designs of transducer pickups: Gibson and Fender. Consequently, new and improved pickups came about and consolidated the electric guitar, the electric bass and other electric instruments, while making many music genres a reality.

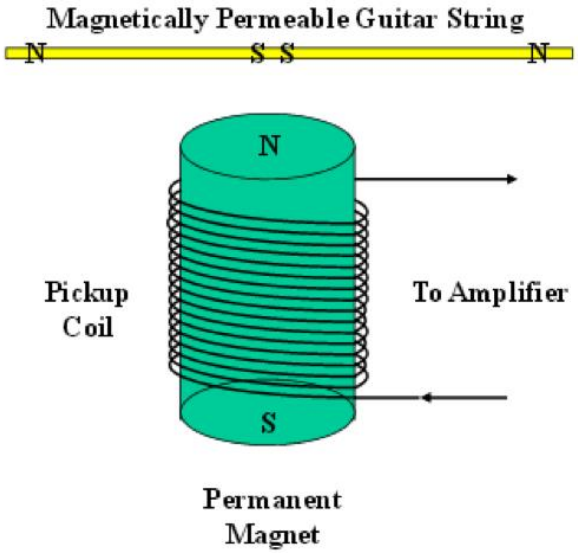

Figure 14: Inductive Pickup Coil, (Source: www.cykelkurt.com)

Operation of Inductive Pickups

Pickups consist of permanent magnets surrounded by a pickup coil, typically #42 or #43 AWG, resting under the instruments string. The strings are made of magnetically permeable material, which, when in proximity to the pickups, becomes magnetized and induces two magnetic poles in the string over the pickup. Thus, the string "is a pair of bucking linear magnetic dipoles, i.e. a collinear pair of bucking magnetic flux tubes". (Errede, 2005) When the string is plucked, it causes a change in the magnetic flux that links it to the pickup coil and, from Faraday's Law, it induces an electromotive force, EMF:

$$\varepsilon(t) = -\frac{d}{dt}[\Phi_m(t)] = -\frac{d}{dt}[B(t) * A_{coil}] \tag{7}$$

Here, ε is the EMF, Φ_m is the magnetic flux, which equals B(t)*A_{coil}-, the magnetic field times the area of the coil. Fortunately, you can also relate the magnetic flux to the inductance in the system by:

$$\Phi_m(t) = L * i(t) \tag{8}$$

Thus,

$$\varepsilon(t) = -L\frac{d}{dt}[i(t)] \tag{9}$$

The following image depicts the simplest model of a guitar pickup. Notice that the potential difference is created by the varying magnetic flux (from the guitar string). Also notice that the same potential difference is proportional to the inductance and the variation of the current.

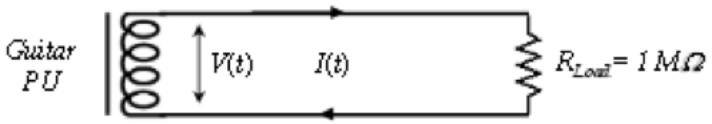

Figure 15: Simplest Model of an Electric Guitar Pickup

Hall Effect Guitar Pickups

Similar to inductive transducers for guitar pickups, linear Hall Effect sensors can be used as a guitar pickup by using a permanent magnet in close proximity to the magnetically permeable strings of a guitar or other stringed instruments. The Hall sensor is usually located in the gap between the magnet and strings as shown in Figure 16. When near the permanent magnet, the guitar strings become magnetized and the vibration of these strings results in proportional changes in the magnetic field, which can then be sensed using a Hall Effect sensor. The output of the Hall sensor is a Hall voltage that is proportional to the magnetic field changes caused by the transverse displacement amplitudes of the strings. This output signal can then be filtered, amplified, or processed using analog or digital signal conditioning circuits to create a desirable and acceptable input signal for the speakers.

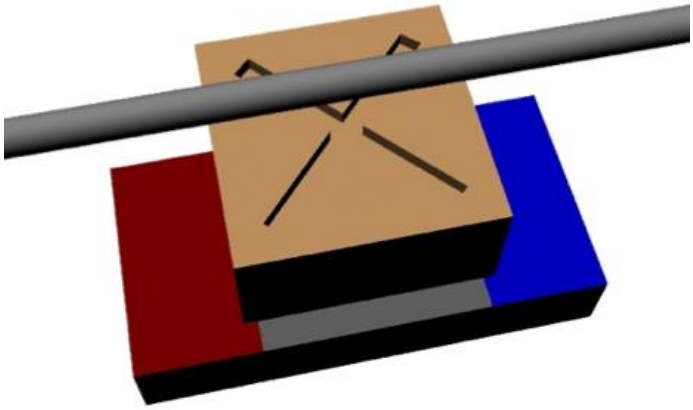

Figure 16: Visualization of a Hall Effect Guitar Pickup: guitar string, sensor (marked with an 'X'), and magnet

Hall Effect pickups also have some notable sonic properties compared to traditional inductive transducers. The frequency response of a Hall Effect sensor is much flatter than that of inductive pickups, resulting in High Fidelity (hi-fi) sound, which refers to high-quality reproduction of sound. (Errede, 2005) Ideally, hi-fi equipment has minimal distortion, noise, and an accurate frequency response, which is potentially useful for low-distortion faithful reproduction type applications such as acoustic guitar, electric bass guitar, violin, mandolin, and so on.

Giant Magnetoresistive Guitar Pickups

As it can be seen in the Figure 11, this sensor consists of a Wheatstone bridge of four magnetoresistive elements (X_1, X_2, Y_1, Y_2). The resistance of the magnetoresistive elements decreases as the magnitude of the surrounding magnetic field increases. The magnetic field may be provided by means of a permanent magnet mounted behind the pickup, or may be generated by a current carried by the vibrating string itself. When a DC voltage is applied across the input terminals (110, 112) of the Wheatstone bridge, an output voltage signal is developed across the output terminals (114, 116) that varies with the changing resistance of the magnetoresistive

elements. A differential amplifier (118) is provided for amplifying the output voltage signal. (Nelson, 2001)

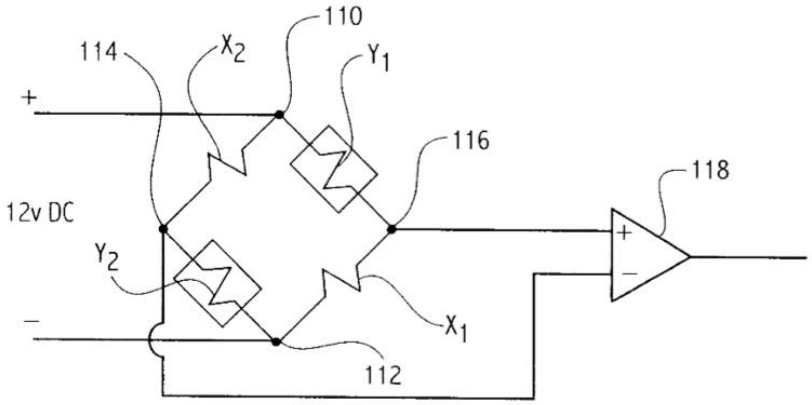

Figure 17: Schematic for Guitar Pickup Using GMR Sensors

In the absence of a magnetic field, or in the presence of a uniform magnetic field affecting each of the GMR resistors in the same way, resistors X1, X2, Y1, and Y2 will all have substantially the same resistance. If the applied magnetic field is non-uniform, however, and is stronger for example, on the side of chip package containing resistors X1, X2, their resistance will be reduced relative to that of resistors Y1, Y2. Under these circumstances the Wheatstone bridge becomes unbalanced and the voltage drop across resistors X1 and X2 will be less than the voltage drop across Y1 and Y2. As a result, the voltage present at the positive output terminal 114 will be less than the voltage at the negative output terminal 116, thus giving rise to a negative sensor output voltage. (Nelson, 2001)

As shown in Figure 17 above, the output voltage of the Wheatstone bridge is a bipolar symmetrical curve about the origin. The output voltage increases in the positive direction as the magnetic field strength increases on the Y elements, and increases in the negative direction as the magnetic field increases on the X resistors. In order to be used as a pickup, the GMR sensors must be biased so that they operate within one of the two linear portions of the curve. This is important

so that the sensor is not affected by the direction of the external magnetic field. When biased, the sensor continuously detects the presence of the bias field. Therefore, the point corresponding to zero external field is shifted from the lowest point on the curve to point 155. Lines 156 represent the maximum vibratory displacement of the string in each direction which is determined by the physical parameters of the string. Note that the curve extends beyond the maximum string displacement so that nonlinear extremes of the response curve are never reached by the string vibrations. (Nelson, 2001)

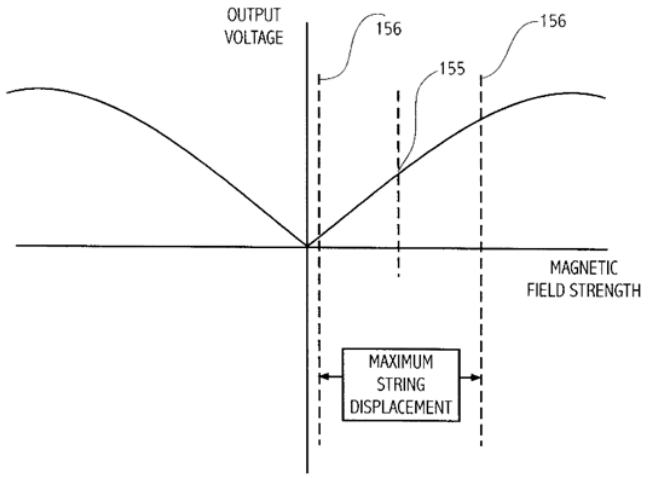

Figure 18: Output Characteristics of the GMR Magnetic Field Gradient Sensor

As shown in Figure 18, a fixed magnet (136) is used to create a uniform magnetic field across the entire sensor. The magnetic flux lines (142) are aligned in an orthogonal direction relative to the axis of sensitivity of the GMR sensor device. When the instrument is played, each string (140) vibrates within a narrow range indicated by circle (141). This vibration creates hysteresis and eddy currents in the ferromagnetic strings. The currents then create their own circular magnetic field around the string which combine with the fixed magnetic field and alter it. (Nelson, 2001)

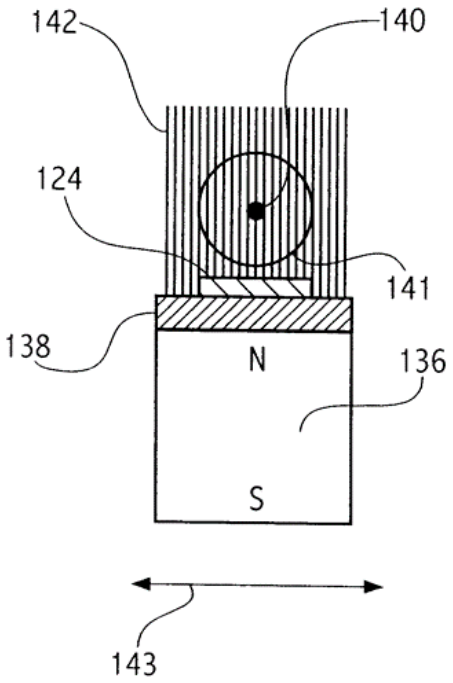

Figure 19: Cross Section of the Alignment of Magnet, GMR Sensor and String

Ideally, the sensor is positioned directly below one of the strings such that when the string is at rest, the longitudinal axis of the string bisects the GMR gradient sensor. This alignment places the sensor pair X_1, X_2 and the sensor pair Y_1, Y_2 on opposite sides of the string and an equal distance therefrom. (Nelson, 2001)

In Figure 14, the GMR sensors for each pickup are shown as blocks 302 with output signals 304 connected to differential amplifiers 306. The output signal 308 from each differential amplifier is connected to a potentiometer R_V and a resistor and finally connected to summing amplifier 310. A feedback resistor R_F is connected between the output of summing amplifier 310 and the input thereof. The gain for each individual string is given by the following equation:

$$G = \frac{R_f}{R_f + R_v} \tag{10}$$

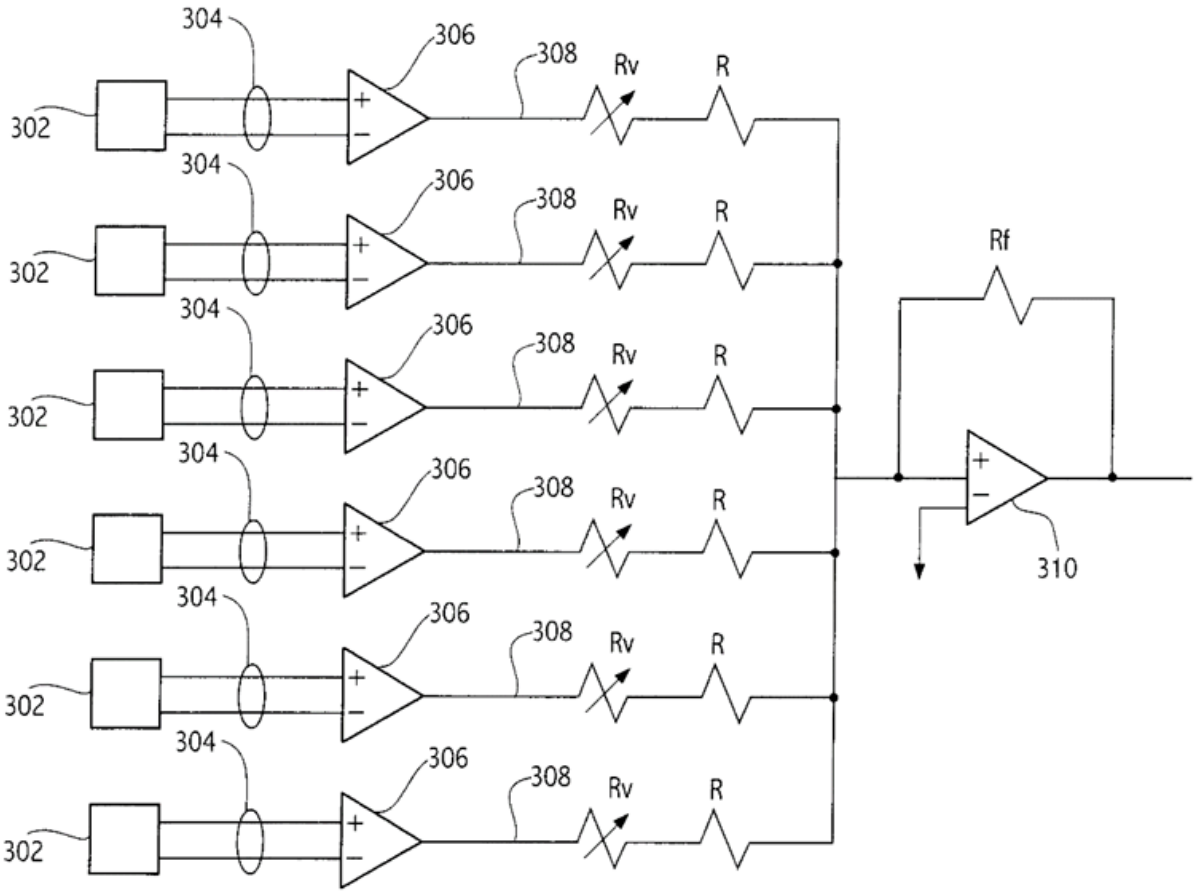

Figure 20: Output Circuit Providing Individual Gain Control for Each Pickup

Comparing Inductive, Hall Effect and GMR Technologies

In general, GMR sensors are used for applications that call for high sensitivities, high bandwidth, and small magnetic fields while Hall Effect sensors are good for high magnetic fields and lower sensitivities. (R & P, 2002)

The saturation field limit of Hall Effect sensors is much higher than that of the GMR sensors, making Hall sensors suitable for high field (usually higher than 1mT) applications. The sensitivity of Hall sensors is quite small usually less than 1 V/AT (Popovic et al., 2002). Lower sensitivity also means a higher electronic gain system must be integrated into the sensor device

thereby limiting the achievable bandwidth of the system. The bandwidth of a typical Hall sensor is in the range of kHz while GMR sensors can go higher than the MHz range. Unlike GMR sensors, the magnetic field must be perpendicular to the Hall sensor device for proper operation.

One other significant drawback of Hall Effect sensors is that they tend to have high sensitivity variation over temperature (AZO Sensors, 2012). According to NVE, one of the leading companies in the practical commercialization of spintronics, GMR sensors shows better sensitivity stability across temperature and supply voltage than unconditioned Hall Effect sensors. On the other hand, the two most significant disadvantages of GMR sensors are their high hysteresis and risk of being destroyed by a large magnetic field.

In conclusion, if no other factors such as power consumption are taken into account, Hall Effect sensors are most suitable for high field range and low bandwidth applications whereas GMR sensors are best for low to mid field range and high bandwidth applications.

Advantages of Magnetoresistive Pickup over Inductive Pickups

Magnetoresistive pickups have several advantages over inductive pickups. These advantages include:

1. Since the resistance of the magnetoresistive elements changes with the instantaneous position of the vibrating string, the output voltage is a true representation of the instantaneous position of the vibrating string. In other words, the output voltage is proportional to the actual string position. (Nelson, 2001)
2. The actual aperture, the length of the sensor geometry, is approximately 0.5 mm, at least 6 to 10 times smaller than a coil-magnet pickup. (Nelson, 2001)

3. A separate pickup is conveniently inexpensive and can therefore be provided for each string of a multi-stringed instrument. (Nelson, 2001)
4. They are much less sensitive to disturbing electromagnetic fields, mainly because their active sensor area is several orders of magnitude smaller (a few mmÂ² instead of cmÂ²). (Lenssen, Somers, & van Zon, 2002)
5. The larger freedom in the choice of the permanent magnets (due to the larger sensitivity of the GMR elements) is advantageous: employing smaller magnets reduces the damping and thus significantly improves the signal. The magnets can be less expensive and more stable magnet materials can be chosen so that aging effects are eliminated. (Lenssen et al., 2002)

Limitations of Inductive Pickup

This section lists various limitations of inductive pickups, which include:

1. Resulted signal does not represent the full range of harmonic tones generated by instrument. The reason is that the output signal does not relate directly to the motion of the strings but rather to the voltage induced in the coil. Thus, sound reproduced will be affected by factors that are unrelated to the acoustics of the instrument such as the number of turns in coil, gauge of wire comprising the coil, number and positions of magnet...etc. (Nelson, 2001)
2. Sound of instrument is determined by the frequency response of the pickup.
    - High impedance pickup (25KΩ - 60KΩ): most of pickups today to match high impedance amplifiers. These pickups have an excellent bass response but don't work well in higher frequency ranges.

- Low impedance pickup (10KΩ - 25KΩ): These pickups have good frequency response in the higher frequency ranges but don't perform well at lower frequencies.

Thus, guitars have to have both high and low impedance pickups and provide some way to switch between the two depending on the type of sound desired. (Nelson, 2001)

3. Coil pickups tend to pick up electrical noise and interference signals from power circuits, radio, television equipment, fluorescent lightning and other sources. "Humbucker" two-coil pickup was developed to reduce the amount of noise. The two coils are spaced apart by the length of the string and are connected with opposite electrical polarities so the noise signals were cancelled out. The drawback of the humbucker is that it sensed string motion from two different points along the length of the string, approximately 0.6 inches apart. Thus, the signals from each coil which were added are slightly out of phase and so the output signal is degraded. (Nelson, 2001)

GMR Pickup

In this section, the methodology and results for characterizing the GMR sensor is presented. For the GMR sensor, the specifications of the part used are included and the circuitry used for testing is discussed. Afterwards, simulation and testing results are presented.

Methodology

This section outlines the procedures that were taken during the design of the GMR pickup. The process consisted of characterizing the sensor, determining the best method for amplification and filtering.

GMR Sensor Functionality

The section investigates the behavior of the chosen NVE GMR sensor, AA005-02, including the hysteresis and magnetic biasing characteristics of the sensor.

Characteristics of the Selected Sensor

The sensor chosen to work with was the AA005-02, manufactured by NVE Corporation. Although the company has other parts for GMR sensors, this part was specifically chosen because it has a large linear range, from 10 Oe to 70 Oe, and a high sensitivity, from 0.45mV/V Oe to 0.65mV/V Oe. The part has an analog output, which makes it easier to work with, considering the areas of expertise of the team and that the preliminary stages of testing were mostly done through bread boarding. (NVE, 2016a)

The sensor circuit is configured as the Wheatstone bridge shown below:

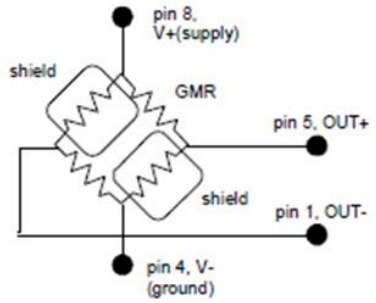

Figure 21: Wheatstone bridge Setup inside GMR Sensor, (Source: NVE Corporation)

The circuit in Figure 21 can operate on any supply voltage from 1V to 24V (NVE, 2016a). 5V was chosen to be the supply voltage for this application because it is large enough to give an output voltage of a decent magnitude but also small enough for a battery-powered application. The resistance of the shield resistors and the GMR devices, with no magnetic field applied, has a nominal value of 5kΩ ± 20% (NVE, 2016a). When a variation in the magnetic field is introduced, the resistance of the GMR devices will change, causing an imbalance in the bridge and producing a differential output across OUT+ and OUT- pins (NVE, 2016a). The AA005-02 part, used in this project, is made of the standard multilayer configuration which has GMR devices that change their resistance in the range of 12% to 16% (NVE, 2016b). It also has a saturation field of about 300 Oe (NVE, 2016b). Shown in Figure 22 is the typical characteristic curve for a GMR sensor with 5V supply.

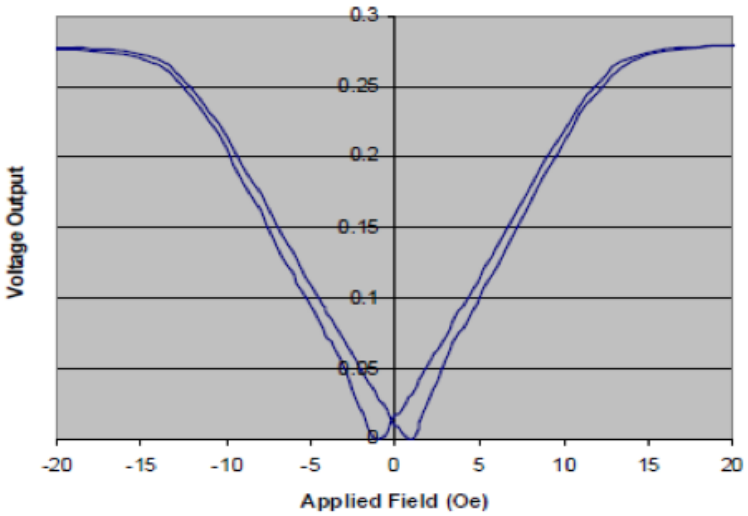

Figure 22: Typical Characteristic Curve for GMR Sensor with 5V Supply, (Source: NVE Corporation)

Hysteresis in GMR Sensors

As shown in Figure 22, the graph representing the sensor's output has two curves. This is caused by an effect called hysteresis. The part used in this project has medium magnetic hysteresis. Hysteresis, in this context, means that the performance of the GMR element is affected by the magnetic history of the material. This means that if the magnitude of the applied field is random in nature, there will be an error at the output, represented as a voltage offset change. For this part, the error can reach a maximum of 4% for a unipolar field and 20% for a bipolar field. Unipolar field is when the applied field at the sensor is always of the same polarity or direction. Bipolar field when the applied field at the sensor changes its direction. Shown below are Figure 23 and Figure 24 with two graphs representing the sensor output when exposed to a saturating unipolar field and a saturating bipolar field, respectively. (NVE, 2016b)

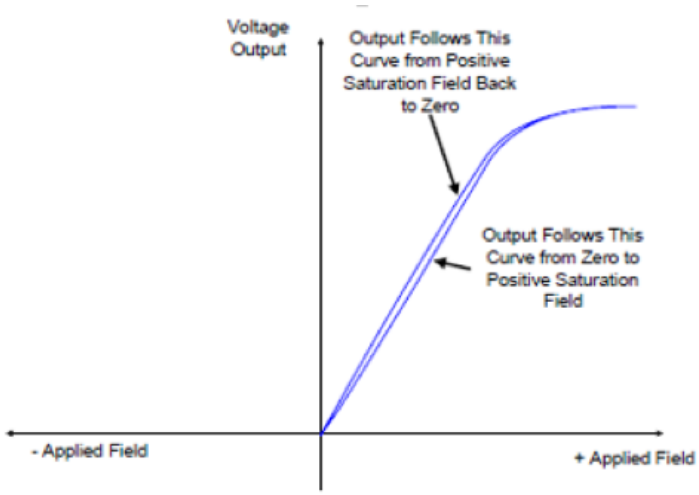

Figure 23: Output Curve with Hysteresis Effect for Unipolar Field, (Source: NVE Corporation)

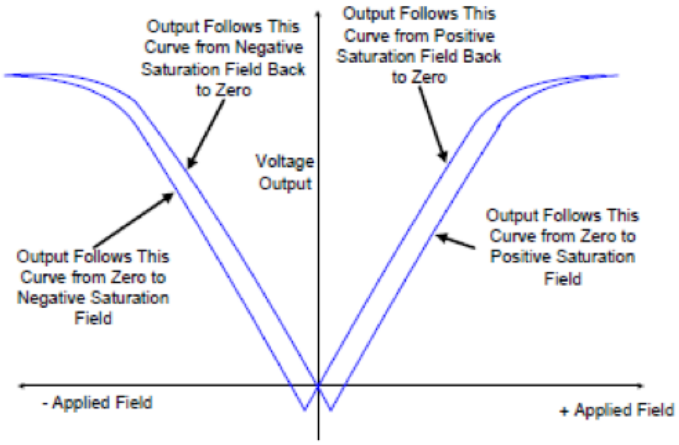

Figure 24: Output Curve with Hysteresis Effect for Bipolar Field, (Source: NVE Corporation)

Note that only the magnitude of the field affects the sensor's performance; time is not an influencing factor. This means that hysteresis actually scales with the applied field; the bigger the field, the more hysteresis the sensor would have. Figure 25 explains this phenomenon graphically. (NVE, 2016b)

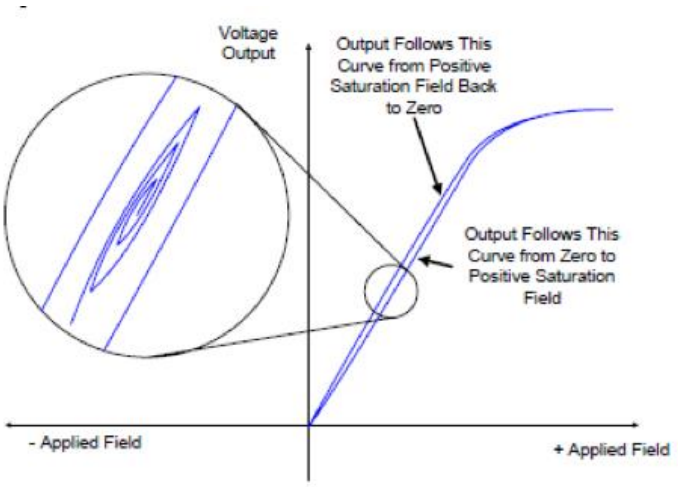

Figure 25: Zoomed-in version of the output curve showing the increase in hysteresis when the applied field increases, (Source: NVE Corporation)

In order to avoid the negative effects of hysteresis, the sensor element has to be biased with an external magnetic field so that the element's magnetic history is always the same. This bias point also needs to be on the linear portion of the characteristic curve. This will guarantee that the magnetic sensitivity of the device will remain the same, no matter how much hysteresis the sensor has. Additionally, ferrous materials and magnetic field producers is preferred not to be in proximity to the sensor. Their presence can increase the magnetic hysteresis and decrease the sensor's output precision. (NVE, 2016b)

Magnetic Biasing of the GMR Sensor

The GMR sensor selected for this project has a primary axis of sensitivity. Figure 26 below shows a cutaway view of the die orientation within an SOIC8 package. The areas labelled as flux concentrators are responsible for gathering the magnetic flux and focusing it at the GMR bridge resistors at the center of the die. To obtain the largest output signal, the applied magnetic field should be parallel to the flux concentrators' axis. (NVE, 2016b)

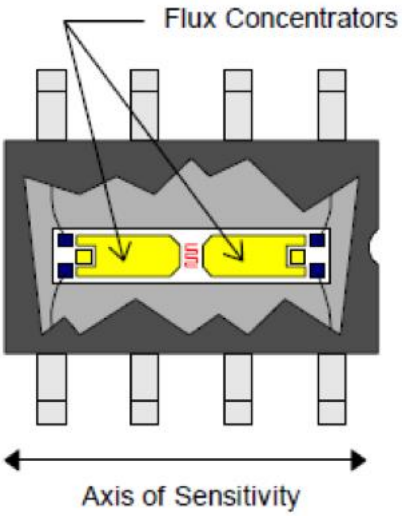

Figure 26: Cut away view of the die orientation within an SOIC8 package, (Source: NVE Corporation)

Biasing magnetic fields can be used either as the magnetic field to be sensed or as a method to create a pseudo zero field. For the application studied in this project, the applied magnetic field is used as the field to be sensed when changes are introduced in that field as the guitar strings are plucked. This is called back-biasing the sensor and its purpose is to create a field that the device can sense for applications where there is no magnetic field present. In order to back bias the sensor, the magnet and the sensor are placed in the orientation shown in Figure 27. This orientation achieves the maximum field in the Z direction and the minimum field in the sensitive X direction. (NVE, 2016b)

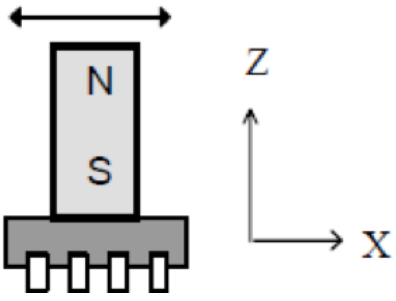

Figure 27: Orientation of the magnet for back-biasing the GMR sensor, (Source: NVE Corporation)

The other kind of biasing is achieved by providing a constant magnetic field in the sensitive direction. This create a pseudo zero field by introducing a DC offset to the output. The resulting curve would look like the curve in Figure 28. One advantage for this kind of biasing is that the sensor is now biased away from the zero field area, where hysteresis is usually larger. (NVE, 2016b)

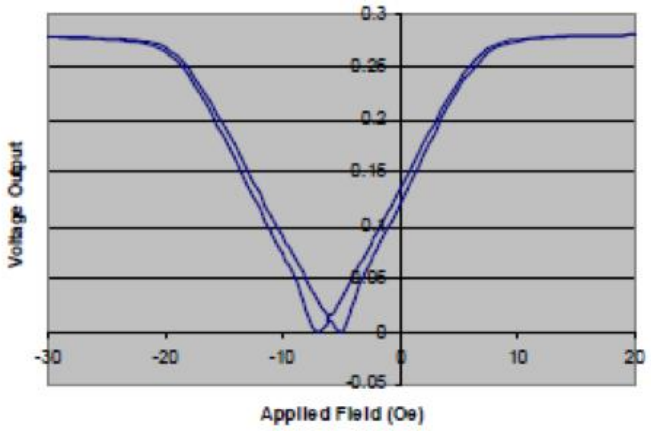

Figure 28: Output curve when the sensor is biased to have a pseudo zero field, (Source: NVE Corporation)

Magnetic Orientation

The magnet chosen for biasing the GMR Sensor is the NSN0548 part from MAGCRAFT. This magnet was specifically chosen because of its relatively small dimensions (0.25” x 0.25”) which would make it easy to fit six magnets under the six guitar strings. It also cylindrical with the magnetization direction along its length as shown in Figure 29. This makes it possible to mount the magnet on a rod and be able to easily change the orientation of the North Pole, relative to the sensor’s axis of sensitivity.

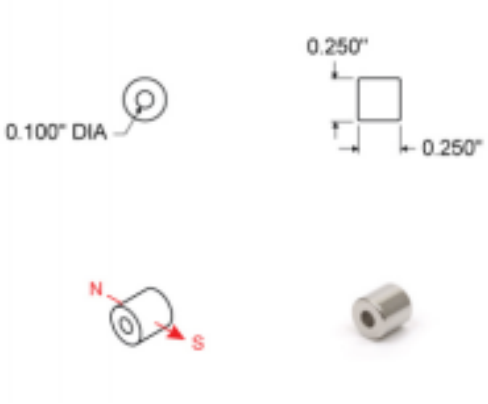

Figure 29: NSN0548 Magnet's Dimensions and Magnetization Direction, (Source: MAGCRAFT Company)

After the magnet was selected, several tests were carried out in order to find the magnet's orientation that would give the best possible output signal. In order to find the ideal orientation for the magnet with respect to the sensor and the string, there are three main dimensions that should be considered:

1. Orientation of the North Pole with relative to the sensor's axis of sensitivity
2. Offset Voltage
3. Distance between the top of the magnet and the string

The first dimension guarantees that the sensor is back-biased correctly, preparing it to sense changes in the magnetic field, as explained earlier. The second dimension guarantees that the sensor is operating at the offset where it has the highest sensitivity. This means that at a specific offset voltage, the magnetic field strength reaching the sensor is equivalent to the point of highest slope on the sensor's characteristic curve. After the sensor is biased at its most sensitive point, the third dimension guarantees that the strings have the biggest effect possible on the magnetic field so that the sensed signal is as close as possible to the actual guitar signal.

For the first dimension, different tests were carried out by the changing the angle between the North Pole and the positive x-axis. The first purpose of these tests was to verify that having the magnetization direction perpendicular to the sensor's axis of sensitivity would be the orientation giving the best output signal. The second purpose was to investigate if there will be a difference when the North Pole and the South Pole are flipped in that orientation. The test results are shown below. For each of the orientations studied below, the blue circle represents the magnet and the red arrow represents the orientation of the North Pole. The grey rectangular block represents a side view of the sensor while the dashed line on top represents one of the guitar strings. In order to make sure that all other variables are constant throughout testing, the top of the magnet and the top of the sensor were both kept at the same vertical level. Also, the distance between the top of the magnet and the string was kept constant. Offset voltage was also kept at the same value (≈ 200mV), which was found to be the most sensitive spot.

<u>Orientation 1: Angle between the North Pole and the positive x-axis is 0 degrees:</u>

Vout (pk-pk) ≈ 500mV

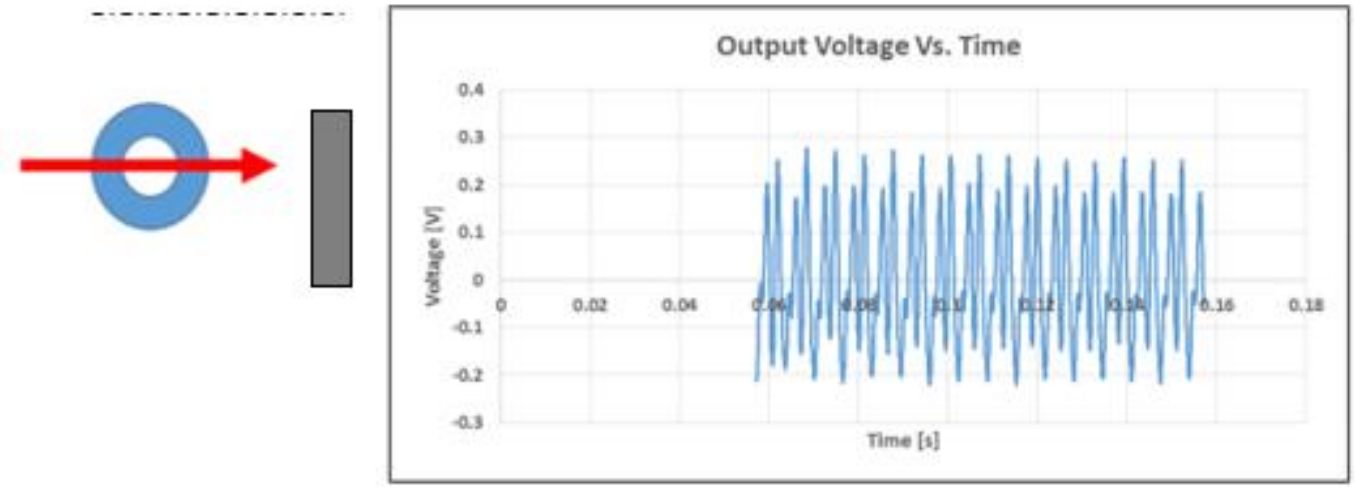

Figure 30: Graph for Output Voltage when the angle between the positive x-axis and the magnet's North Pole is 0 degrees

Orientation 2: Angle between the North Pole and the positive x-axis is 45 degrees:

Vout (pk-pk) ≈ 700mV

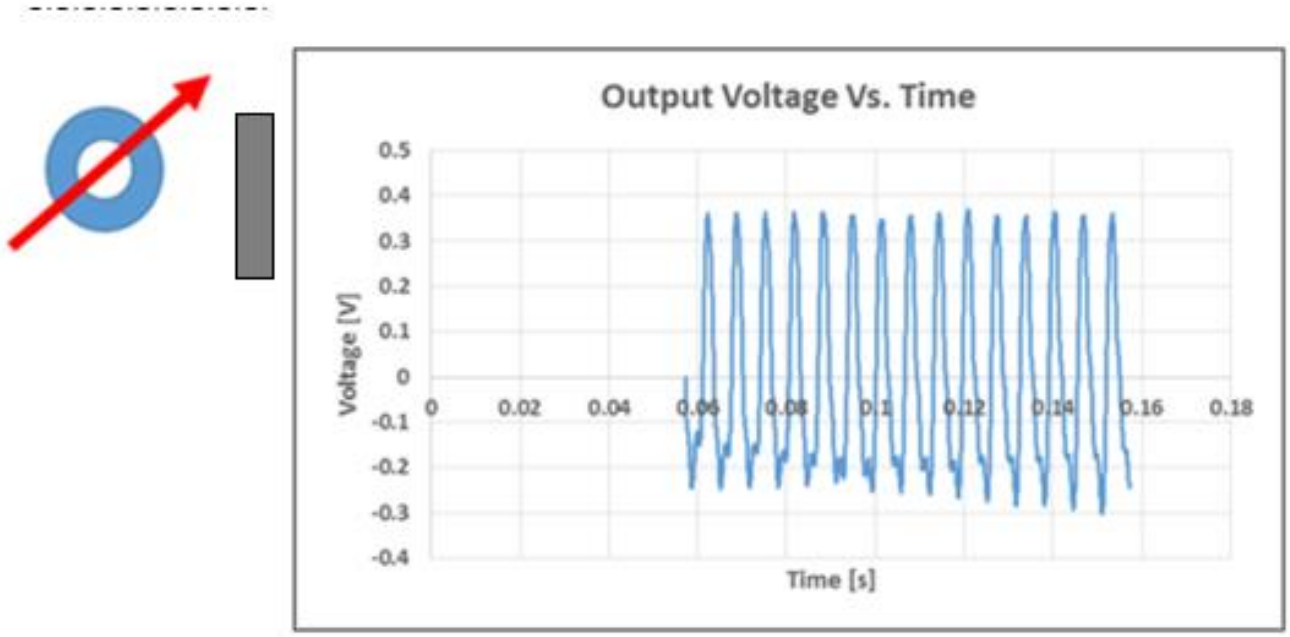

Figure 31: Graph for Output Voltage when the angle between the positive x-axis and the magnet's North Pole is 45 degrees

Orientation 3: Angle between the North Pole and the positive x-axis is 90 degrees:

Vout (pk-pk) ≈ 170mV

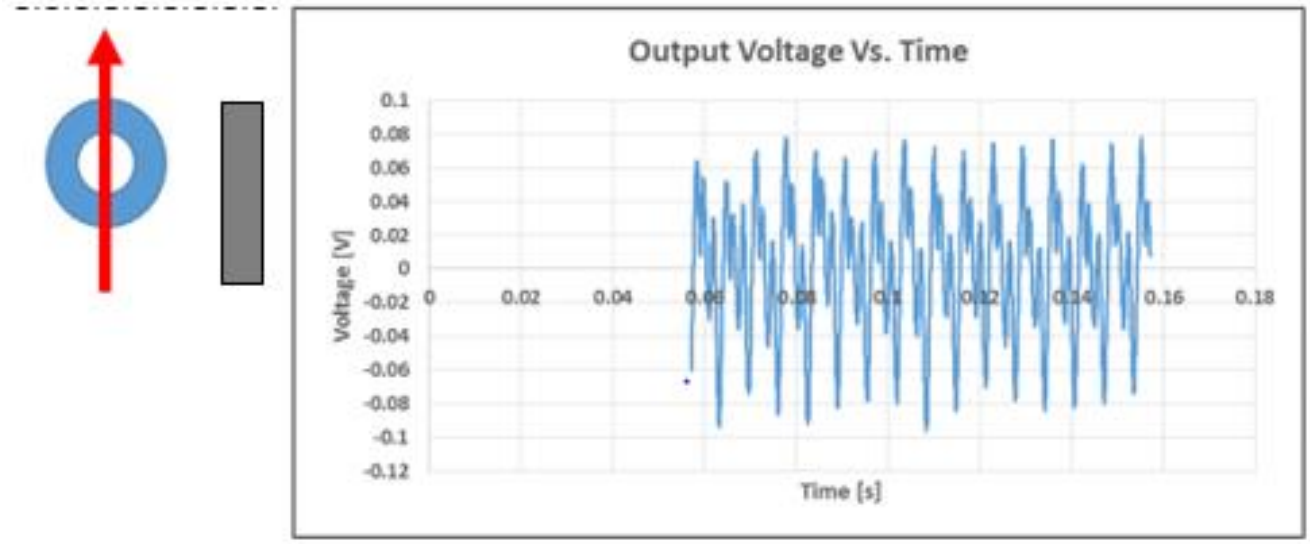

Figure 32: Graph for Output Voltage when the angle between the positive x-axis and the magnet's North Pole is 90 degrees

Orientation 4: Angle between the North Pole and the positive x-axis is 135 degrees:

Vout (pk-pk) ≈ 420mV

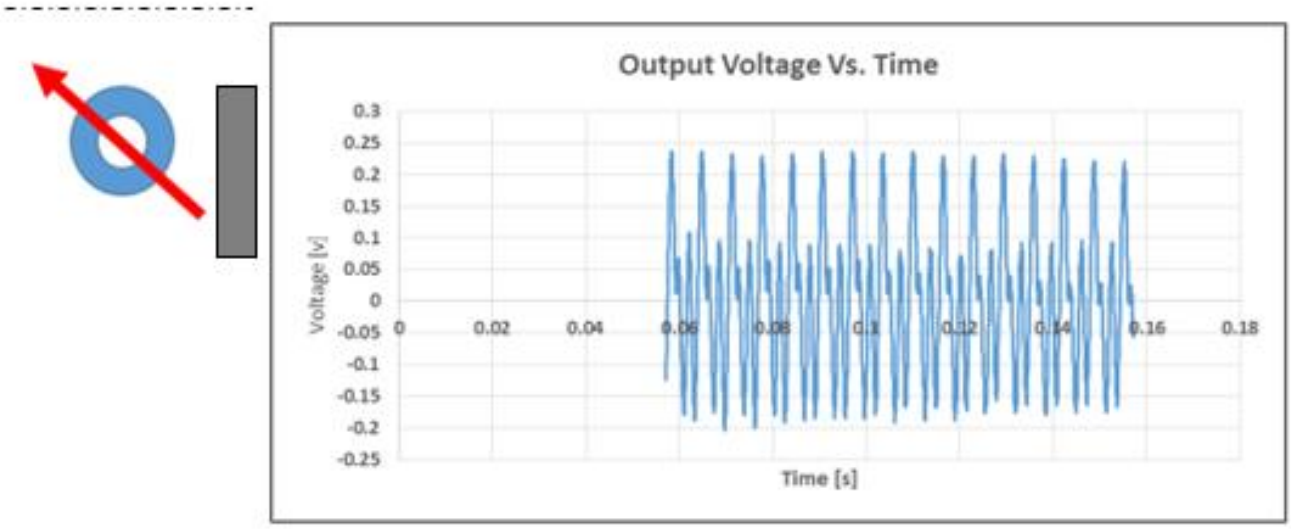

Figure 33: Graph for Output Voltage when the angle between the positive x-axis and the magnet's North Pole is 135 degrees

Orientation 5: Angle between the North Pole and the positive x-axis is 180 degrees:

Vout (pk-pk) ≈ 900mV

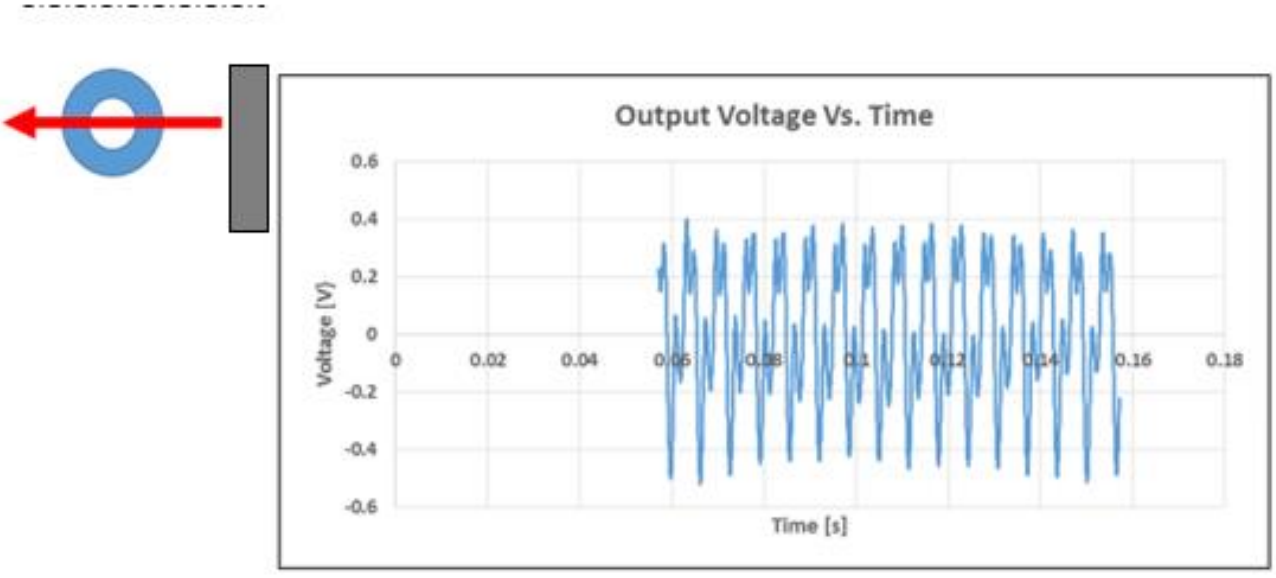

Figure 34: Graph for Output Voltage when the angle between the positive x-axis and the magnet's North Pole is 180 degree

Orientation 6: Angle between the North Pole and the positive x-axis is 225 degrees:

Vout (pk-pk) ≈ 500mV

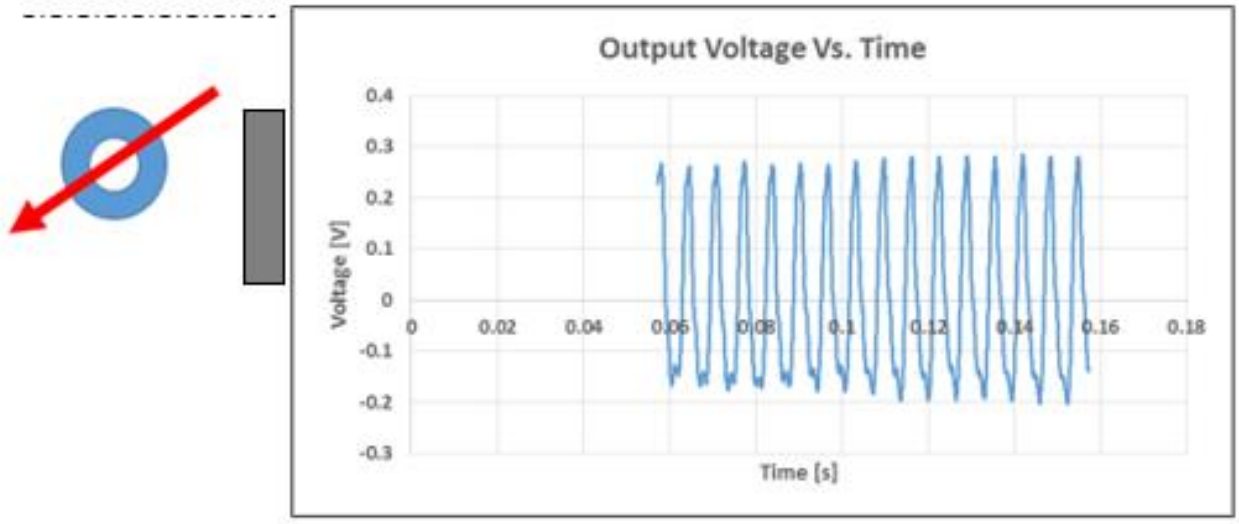

Figure 35: Graph for Output Voltage when the angle between the positive x-axis and the magnet's North Pole is 225 degrees

Orientation 7: Angle between the North Pole and the positive x-axis is 270 degrees:

Vout (pk-pk) ≈ 300mV

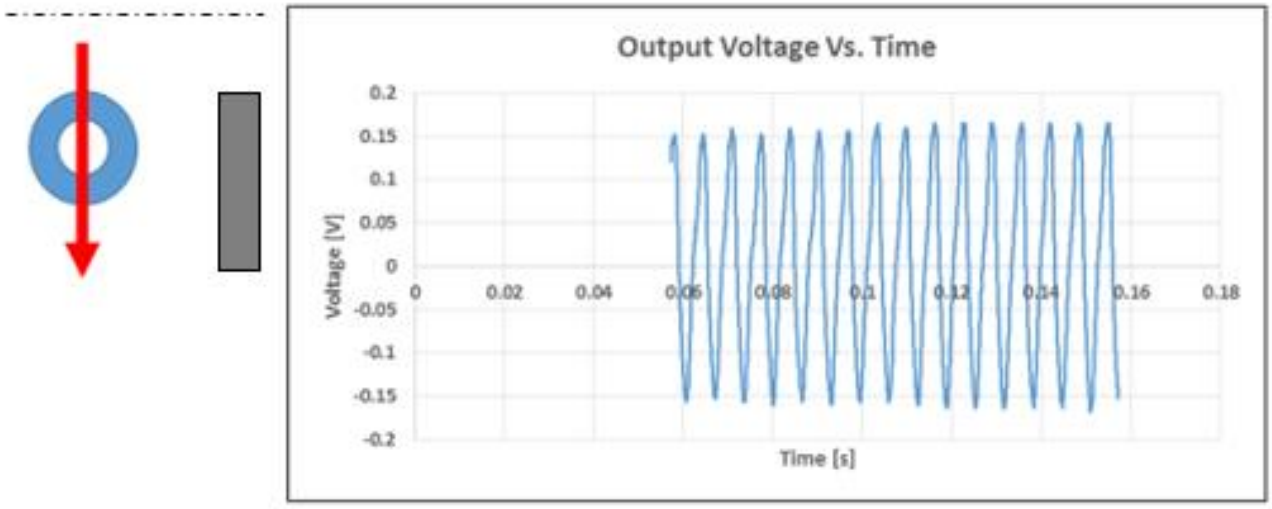

Figure 36: Graph for Output Voltage when the angle between the positive x-axis and the magnet's North Pole is 270 degrees

Orientation 8: Angle between the North Pole and the positive x-axis is 315 degrees:

Vout (pk-pk) ≈ 400mV

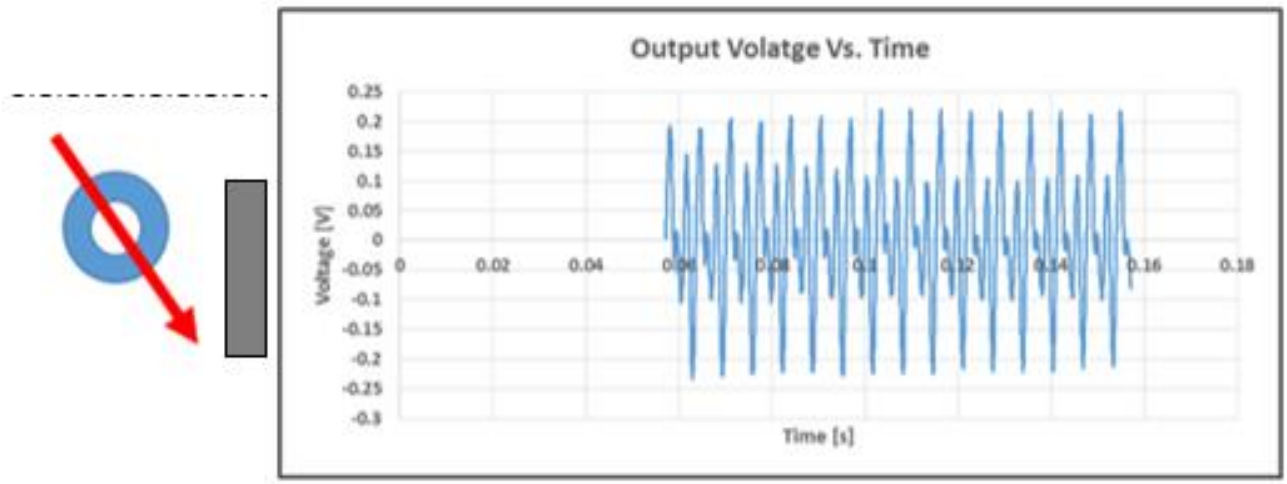

Figure 37: Graph for Output Voltage when the angle between the positive x-axis and the magnet's North Pole is 315 degrees

From the results shown above, it is confirmed that the sensor gives the largest output when the magnetic field is perpendicular to the sensor's axis of sensitivity. Additionally, it was discovered that having the North Pole pointing away from the sensor gives a larger output than having it facing the sensor.

Testing the GMR Sensor

To prepare the sensor for testing, a magnet was used for biasing. The D string was plucked multiple times to ensure accuracy and the typical resulting signal was as follows:

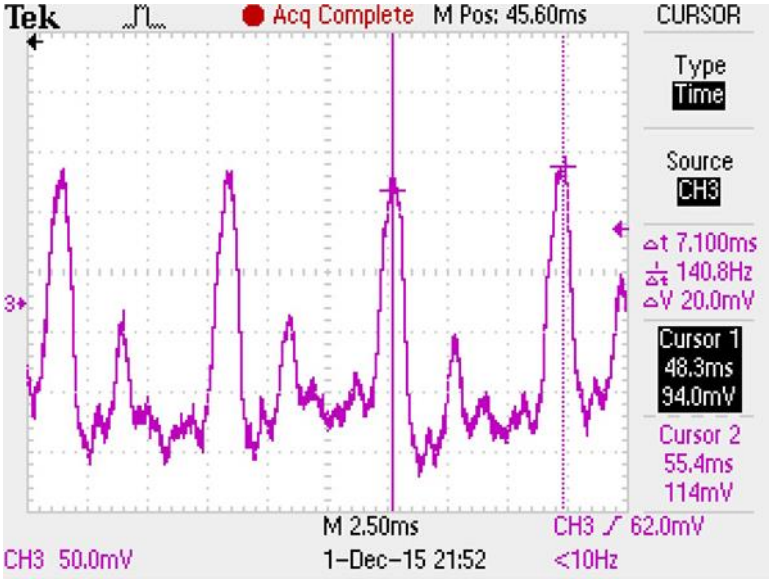

Figure 38: Typical Differential Output Signal from GMR Sensor

As shown in Figure 38, the amplitude of the output signal is around 230mV. When the sensor is connected to the guitar amplifier, no output is heard. This is because the signal amplitude is too small so a preamplifier is needed to increase the amplitude to a detectable level. Additionally, there is an offset voltage due to the magnetic biasing of the sensor. This offset will need to be adjusted such that the sensor exhibits the highest sensitivity, producing the best possible output signal. The signal produced was also noisy, thus, some kind of filtering will be needed at the output.

GMR Recommended Test Circuit

Figure 39 shows one of the signal conditioning circuits that were recommended by NVE. NVE claims that this configuration has significant advantages in noise and performance over other op-amp implementations.

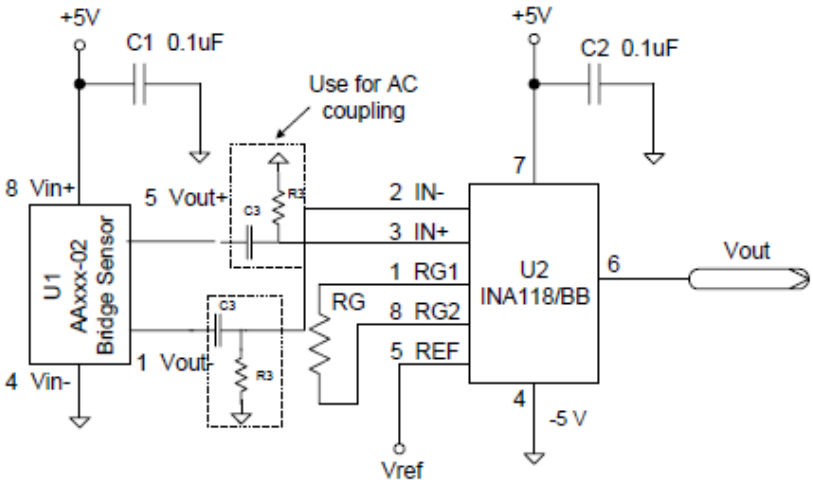

Figure 39: Instrumentation Amplifier Bridge Preamplifier Circuit, recommended by NVE, (Source: NVE Corporation)

With instrumentation amplifier circuits, resistor matching is no so important for common mode rejection. Additionally, gain-bandwidth product for instrumentation amplifier circuits can be higher than operational amplifier circuits. (INA datasheet Info) The gain for the circuit in Figure 39 can be calculated by the following equation:

$$Vout = \left(1 + \frac{50K}{RG}\right) Vin + Vref \tag{11}$$

For the GMR sensor output, the desired gain is 1000 so that the signal is amplified to a detectable amplitude, and so RG was chosen to be 50Ω and Vref is 0V. The cutoff frequency for the high pass filter can be calculated using the following equation:

$$f3db = \frac{1}{2\pi R3C3} \tag{12}$$

The lowest frequency played on guitar strings is around 70 Hz and so f3db is adjusted at that value. Thus, R3 and C3 were chosen to be 10kΩ and 0.227uF accordingly. The circuit was then simulated in Multisim in order to study its behavior.

GMR Pickup Circuit Description

This section will discuss and explain the design ideas behind the final circuit design for the GMR pickup. It will also highlight the various breadboard tests that were carried out towards the final circuit design. Figure 40 shows the circuit schematic of the final GMR pickup for one string along with non-inverting summing amplifier and second order low pass filter.

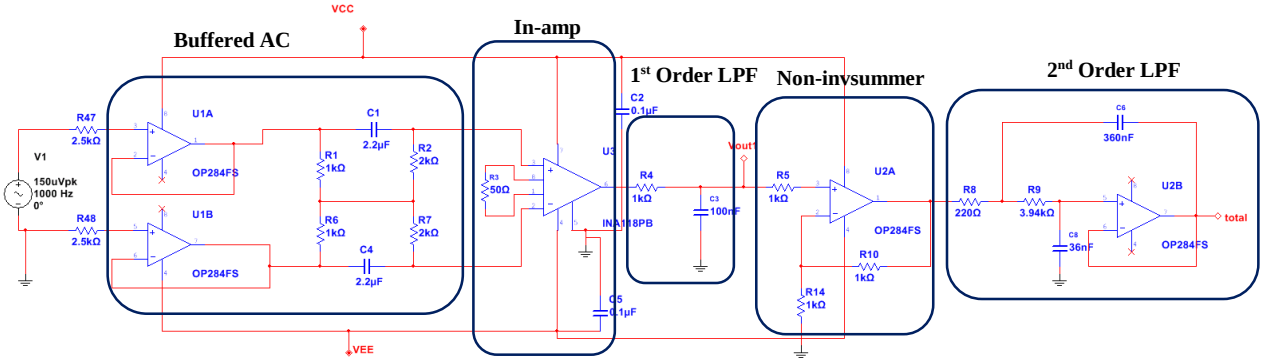

Figure 40: Final GMR pickup circuit schematic for one string plus summing amplifier and Sallen-Key LPF

Buffered AC Bridge

Since the differential outputs of the GMR sensor were magnetically biased to have 200mV DC offset, AC input coupling was needed for each input in order to delete the DC component before feeding it to the in-amp. A simple differential high pass filter as shown in Figure 41 can be used between the sensor and in-amp to accomplish the task.

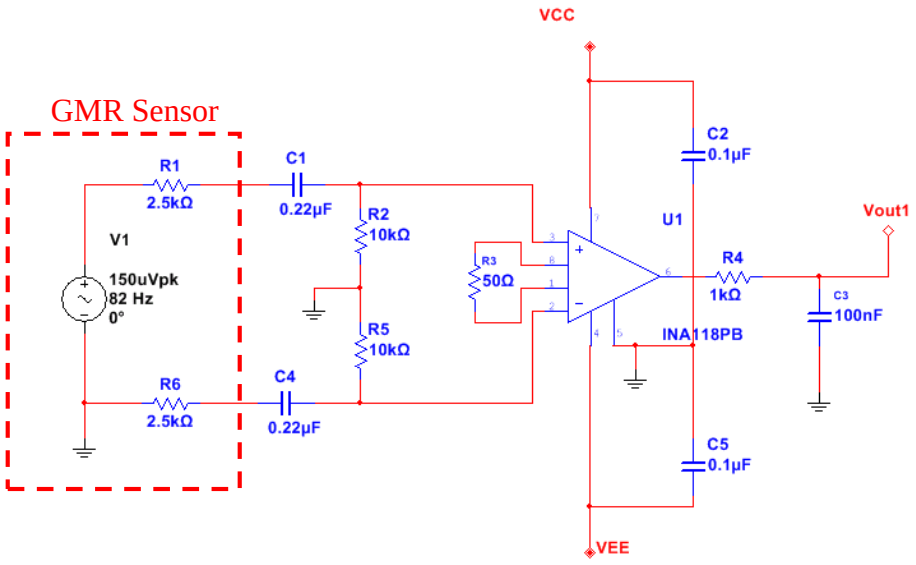

Figure 41: GMR circuit design with traditional differential high pass filter (HPF)

However, since C1 and C4 will become shorted out at the passband regions, R2 must be significantly larger than the source output resistance R1 or considerable signal loss will occur. Moreover, the grounded resistors, which provide bias current path for in-amp, degrade the common mode rejection ratio (CMRR) (Spinelli et al. 2003). Therefore, a novel different AC coupling network that provides a bias path without any connection to ground was used as shown in Figure 42. Moreover, this network also provides AC coupling only for the differential signals and DC coupling for common mode signals, which makes the network compatible with single supply amplifiers (Spinelli et al. 2003). OP284 op-amp was then used to buffer the outputs of the GMR sensor, which will reduce the resistor loading effect since the op-amp output impedance is usually very low.

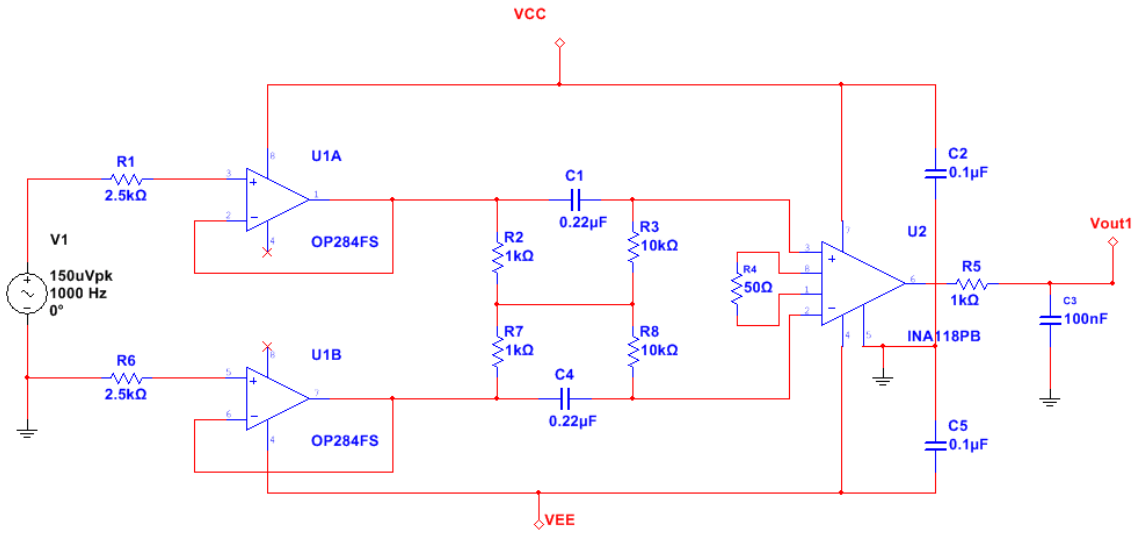

Figure 42: GMR circuit design with buffered AC Bridge

The two circuits were also built on a breadboard and tested for noise and offset. The results from these experiments are shown in Figure 43 and Figure 44. It was observed that using the buffered AC bridge results in both smaller noise by $0.3187mV_{rms}$ and smaller offset by 16.35mV than the traditional high pass filter. The final design uses 2.2uF as C1 and 2kΩ as R3, which reduces the high pass cutoff from 72Hz to 36Hz and reduces the noise generated from R3 and R8. The high pass cutoff was reduced to a lower frequency to achieve a more even passband gain for the fundamental frequency of the lowest guitar note at 82Hz.

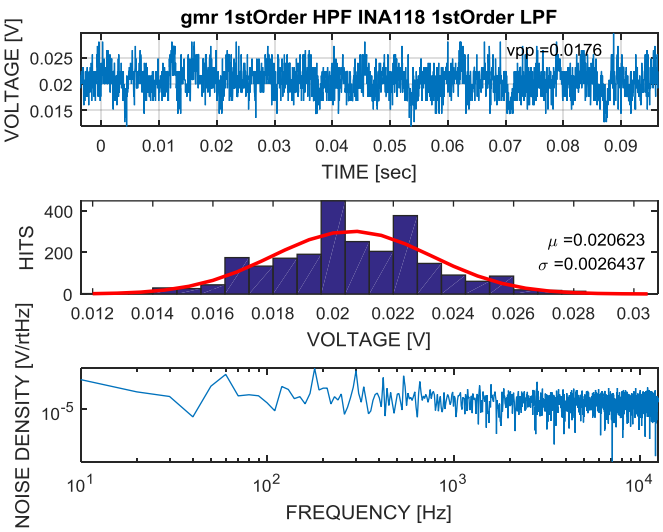

Figure 43: MATLAB noise analysis for differential HPF circuit

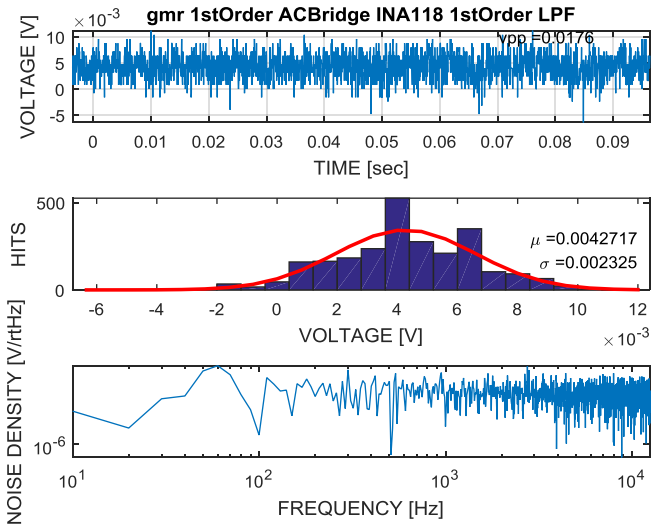

Figure 44: MATLAB noise analysis for AC bridge circuit

Instrumentation Amplifier (In-Amp) Selection

Two in-amps were used in the preliminary breadboard tests. NVE recommended the INA118 and Analog Devices' lowest noise in-amp, the AD8429. A brief comparison between

several specifications of the two in-amps is shown in Table 1. It can be seen that the AD8429 has a noise voltage rating ten times better than the INA118, however, the AD8429 has worse current noise level, offset current, bias current, and finally and most importantly, supply current consumption. Since the AD8429 has significantly lower voltage noise than the INA118, two circuits were built using both in-amps and tested in lab for output noise levels.

Table 1: INA118 Vs AD8429

Specs	INA118	AD8429	Unit
Offset voltage	±50.5	50	µV
CMRR (G = 1000)	125	134	dB
Bias current	±5	150	nA
Offset current	±5	30	nA
Noise voltage (1kHz)	10	1	nV/rtHz
Noise current (1kHz)	0.3	1.5	pA/rtHz
-3dB bandwidth (G = 1000)	7	150	kHz
Supply current	±0.385	7	mA

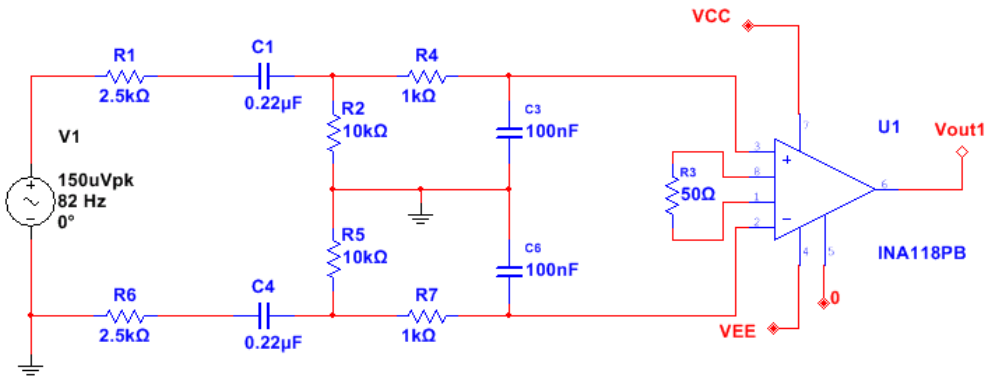

Figure 45: Test circuit for INA118

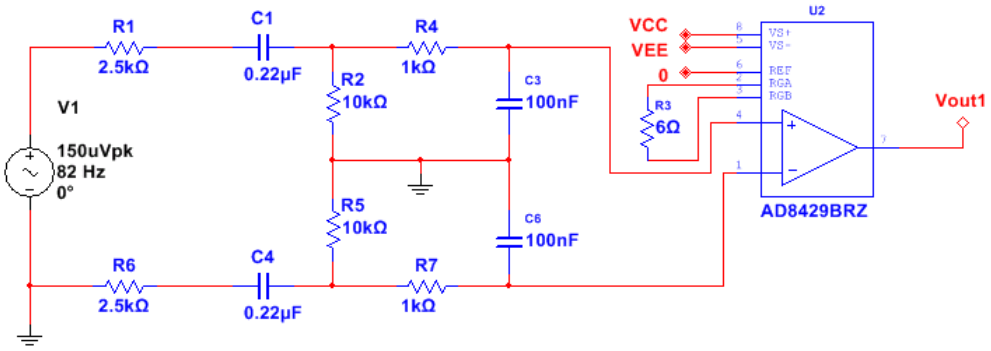

Figure 46: Test circuit for AD8429

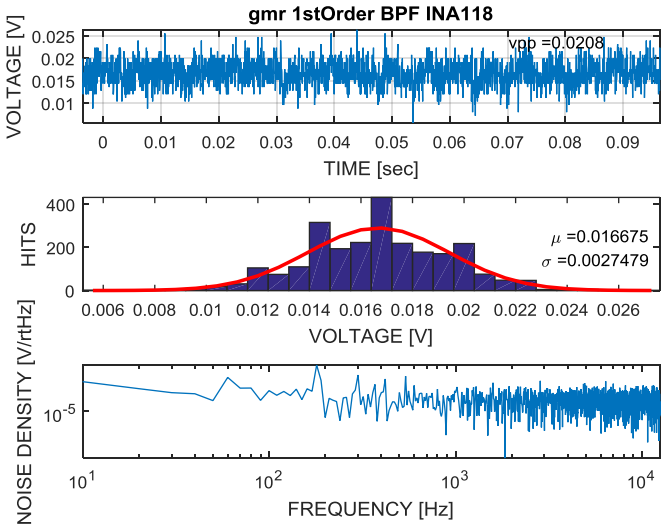

Figure 47: MATLAB noise analysis for INA118 circuit

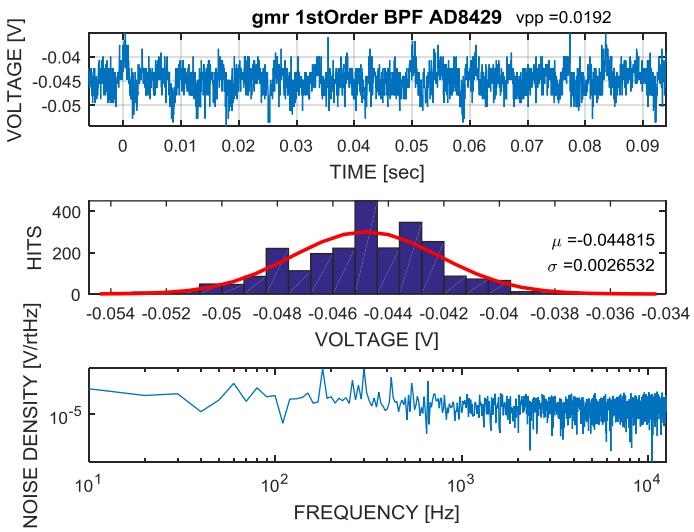

Figure 48: MATLAB noise analysis for AD8429

As expected, the AD8429 circuit resulted in providing a voltage noise that was 3.4% better than the INA118 circuit. However, the AD8429 circuit draws 18x more current than the INA118, making the AD8429 unsuitable for a battery operated pickup application regardless of the low voltage noise. Moreover, it was observed that the AD8429 also produces a larger offset (μ – mean value in MATLAB figures) than the INA118. Therefore, the INA118 was chosen as the final in-amp for the prototype design.

Low Pass Filtering After In-amp

In order to construct the desired bandpass filter, a lowpass filter was added to the circuit design. The challenge was to investigate whether the lowpass filter should be placed before the in-amp or after the in-amp. Therefore, two test circuits shown in Figure 49 and Figure 50 were built on a breadboard and tested for differences between the two circuits in terms of noise.

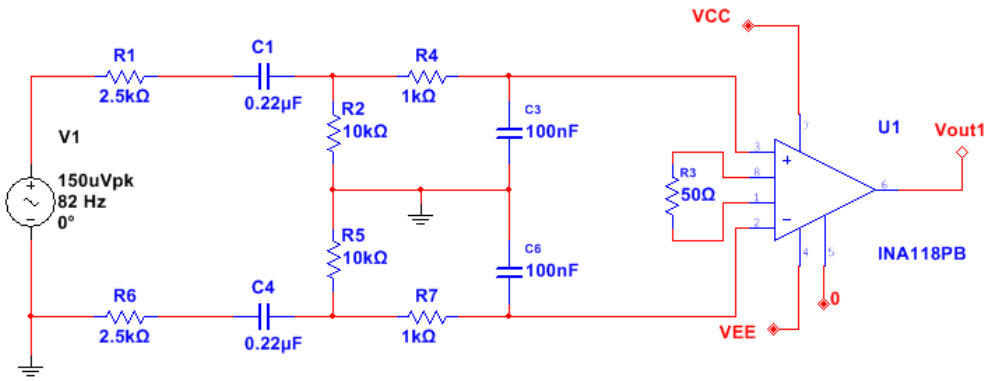

Figure 49: Test circuit with low pass filter before INA118

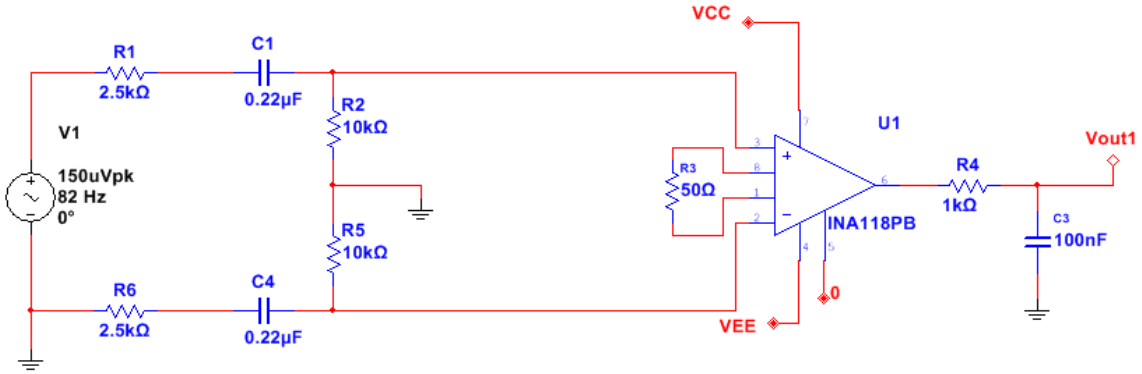

Figure 50: Test circuit with low pass filter after INA118

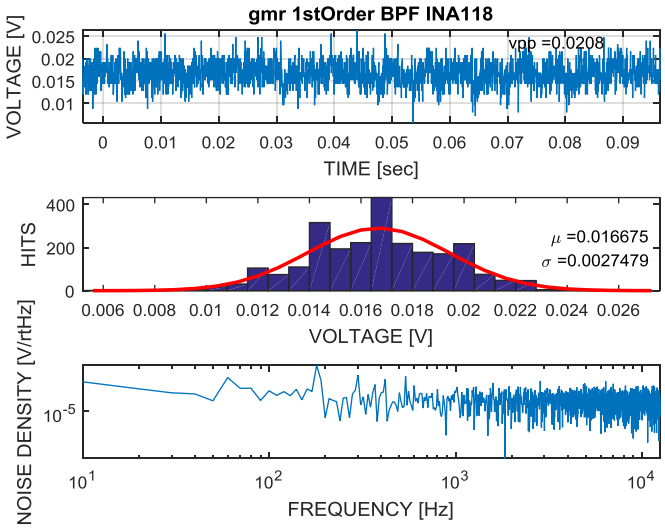

Figure 51: MATLAB noise analysis for LPF before in-amp circuit

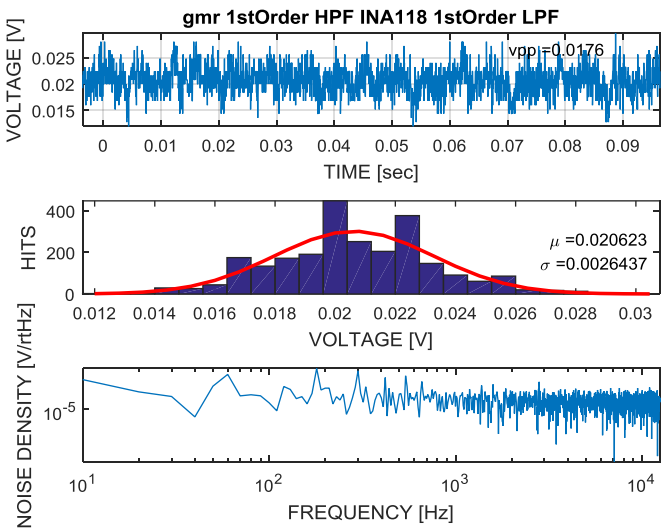

Figure 52: MATLAB noise analysis for LPF after in-amp circuit

As seen from Figure 51 and Figure 52, having the low pass filter after the in-amp results in a lower noise level than having it before the in-amp. Moreover, through listening the output of the circuits, it was confirmed that high frequency hissing noise was heard when the low pass filter was placed before the in-amp. Therefore, it was decided that the low pass filter be placed after the in-amp for the best noise performance, which also resulted in using fewer circuit components and thereby reducing the power consumption of the circuit. The cutoff frequency was designed to be 1.6kHz, which also covers all of the high frequency guitar notes and a few crucial high frequency harmonics.

Non-inverting Summing Amplifier

First order low pass filters are needed after the in-amps in order to filter out the high frequency hissing noise for individual string control outputs. However, the filters causes the summing signal source to become a high impedance output. Using an inverting summing amplifier in this case would result in severe signal loss due to the low input impedance of the inverting

summing amplifier. If necessary, an inverting summing amplifier could still be used by buffering the summing signal sources; however, doing so would require an additional op-amp per string, which is undesirable since the PCB board area is limited and it is necessary to keep the number of components manageable for PCB trace routing and manual soldering. Therefore, it was decided that non-inverting summing amplifier be used, avoiding the need for six more op-amps. Moreover, using the non-inverting summing amplifier resulted in an unloaded signal at the output of the LPF, which can directly be routed to become output access nodes for individual string control whereas with inverting summing amplifiers, it would require six more buffer op-amps. If the board size was not a limiting factor, an inverting summing amplifier would have been used due to the fact that it provides a constant input impedance set by the RI_x and the individual signals do not get smaller with increasing number of summing input signals. Table 2 also lists some pros and cons of using inverting and non-inverting op-amp summing amplifiers.

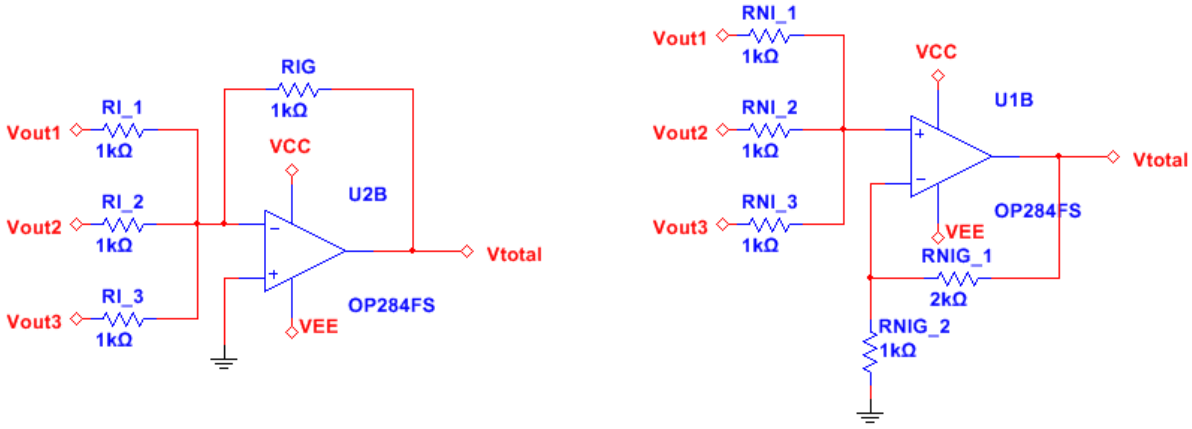

Figure 53: Inverting Vs non-inverting op-amp summing amplifiers

Table 2: Some pros and cons of inverting and non-inverting summing amplifiers

Inverting Summing Amplifier	Non-inverting Summing Amplifier
Equation $$Vtotal = -(\frac{RIG}{RI_1}Vout1 + \frac{RIG}{RI_2}Vout2 + \frac{RIG}{RI_3}Vout3)$$ Pros • Input impedance is set by RI_x and held constant by virtual ground. No interaction between stages. • Number of input summing signals does not affect the sum components. • Smaller common mode voltage Cons • Input impedance is very small compared to non-inverting summing amplifier. Need summing signal sources to originate from the output of previous op-amps or tremendous signal loss will occur.	Equation $$Vtotal = (1 + \frac{RIG}{RI_1})\frac{(Vout1 + Vout2 + Vout3)}{\#\ of\ input\ sums}$$ Assuming RNI_1 = RNI_2 = RNI_3 Pros • Very high input impedance. Cons • The non-inverting pin is exposed to varying voltages, which can affect the input impedance of the summing amplifier. The fact that input impedance varies on other voltage levels shows that there can be strong interactions between various input stages, which could give rise to unforeseen results in multistage designs. • The more input summing signals there are, the smaller the sum components are. Bigger feedback resistor needed to achieve a gain of 1. • Bigger common mode voltage. Need care to ensure the input does not exceed common mode spec

2nd Order Low Pass Filter

Since one op-amp has been used as a summing amplifier in the previous stage, and most op-amps come in a dual package, it was decided that a 2nd order Sallen-Key low pass filter be used as the final stage to further eliminate the white noise outside of the desired bandwidth. The cutoff frequency was decided to be about 1.5kHz since the highest guitar note fundamental frequency is about 1200Hz. The filter was designed using an online filter resource from Analog Devices Inc. called Filter Wizard, which can be found at this URL link http://www.analog.com/designtools/en/filterwizard/. There is also an interesting feature in Filter

Wizard that enables the users to adjust the size of the resistors or capacitors in the filter design, which is very useful in this project since low resistor values are desired to keep the thermal noise of the circuit in a reasonable range.

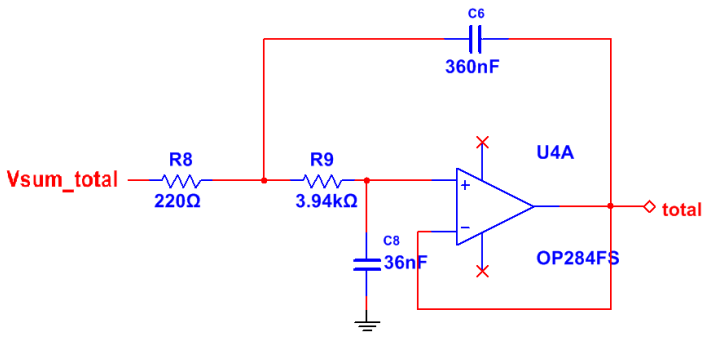

Figure 54: 2th Order Sallen-key LPF of the final GMR pickup circuit design

Final Design Simulation

After all the different circuit parts were constructed, the whole final design for all six strings was simulated using NI SPICE Simulation Environment Multisim. The results are shown in Figure 57 and Figure 58.

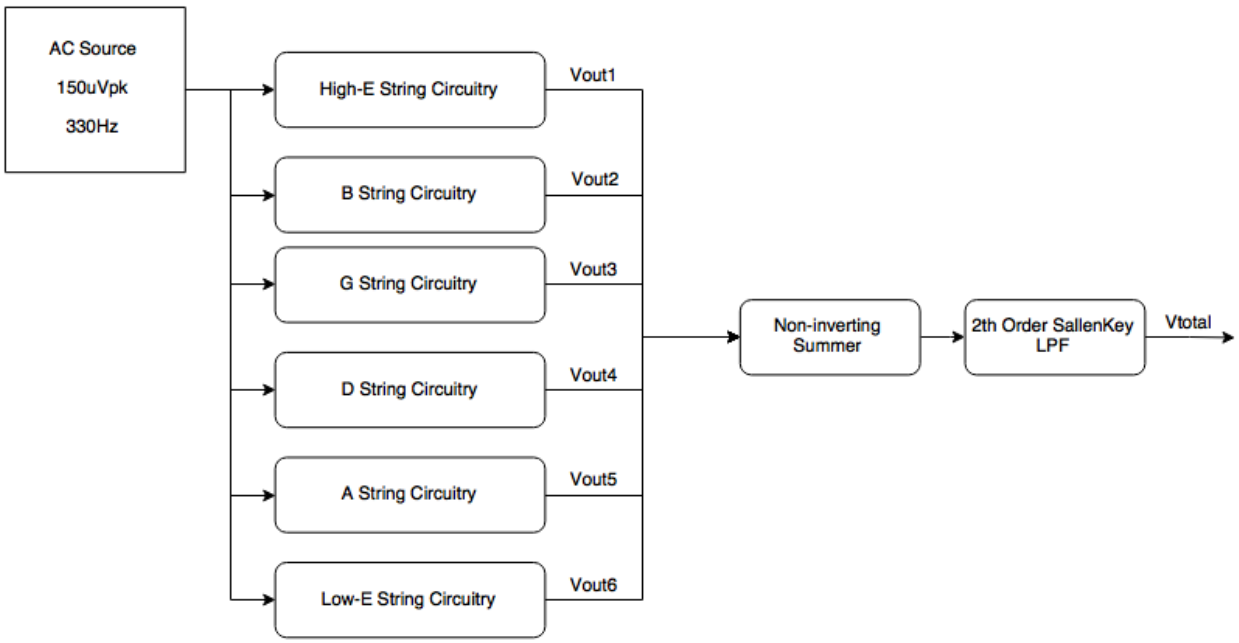

Figure 55: Block diagram of the simulated circuit

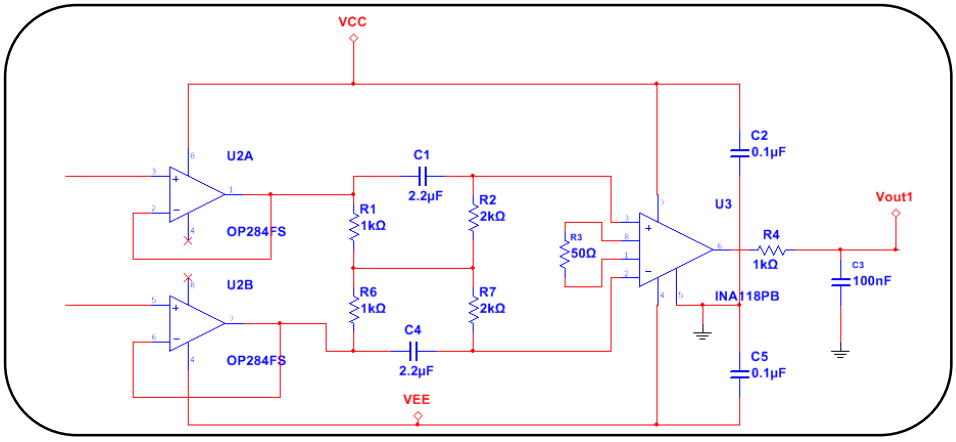

Figure 56: Signal conditioning circuit for each string

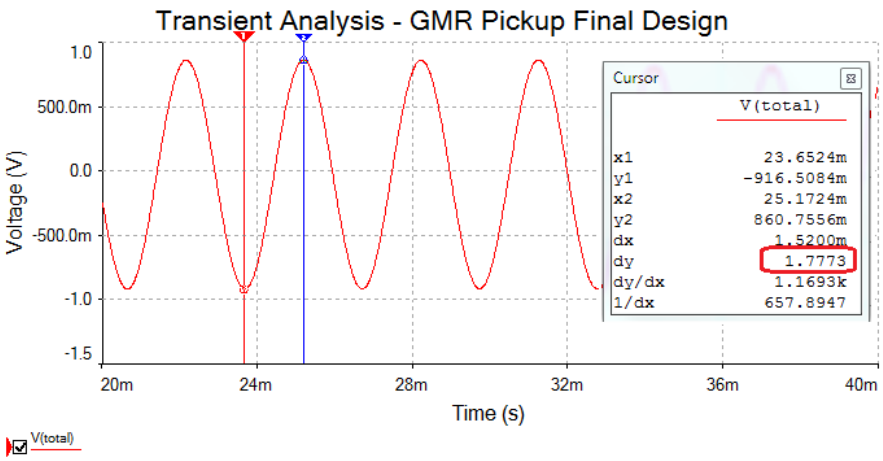

Figure 57: Result for transient analysis of final design

The expected V_{total} output was calculated to be

$$V_{total} = 300uVpp * 1000 * 6 = 1.8Vpp \quad (13)$$

The V_{total} output size of 1.7727V confirms that every part of the circuitry is working as expected. Moreover, the frequency response of the circuit was also simulated.

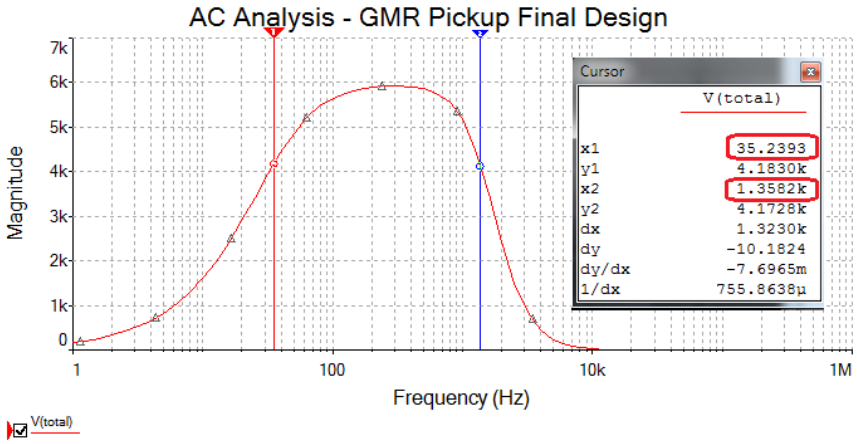

Figure 58: Result for AC analysis of final design

The two low and high cutoff frequencies were confirmed to be less than 82Hz and greater than 1200Hz, which is the guitar frequency range. Moreover, the gain of the circuit is also confirmed to be about 1000V/V per string circuit.

Designing the GMR Pickup Printed Circuit Board

Once simulation of the final design was successful, the PCB layout design was started. Access points to individual string output were also made available as output pins on the 1x10 header to allow for individual string tone, volume, and distortion control. Once the simulation part was completed, the correct device footprints were assigned to the components. Surface mount packaging was selected for all devices so that all 100 devices can be placed on a board area of approximately 1” x 3”, which is determined by the traditional inductive guitar pickup housing.

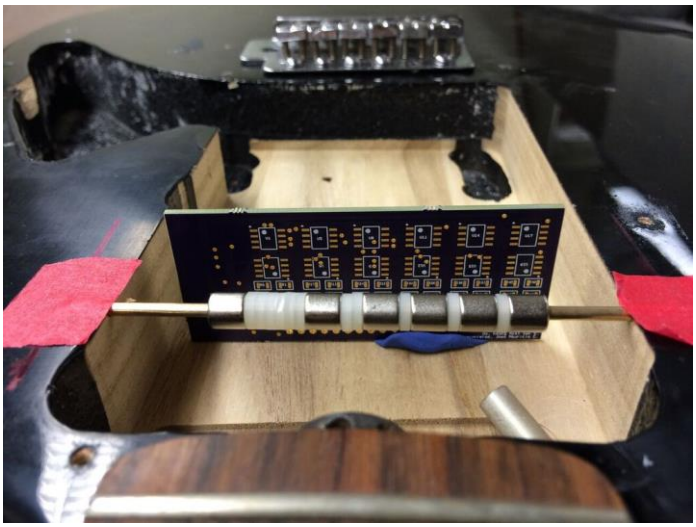

Figure 59: GMR PCB board placed in the pickup housing (Note: the housing was trimmed down to fit the PCB board)

The footprint for resistors and capacitors were chosen to be 0805 Imperial code, which provides both relatively small size and ease of manual-soldering capability. After that, the Multisim circuit was transferred to National Instruments rapid printed circuit board prototyping environment, Ultiboard. Since most of the circuitry was the same for each string, the PCB layout was designed to reflect the circuit schematics by grouping the components by string. In order to fit all the components on the limited board area, both sides of the two-layer PCB board, copper top and bottom, were utilized.

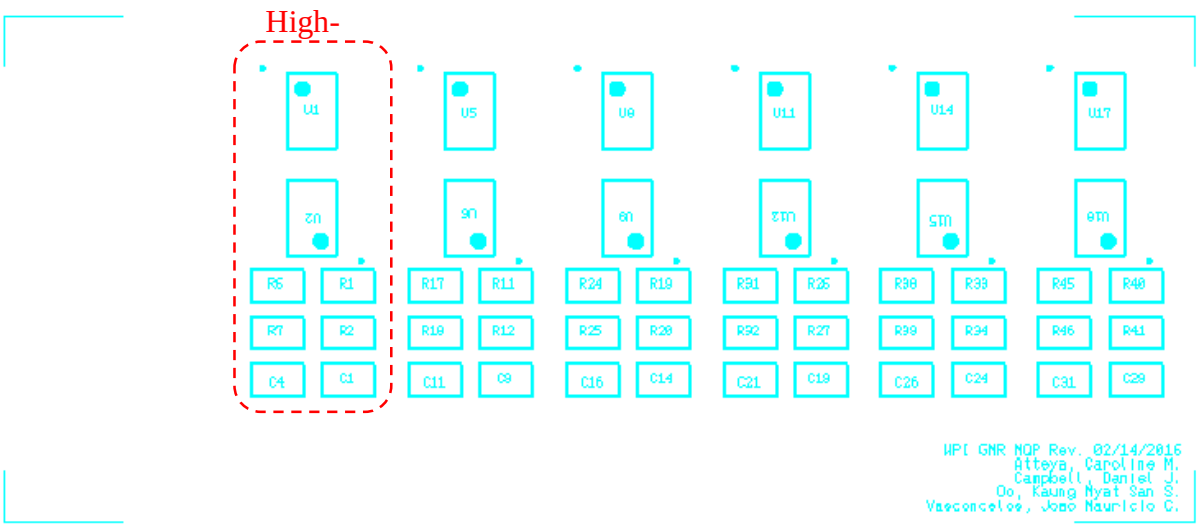

Figure 60: Silkscreen bottom of the designed PCB

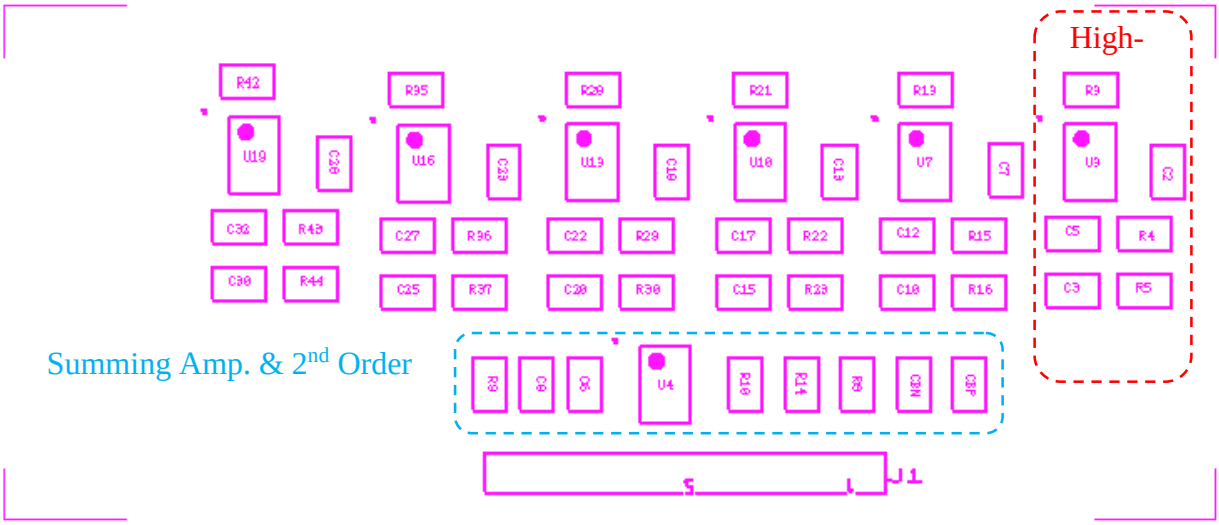

Figure 61: Silkscreen top of the designed PCB

After the components were placed in groups with respective to the strings, interconnecting traces (traces excluding VCC, GND, VEE, and output pin connections) were routed manually to achieve repetitive and recognizable layout pattern for each string since the auto-routing feature in Ultiboard does not follow the same routing pattern even with repeating component layouts. Once all the interconnecting traces were routed, the remaining traces, which are power and output traces,

were routed using the auto-routing feature. Even though manual-routing can achieve better PCB trace design, auto-routing was used for finishing up the remaining traces since the size of the board is small and the components are tightly placed. Moreover, manual-routing in this case would require more intensive labor and time investment in the PCB design.

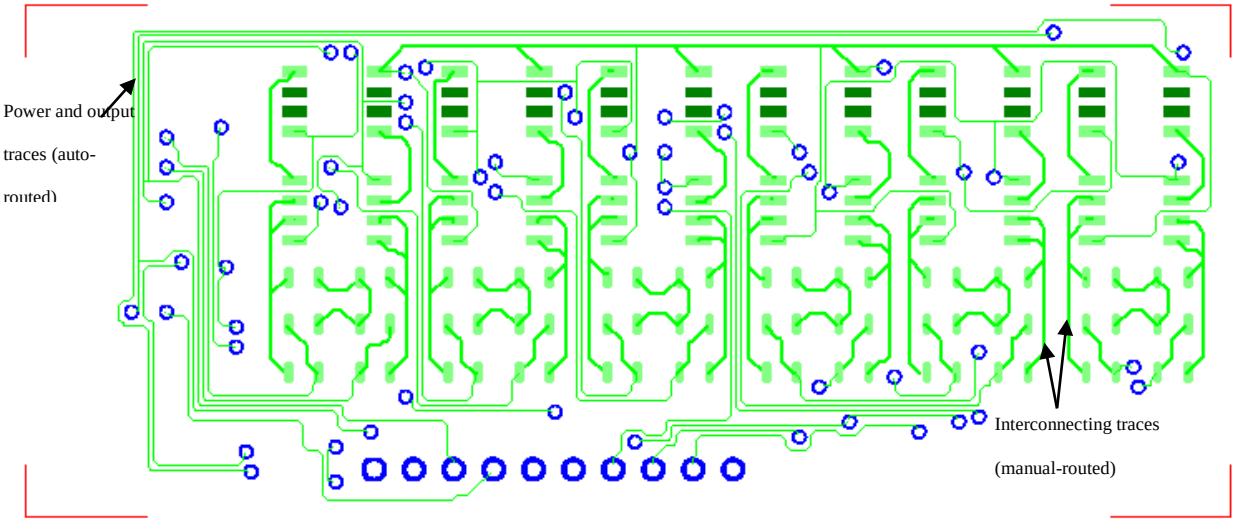

Figure 62: Copper top of the designed PCB

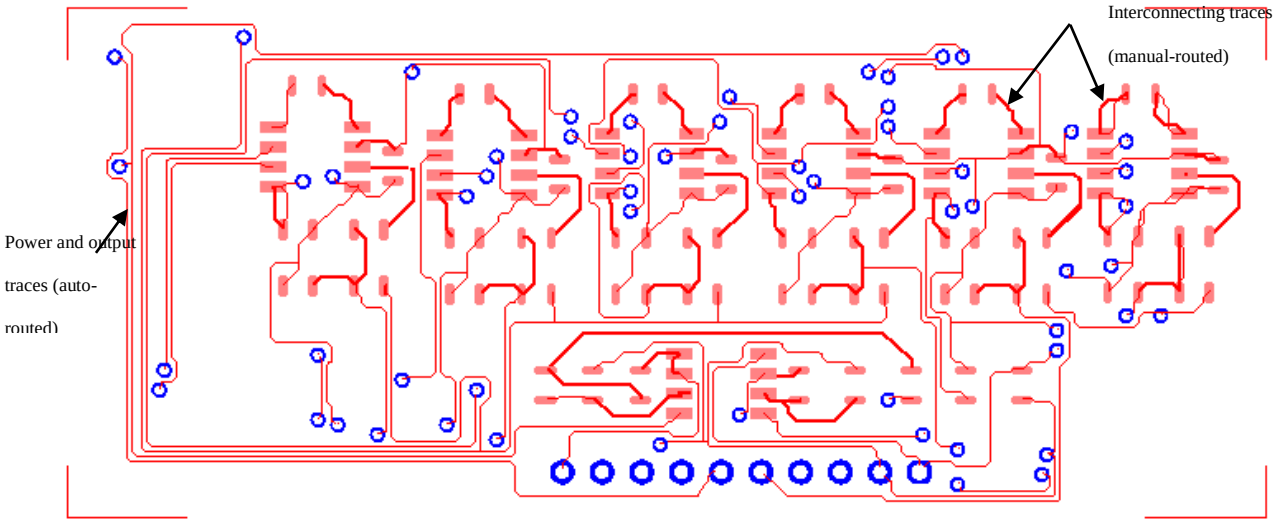

Figure 63: Copper bottom of the designed PCB

The first few attempts at auto-routing the remaining traces were not successful due to the tight placing of components. Therefore, the trace widths and trace tolerances were reduced to 6 mils, which is the minimum design rule specified by the PCB board manufacture of choice, OSH Park. With the new design specifications, Ultiboard was able to complete the auto-routing process for all the remaining traces. After the adding ground planes on both sides of the board and checking for connectivity errors, the finalized PCB layout Gerber files were sent out to the board manufacturer.

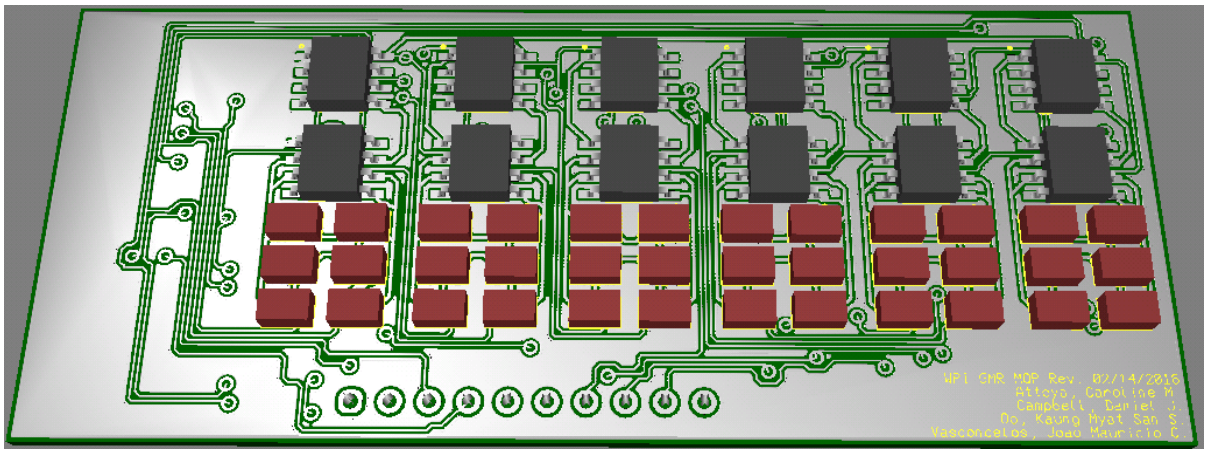

Figure 64: 3D rendering view of the designed PCB

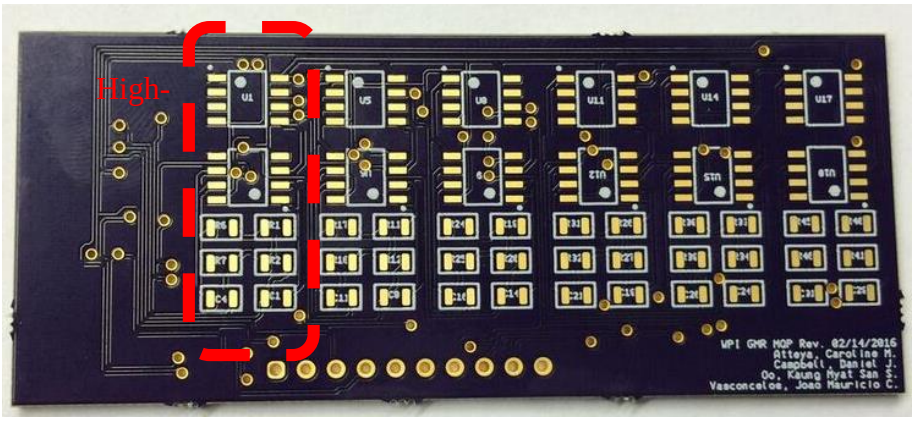

Figure 65: GMR pickup PCB board from OSH park - front view

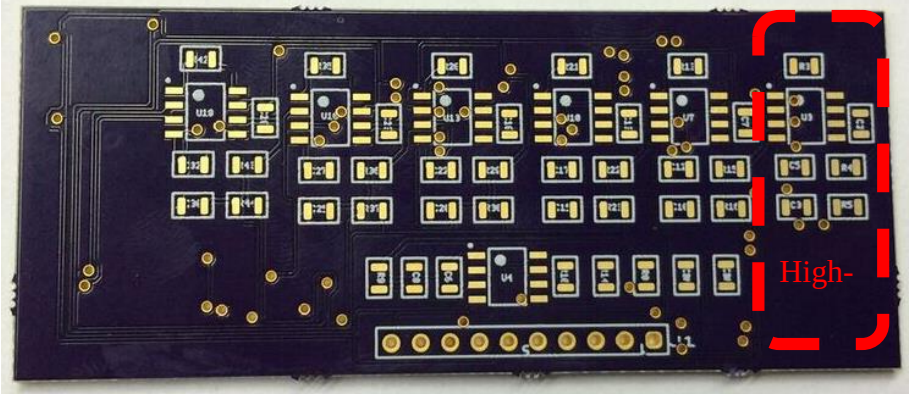

Figure 66: GMR pickup PCB board from OSH park - back view

PCB VCC and GND Short Issue

In order to allow ample time to conduct tests on the final GMR pickup PCB, the 'Super Swift' option was chosen by spending an additional $ 89 on top of the board cost, which reduces the turn time to 5 business days as opposed to 12 business days. The boards arrived in about one week including the shipping time, however, it was found that all three PCB boards were shipped with a manufacturing defect, a short between VCC and GND. Several attempts were made in hopes of locating the shorted connection and eventually, a rough location of the shorted connection was pinpointed after directly connecting a wall plug between VCC and GND of one of the boards, which burnt out the shorted connection along with a couple other VCC and GND traces. These burnt traces can be seen in Figure 67 (bottom right) which shows the PCB board that was subjected to the wall plug. Further email support from OSH Park confirmed that the burnt VCC trace under U3 was indeed the trace that connects VCC and the GND plane. One of the PCB boards was then salvaged by slicing the VCC trace under U3 and it was confirmed that the VCC and GND short bug was eliminated. However, doing so also resulted in disconnecting the VCC net from U3, which left the whole High-E string circuitry non-functional.

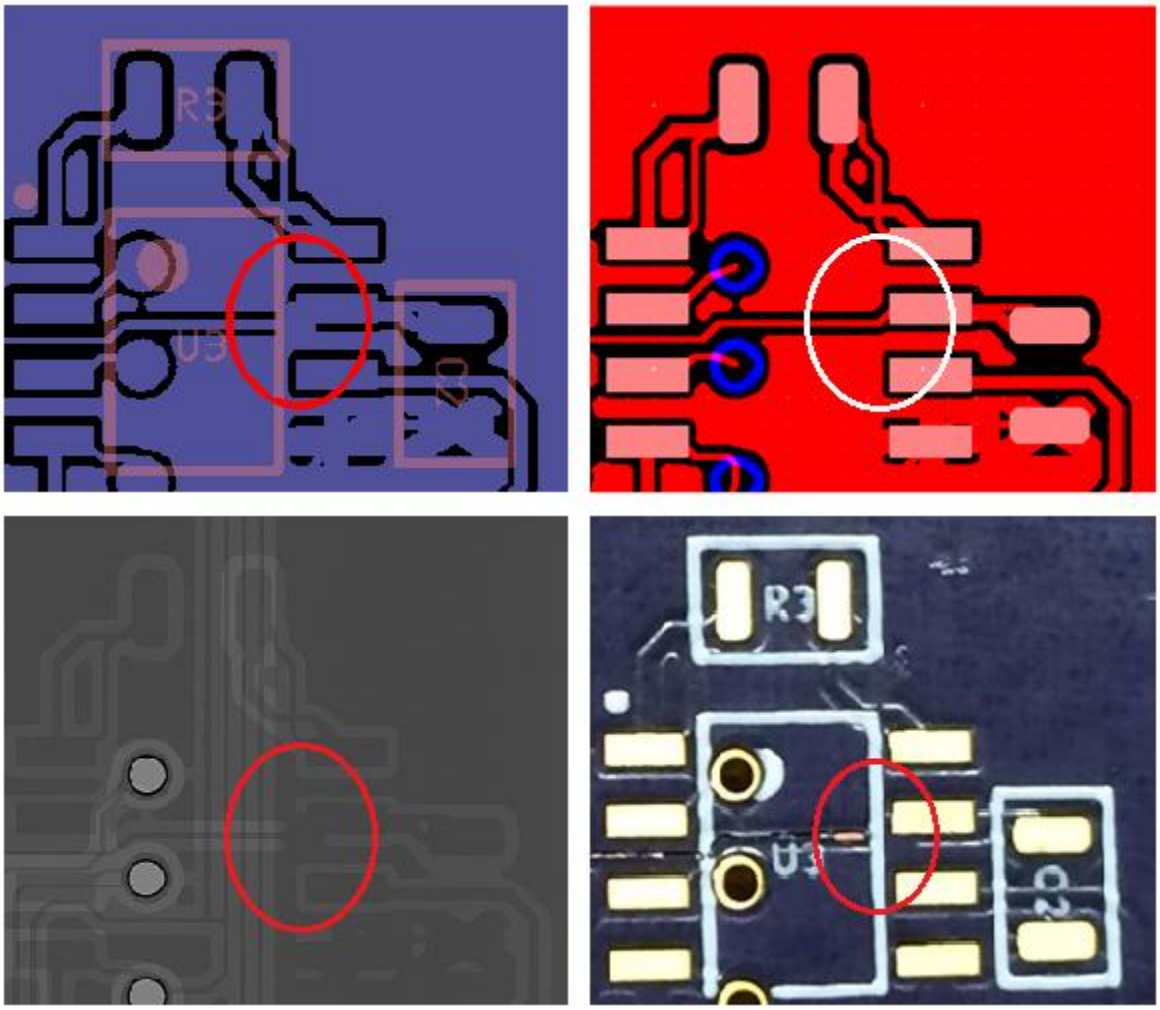

Figure 67: VCC and GND short connection location (top left - OSH park machine layout, top right - Ultiboard layout, bottom left - X-ray image showing the short connection, bottom right - OSH park PCB board subjected to AC wall plug)

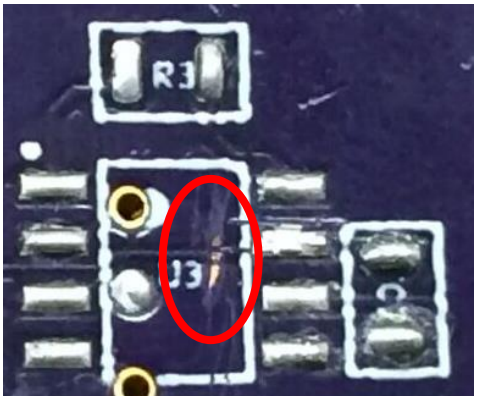

Figure 68: Salvaged PCB showing the sliced connection

GMR Pickup Testing Results

This section will discuss the results of testing the salvaged PCB with G and D string circuitries, non-inverting summing amplifier, and second order low pass filter. The equipment used in this testing included:

- Tektronix TDS 2004B Oscilloscope
- Tektronix AFG 3021 Function Generator
- GW INSTEK GPS-3303 Power Supply
- Agilent 34405A DMM

Ideal Magnet and Sensor Position and Orientation Relative to String

In order to achieve the best signal shape and size from the GMR pickup, the magnet and sensor orientation as shown in Figure 69 is used. NSN0548 magnet was placed such that the top part of the inner ring lies in a straight line with the top of the GMR sensor. The north pole of the magnet must be pointing away from the sensor at 180 degrees. The distance between the magnet and sensor is determined by the desired magnetic bias offset of the sensor, which directly determines the sensitivity of the sensor. The distance between the top of the sensor and the string should be less than 250mils in order to achieve a signal that is not distorted harmonically.

Since the current test fixture for holding the magnet and the circuit board in place was made using Play-Doh, the ability to repeat these tests for achieving a certain output signal size was limited. However, if the configuration shown in Figure 69 was followed closely, signal sizes ranging from $1V_{pp}$ to $4V_{pp}$ can be achieved for guitar frequencies less than 150Hz. For the final GMR pickup prototype, a 3-D printed adjustable fixture as shown in Figure 69 will be made.

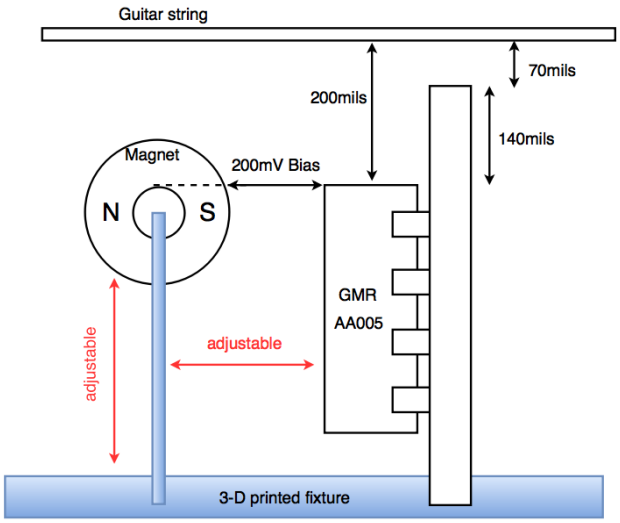

Figure 69: Magnet and sensor fixture footprint

Circuit Under Test

Figure 70 shows the PCB circuit that was used for testing. G and D string circuit components were soldered onto the salvaged PCB board to test the non-inverting summing amplifier. The different string circuit sections will be referenced as V_{out1} for high E string and V_{out6} for low E string in the following parts of this paper.

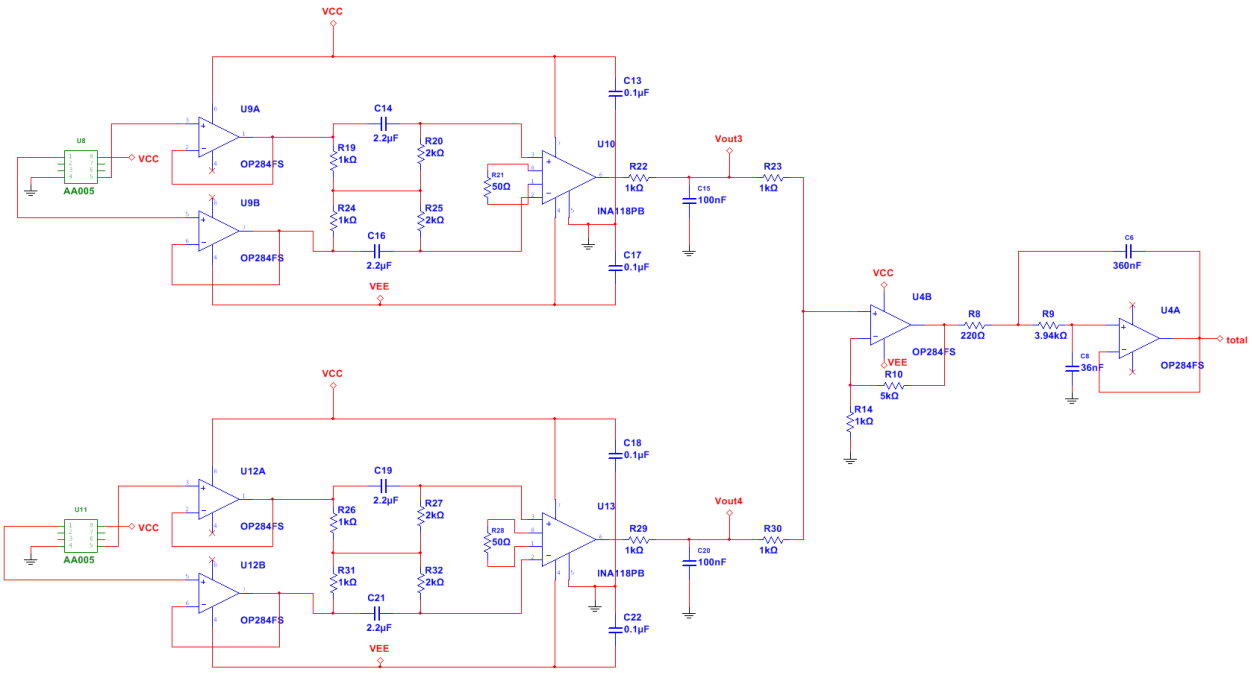

Figure 70: Schematic of the tested circuit (Note: R10 value was 1kΩ for the test circuit)

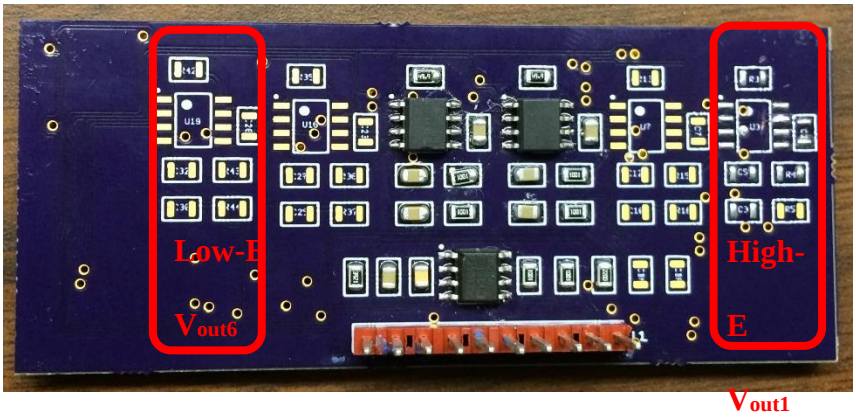

Figure 71: Tested circuit on the salvaged PCB

Signal Size

First, the G string was put onto the guitar and over the V_{out3} section of the PCB board. A round-hole magnet was then placed in front of the V_{out3} GMR sensor and the string was plucked

at a normal pace. Tektronix TDS 2004B four channel digital storage oscilloscope was used to capture the CSV waveform data.

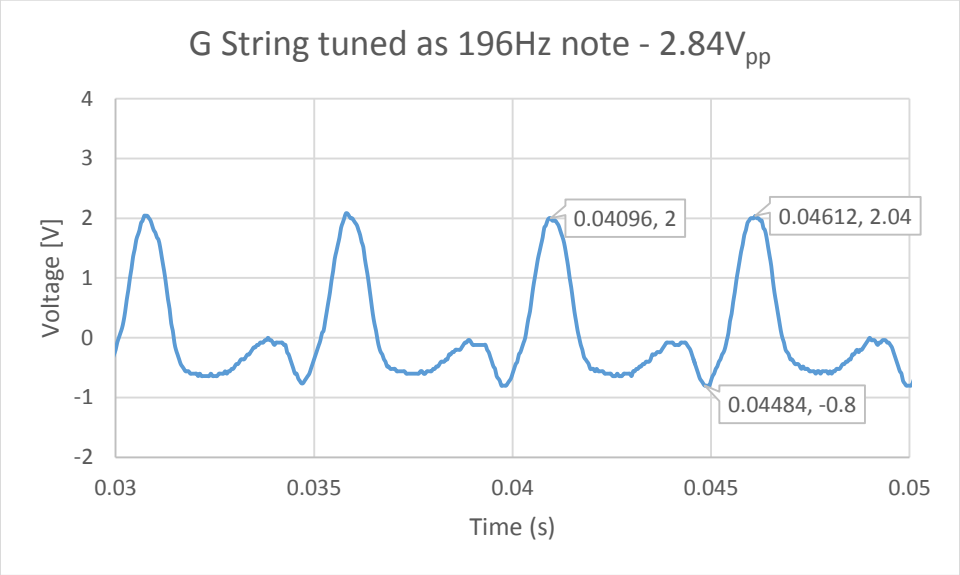

Figure 72: 196Hz note on G string

Next, the magnet was moved in front of the V_{out4} GMR sensor and the same procedure was carried out again with the low E string.

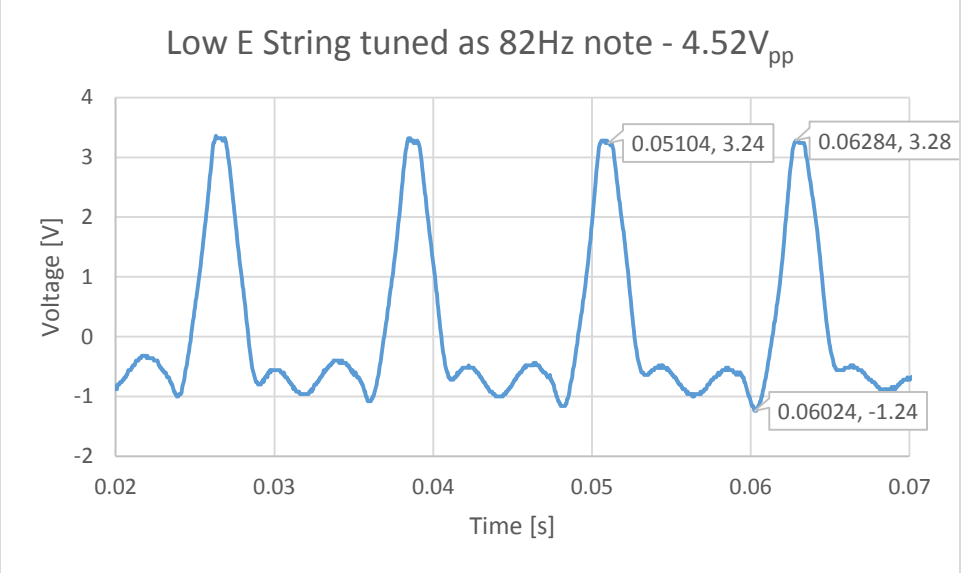

Figure 73: 82Hz note on low-E string

As can been seen from Figure 72 and Figure 73, the amplitude of the 196Hz note signal is much lower from that of the 82Hz note, which raises the question of having an unforeseen low pass filter action. Therefore, the high E string was put on the guitar replacing the G string and tested with the same magnet and sensor orientation that was used to test the other two low E and G strings. The high E string was first tuned as the open high E note with a frequency value of 329Hz, plucked, and recorded the waveform. Then, the same procedure was performed with that same high E string tuned as open B note with a frequency of 247Hz. The two resulting waveforms are shown in Fig 81 and 82.

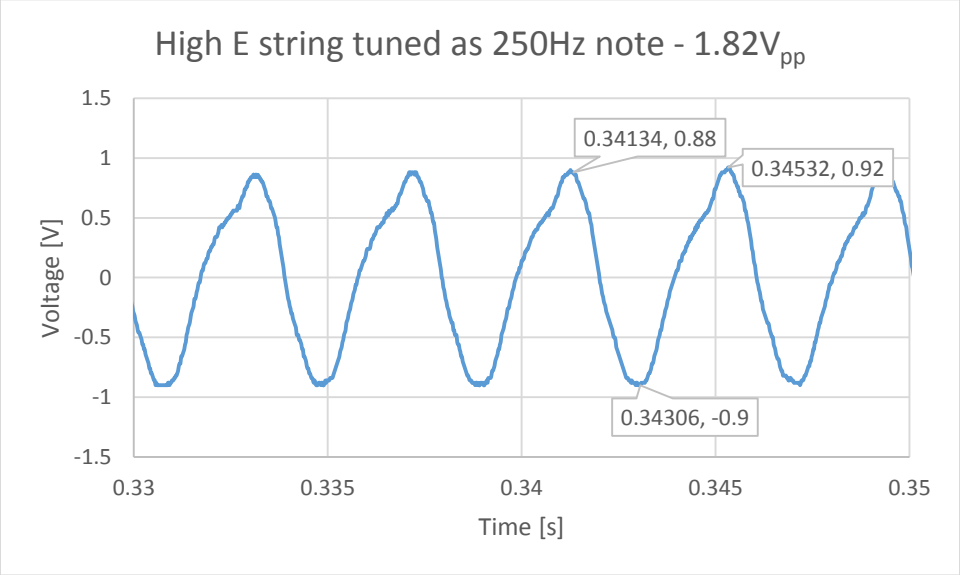

Figure 74: 250Hz note on high E string

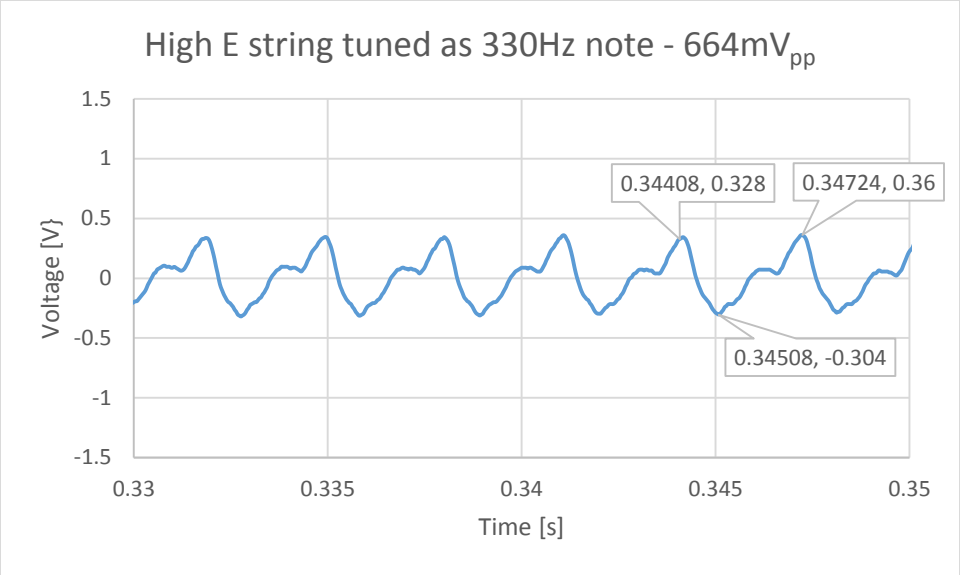

Figure 75: 330Hz note on high E string

It was observed that the signal size of the 330Hz note is only 632mV$_{pp}$, which is only 36% of the 250Hz note signal size of 1.78V. Since the only varying parameter in this test was the frequency of the high E string, the massive difference in signal sizes suggests that the frequency response of the PCB circuit could be incorrect. Simulating the frequency response of one string circuitry shows that the frequency response of the designed circuit is working as expected. Figure 77 shows the results of AC response simulation. Note that V$_{out1}$ circuitry was simulated instead of V$_{out3}$ but they are identical.

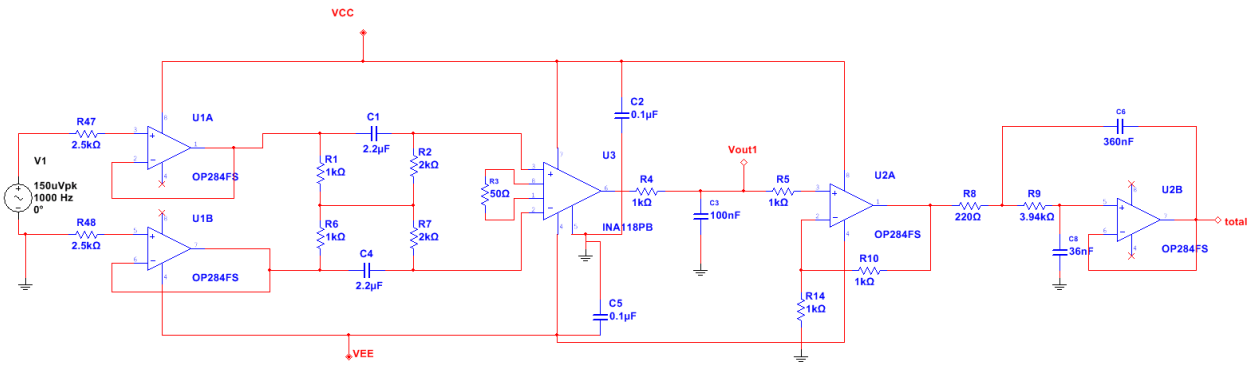

Figure 76: Schematic of the simulated test circuit

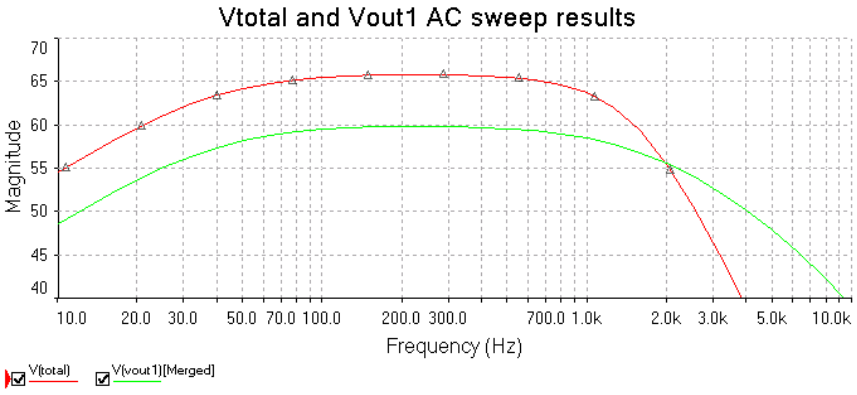

Figure 77: Simulated AC response of the test circuit

Therefore, frequency response of the PCB circuit board was again tested using a Tektronix AFG3021 function generator in the lab to ensure that the physical circuit board behaves in the same way as the simulated one. The V_{out3} GMR sensor was de-soldered and two thin wires were soldered to the inputs, which are pin 1 and 5 GMR pads on the PCB board. Since the lab function generator can only give a minimum of $20mV_{pp}$ signal whereas the gain of the circuit is 1000, a voltage divider circuit using 5kΩ and 13kΩ resistors was constructed to get a $5.5mV_{pp}$ signal, which becomes a $5.5V_{pp}$ signal after the in-amp gain of 1000, to avoid signal clipping. Figure 79 shows the measured AC response of V_{out3} circuitry.

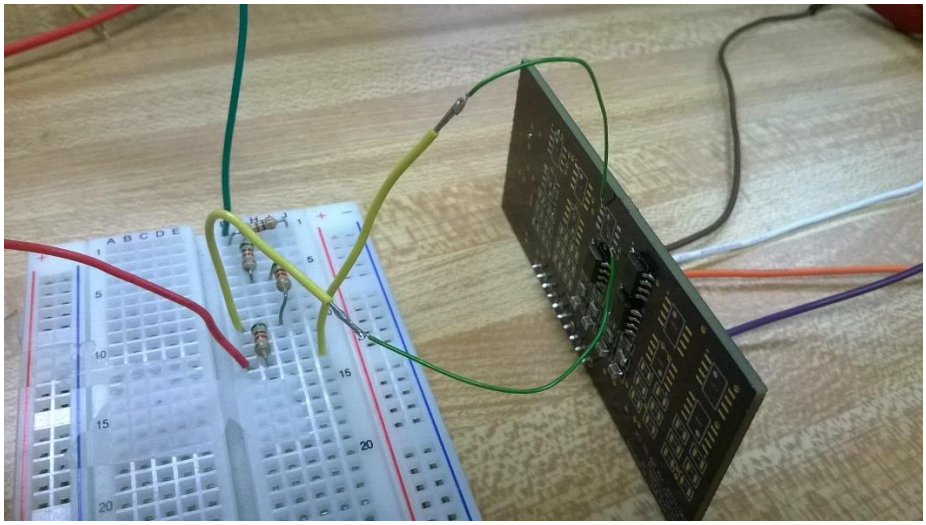

Figure 78: Testing the frequency response of the PCB circuit using function generator

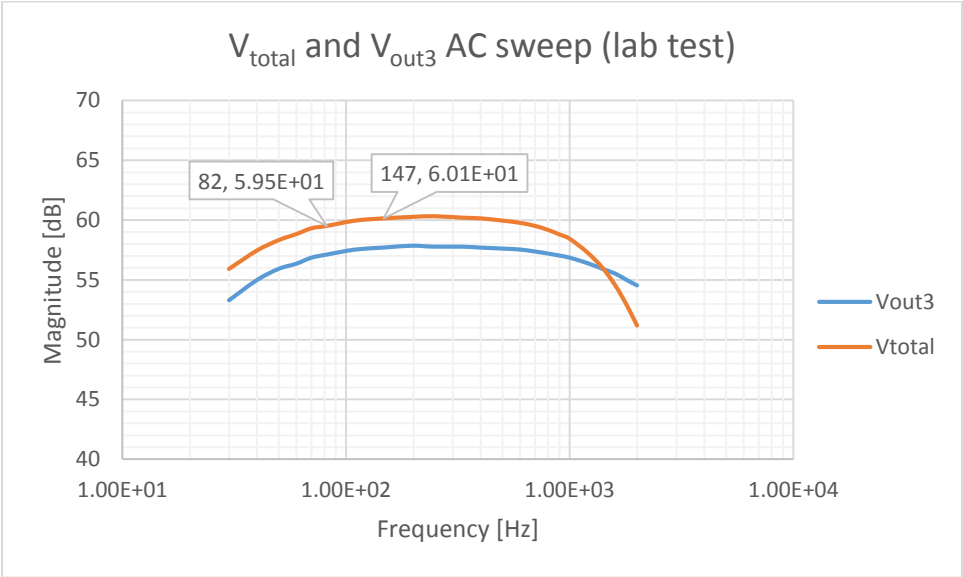

Figure 79: Measured frequency response of the PCB circuit

From Figure 79 and Figure 77, it is obvious that the measured frequency response of the designed circuit matches that of simulation with a relatively flat passband from 80Hz to 1000Hz. The measured flat band gain has approximately a 5dB discrepancy when compared to the simulated gain due to resistor, capacitor, and in-amp gain tolerances. However, the flat passband gain indicates that the GMR sensor, the only component that was omitted from the circuit during

this test, is responsible for picking up very different signal sizes for varying frequencies under 1kHz. The manufacturer's datasheet of the GMR sensor was then consulted again to confirm that the sensor is suitable for applications with frequencies up to and above 1MHz.

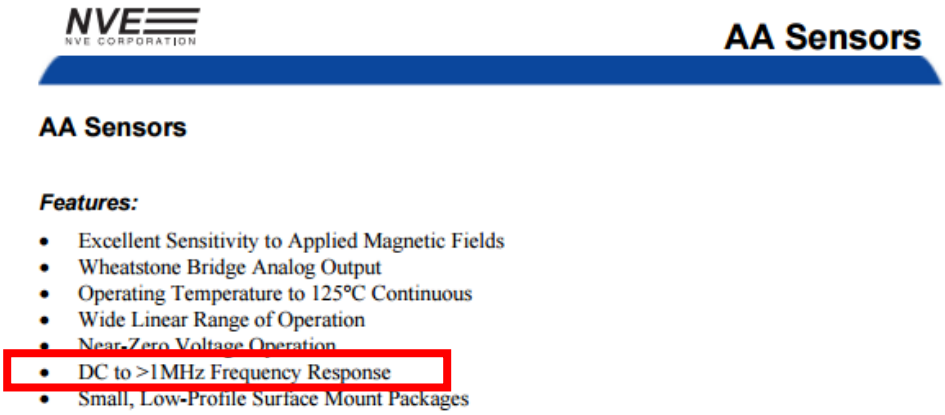

Figure 80: Frequency response of GMR sensor AA005 according to NVE, (Source: NVE Corporation)

Despite NVE's claim regarding the frequency response of the sensor, the lab tests show that the frequency response of AA005 might be severely corrupted starting at frequencies as low as 100Hz. Figure 81, Figure 82, and Figure 83 show three more scenarios of this issue where the low E string was used. In order to ensure that the only variable is the string frequency, the high E string was carefully replaced with low E string without affecting the clay fixture of the magnet.

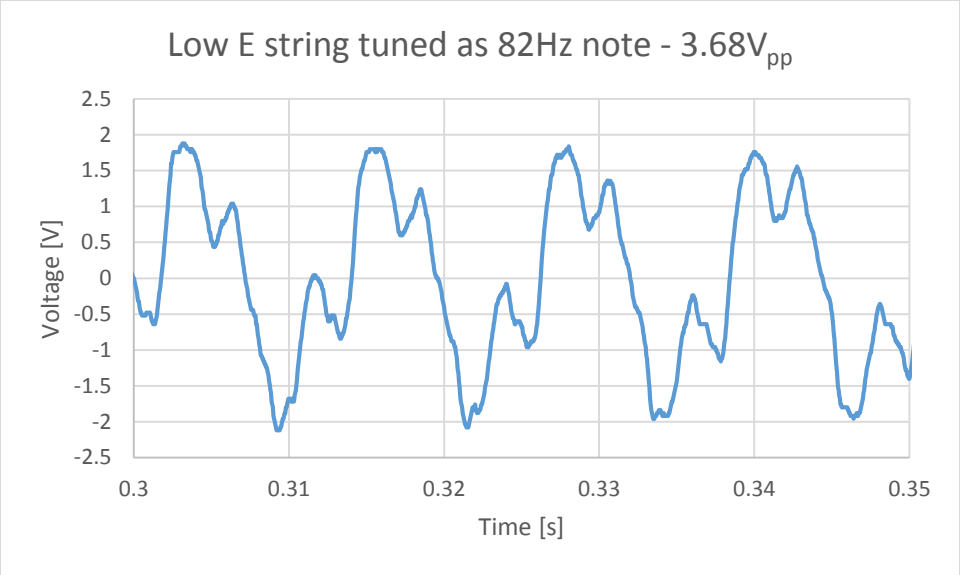

Figure 81: 82Hz note on low E string

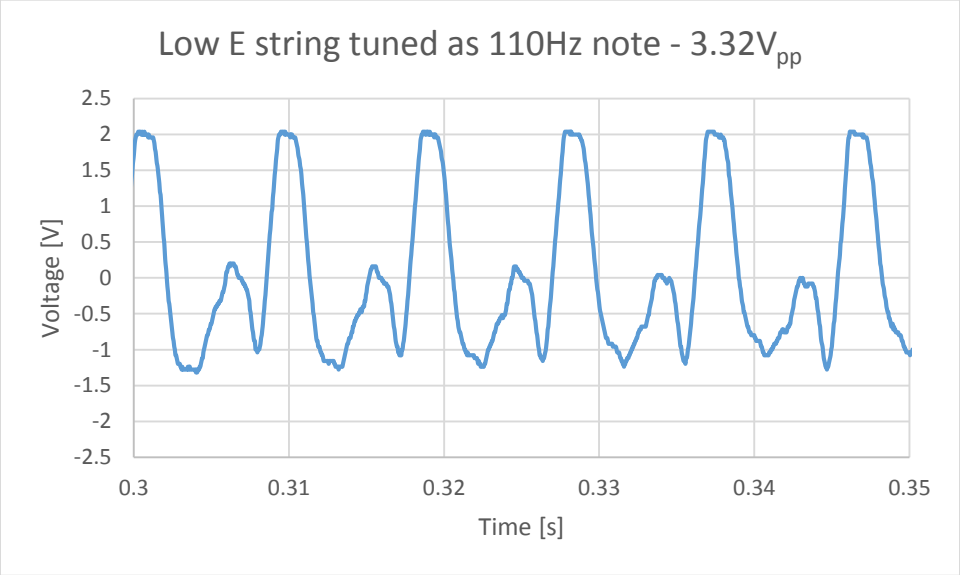

Figure 82: 110Hz note on low E string

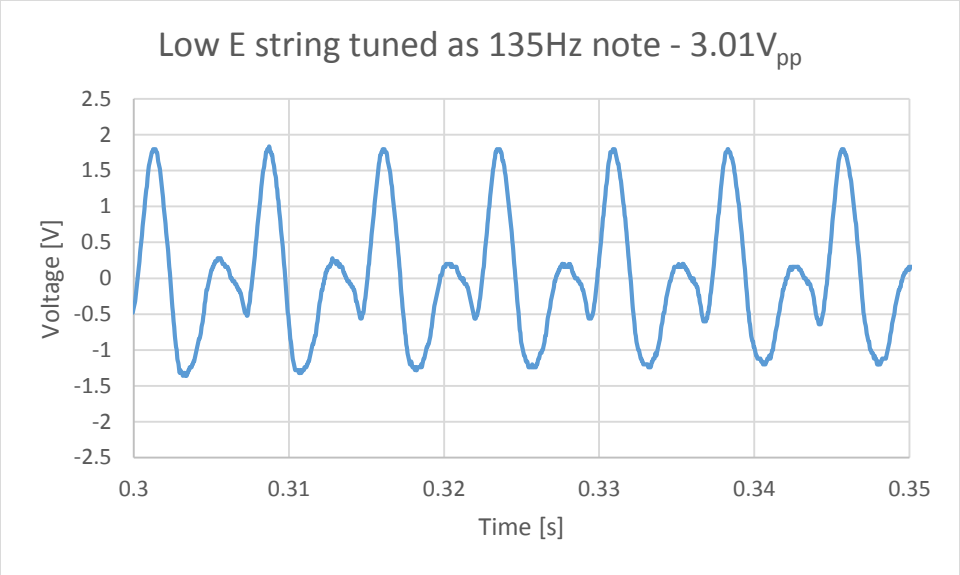

Figure 83: 135Hz note on low E string

Once again, the pattern of decreasing amplitude with increasing frequency was observed even though the frequency response magnitude of the rest of the circuit except the GMR sensor is slowly increasing from 59.5dB (82Hz) to 60.1dB (147Hz) as shown in Figure 79. This unforeseen severe low pass filter action of the sensor introduces a major setback on using this GMR sensor in the guitar pickup application. However, this issue can still be tackled by adjusting the in-amp gains of each individual string to achieve roughly equal amplitudes for all interested guitar notes.

The amplitude of the lowest guitar note (82Hz, $3.68V_{pp}$) is very massive compared with the typical output of a traditional inductive guitar pickup, which ranges from $100mV_{rms}$ to $1V_{rms}$ for high power output. Therefore, the gain of the low frequency strings will be reduced accordingly to achieve about $600mV_{pp}$ signal size for all guitar notes for the final prototype.

Noise

The noise of at the output access node V_{out3} and V_{total} were measured using the oscilloscope in AK227 lab. The noise data was also imported into MATLAB to compute the RMS noise value

as well as the spectrum of the noise. It was also observed that the output noise is lower amplitude and more similar to white noise when the sensor was not under the influence of the magnet and that some low frequency oscillations were witnessed when the sensor was near the magnet. Figure 84, Figure 85, Figure 86, and Figure 87 show the results of noise measurement at V_{out3}, V_{out4}, and V_{total}.

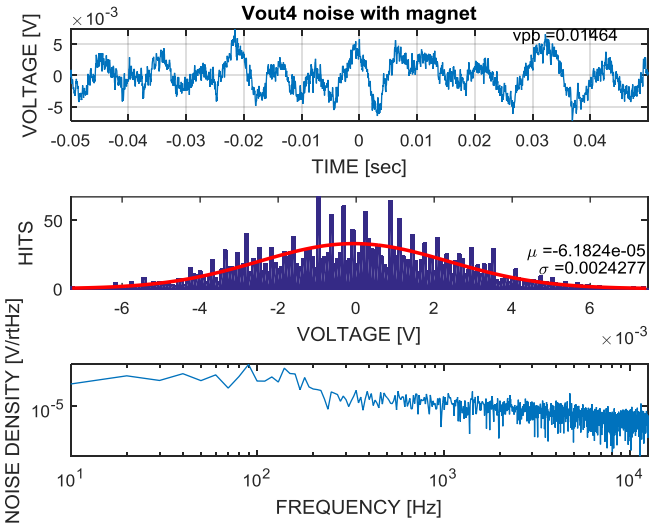

Figure 84: Output noise at V_{out4} node under magnet influence

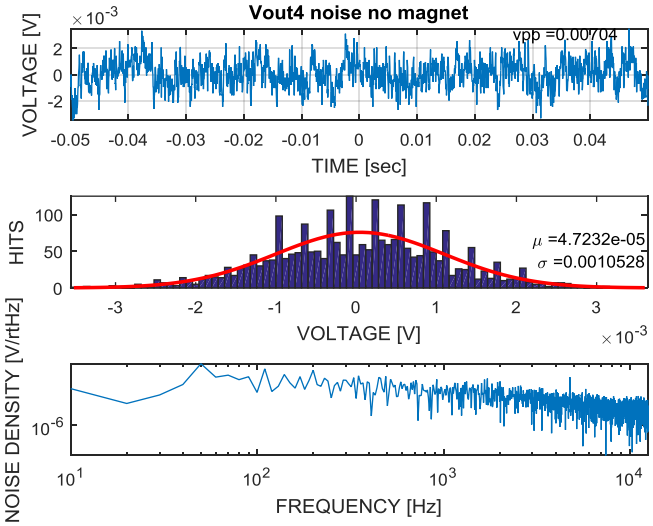

Figure 85: Output noise at V_{out4} without magnet nearby

V_{out3} output noise is also supposed to be the same as V_{out4} since all string circuitries are identical. However, in this case, the low pass filter capacitor after the in-amp was removed from the V_{out3} circuit and therefore, high frequency noise components were detected in the data collection. It is observed that the noise increased by $0.5115mV_{rms}$ when the low pass filter after the in-amp is not present.

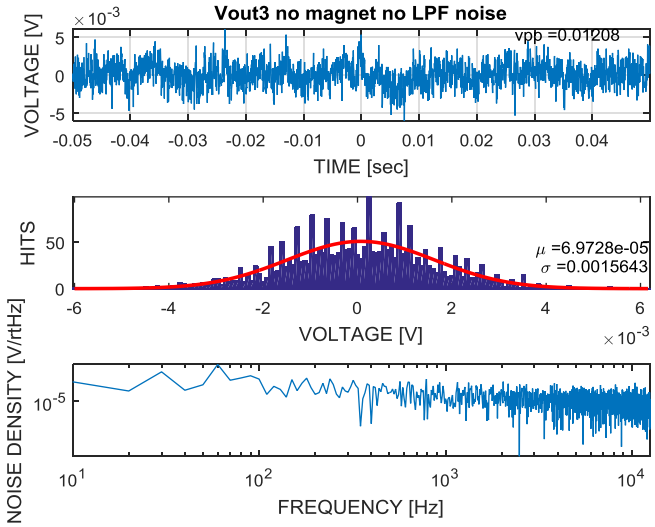

Figure 86: Output noise at V_{out3} without magnet influence

V_{total} output noise, which is the sum of V_{out3} and V_{out4}, was also measured and it was observed that the noise does not differ much from V_{out3} noise.

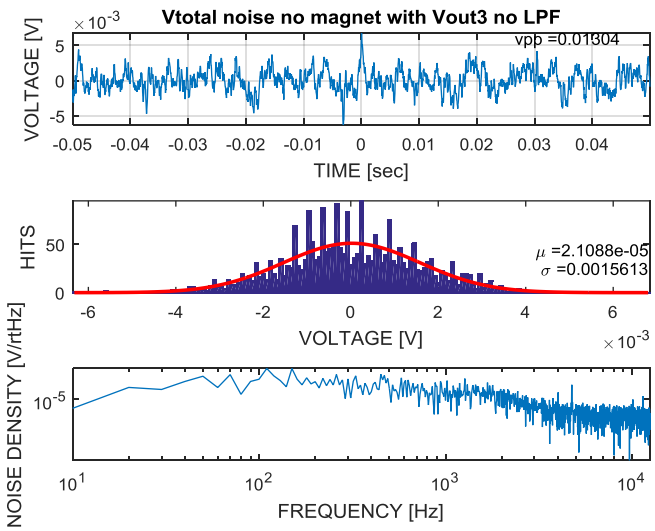

Figure 87: Output noise at V_{total} without magnet nearby

Moreover, V_{out3} noise without the GMR sensor was also measured by grounding the inputs. The V_{out3} GMR sensor was de-soldered and two thin wires were soldered to the inputs, which are pin 1 and 5 GMR pads on the PCB board.

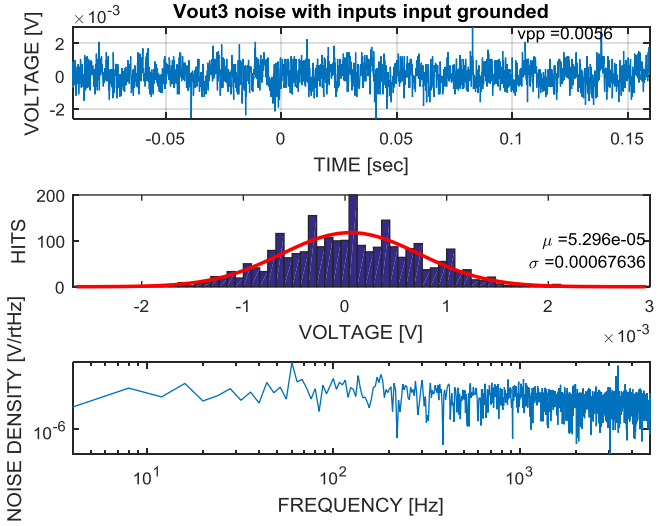

Figure 88: Output noise at V_{out3} without the GMR sensor and with inputs grounded

Comparing Figure 88 with V_{out4} output noise without magnet influence as seen in Figure 85, it was observed that the GMR sensor itself adds about 0.376mV_{rms}, which is 36% of the total V_{out3} noise.

Signal-to-noise Ratio (SNR)

After the signal amplitude and signal noise data were collected, the SNR of the GMR guitar pick for one string was calculated using the following equation

$$SNR = 20\log(\frac{Vsig_{rms}}{Vnoise_{rms}}) \quad (14)$$

Taking the largest signal size observed during the tests and the RMS noise without magnet influence, the highest achievable SNR was calculated to be

$$SNR = 20\log\left(\frac{4.52Vpp * 0.3536}{1.0528mVrms}\right) = 63.6dB \quad (15)$$

However, due to the unreliable frequency response of the GMR sensor AA005, the SNR value in Equation 13 holds true only for guitar note frequencies below 130Hz. For the high frequency guitar notes starting at 330Hz, the SNR drops down to

$$SNR = 20\log\left(\frac{664mVpp * 0.3536}{1.0528mVrms}\right) = 47dB \quad (16)$$

Offset

It was observed that the offset at V_{out3} to be about 4.5mV while the offset at V_{out4} to be about 19mV. With a gain of 1000 at the in-amp stage and without high pass filters at the end of the in-amp, an offset of 19mV is considered to be very small. Assuming that 19mV to be the worst case offset, the maximum offset voltage at V_{total} is calculated to be about 114mV, which could still

be considered to be acceptable since it does not impact the operation of the circuit with +5V and -5V supply rails. Note that the V_{out3} offset data was collected without the 1.6kHz low pass filter after the in-amp and therefore, contains more noise than the V_{out4} waveform.

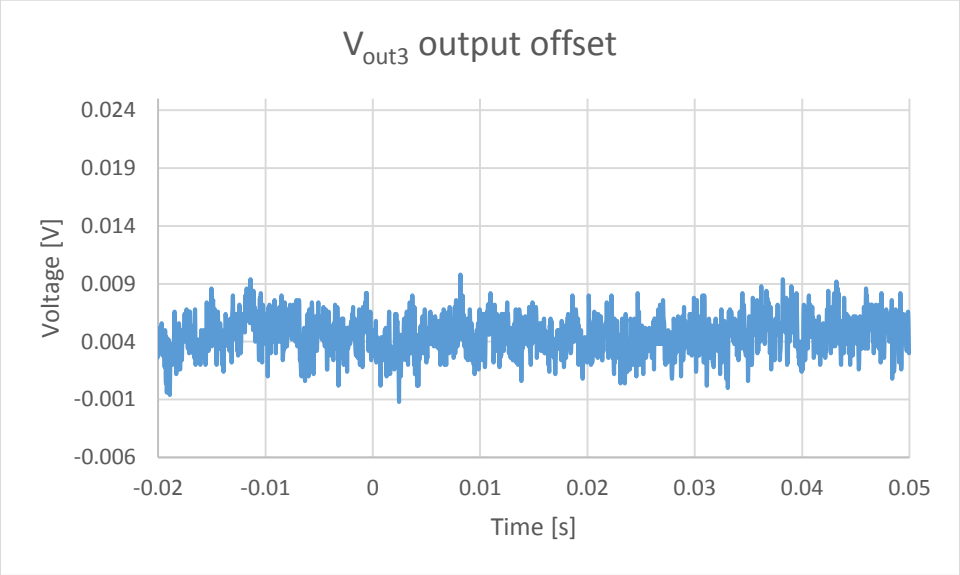

Figure 89: Output offset at V_{out3}

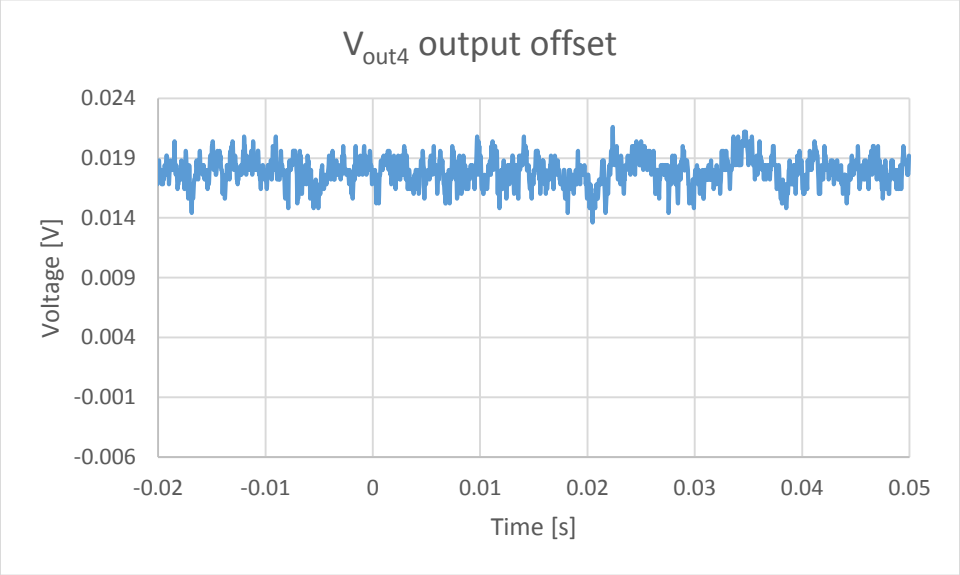

Figure 90: Output offset at V_{out4}

Power Consumption Using ±5V Supplies

Using Agilent 34405A $5^{1/2}$ Digit Multimeter, the current draw of the test PCB circuit board was measured.

Table 3. Measured current draw of the test PCB board

Path	Current
5V supply	8.84mA
-5V supply	-7mA
GND	-1.84mA

Table 4. Max current draw (datasheet) calculation of test PCB board

Parts	Count	Max Is/part (from Datasheet) [A]	Total [A]
AA005	2	5.00E-04	1.00E-03
OP284	6	1.45E-03	8.70E-03
INA118	2	3.50E-04	7.00E-04
		Total	1.04E-02

From Table 3 and Table 4, it was observed that the total measured current draw for the test PCB was 8.84mA with the calculated maximum current draw according to the datasheets being 10.4mA.

Table 5. Max current draw estimation for complete PCB board (all 6 strings)

Parts	Count	Max Is/part (from Datasheet) [A]	Total [A]
AA005	6	5.00E-04	3.00E-03
OP284	14	1.45E-03	2.03E-02
INA118	6	3.50E-04	2.10E-03
		Total	2.54E-02

For the complete circuit with 6 strings, the total current draw was estimated to be 25.4mA. Using a 9V 550mAhr battery as the supply, the battery life of the GMR pickup was calculated to be 21.65 hours. The final prototype will use ADA4084, which has the same noise spec ($3.9\frac{\text{nV}}{\sqrt{\text{Hz}}}$) as OP284 but draws only 0.6mA as opposed to 1.45mA, resulting in an expected battery life of 42 hours. Furthermore, if low power operation is required, low power low noise op-amps such as AD8622 can be used, which will provide a battery life of 69 hours for a small tradeoff in noise.

Hall Effect Pickup

In this section, the methodology and results for characterizing the Hall Effect sensor is presented. For the Hall Effect Sensor sensor, the specifications of the part used are included and the circuitry used for testing is discussed. Afterwards, simulation and testing results are presented.

Methodology

This section outlines the design of the Hall Effect pickup. The process included filter design, selection of amplifiers, and the design of a battery power supply.

Hall Effect Sensor Behavior

In order to fully understand the performance of the GMR technology in a guitar pickup application, similar tests have to be conducted on the technology that currently dominates the market: the Hall Effect. Comparing the GMR technology to the Hall Effect technology will provide better grounds to determine how suitable these technologies are to the guitar pickup application and, most importantly, how sensitive they are. Thus, the following experiments are dedicated to the study of the Hall Effect technology in a guitar pickup application. Further tests were conducted to evaluate the circuit required to power and amplify Hall sensor's signal.

Design of Test Circuitry

First, the team designed the circuit for the Hall Effect Sensor for basic tests to understand the behavior of the sensor before designing a more complex sensor. The datasheet of the sensor, part number A1324, describes the sensor as a linear, analog magnetic-field sensor with a constant DC-bias of 2.5V. Thus, the first efforts in the circuit design were to eliminate this DC-bias such that only the variable signal-output was amplified. A simple high pass circuit, capacitor and

resistor, was chosen to chop off the DC-bias. In order to lower the corner frequency, a large resistor had to be used (1MΩ). Yet, resistor R1, from the circuit diagram in Figure 91, imposes a risk due to the op-amps' bias current. This bias current could be amplified and jeopardize the signal. Fortunately, the bias current is very small (in the low nA range), which means that the input bias voltage is in the low mV range. Since the amplification of the circuit is 5 V/V, this bias doesn't have a major effect in the output signal. In Figure 91, the output signal is represented by pin 6 of the op-amp.

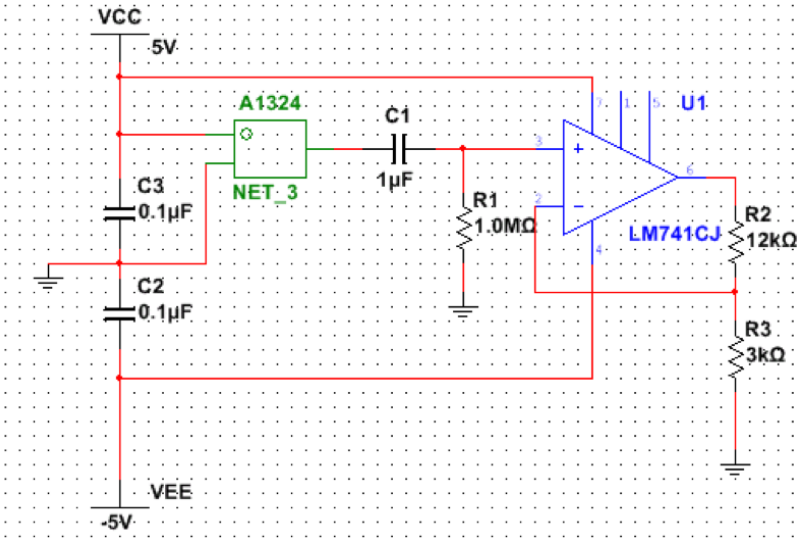

Figure 91: Schematic for Hall Effect Test Circuit

Testing for Saturation

The device's datasheet claims that device will saturate once a strong magnetic field is detected by the sensor. Thus, a weak magnet was used to check whether the sensor would saturate and then the results were compared to a stronger magnet. It was clear that the device didn't saturate with the 'weak' magnet because, once the 'strong' magnet was used, the output waveform hit either one of the output rails (0V or 5V). Figure 92 shows the output from the experiment with the

‘strong’ magnet. These tests were valuable for the understanding and the verification of the validity of sensor’s operation. The output waves were taken at the output of the sensor and at the output of the op-amp, pin 6.

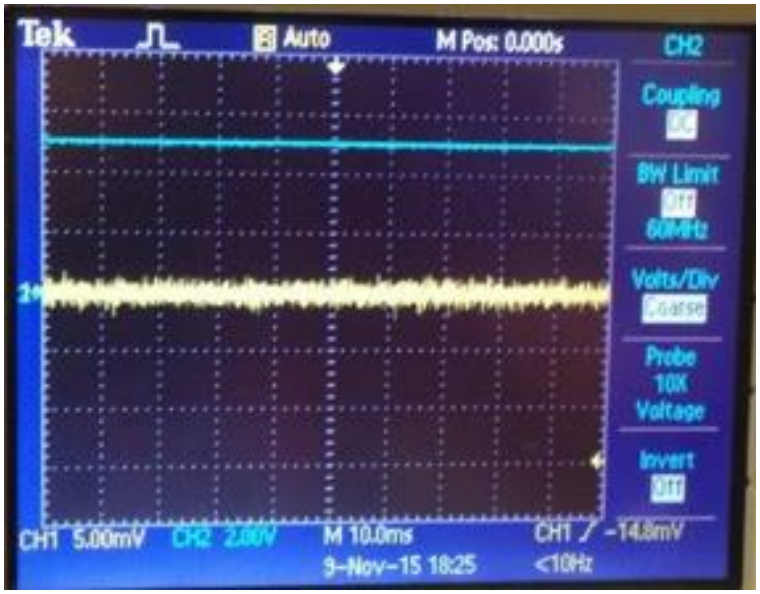

Figure 92: Output Waveforms resulting from saturating the sensor

Notice that there are two output waves in Figure 92. CH2’s signal represents the waveform at the output of the Hall Effect sensor. CH1 is the signal at the output of the op-amp. Since the device is saturated, there is only a DC signal. Capacitor C1 decouples the DC signal from any AC waveform, and therefore the output of the circuit is 0V, while the output of the sensor is 5V. If the magnet used to bias the sensor were flipped, i.e. change the polarity of the field, the output from the sensor would be saturated at 0V. This information helped us to determine the magnet that should be used in our application. It is necessary to have a large dynamic range and that there is no way the signal will get cut off by the rails.

Testing with Guitar String

The following figure shows the setup used to test one of the strings in the guitar. Notice that the sensor is sitting on top of the magnet from the inductive pickup. This is one of the 'weak' magnets that did not saturate the device even when it was in contact with one of the magnets faces. Further notice there is nothing else in the guitar except for the string and the magnets used for the inductive pickup.

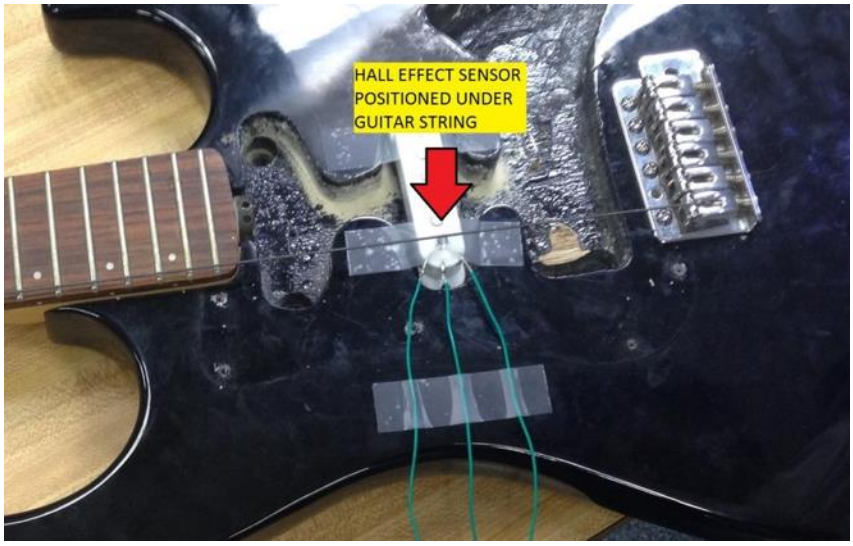

Figure 93: Testing Setup for Hall Effect Sensor

Figure 94 shows the output waveform once the lowest frequency string (82.4 Hz, when in tune) is plucked. Notice that the signal in CH1 of Figure 92 does indeed represent that of guitar string. This signal has been filtered and therefore only shows the variable signal from the guitar. The other signal, CH2, represents the output with the DC-bias. Since the wave in CH1 is so small, without the amplification, it can't be visually detected riding on CH2's wave. Even though the signal is in the tens of millivolts, this signal should be large enough to be connected to a guitar amplifier and audible. This signal is comparable to the one in Figure 95 in which the oscilloscope was connected to the output of an electric guitar using its regular inductive pickups. The signal of

the inductive pickup is obviously over ten times larger. Yet, the signals are both large enough to be plugged to an electric guitar amplifier and/or tweaked to attain larger signal values. Two different strings were used for the experiments below. This is the reason for the difference in signal frequency (both frequencies are highlighted).

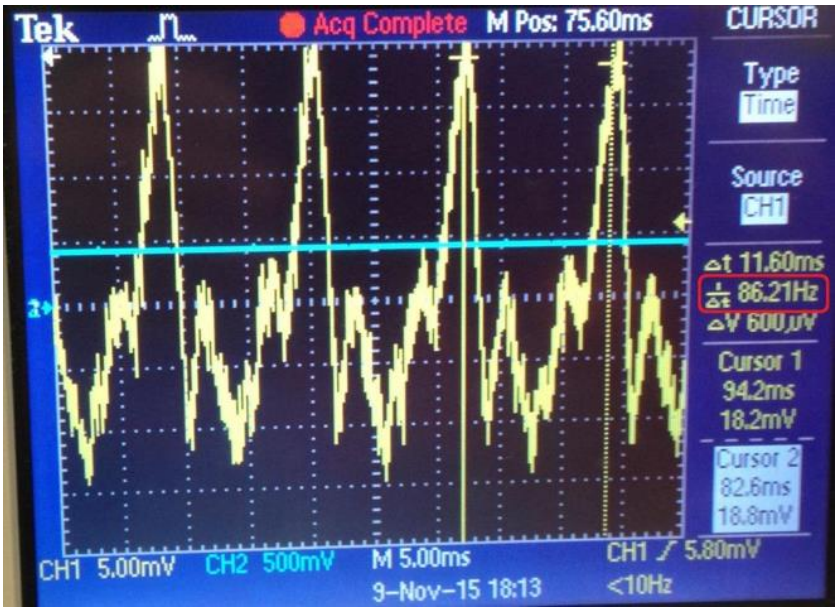

Figure 94: Output Waveform from Hall Effect Sensor Pickup

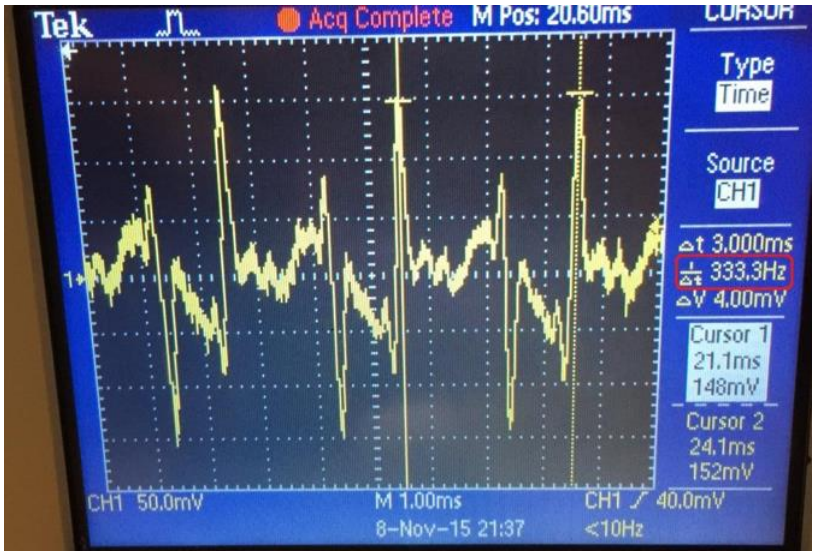

Figure 95: Output Waveform from Inductive Pickup

Circuit Design

The approach used in the design of the circuit for the Hall Sensor guitar pickup followed an intuitive track. Even though there were several iterations of the design, the fundamental stages of the circuit – power supply, sensors, filtering and amplification – were always present in the design. Other stages were added gradually in order to augment the quality of the signal over noise, while others were modified in order to fit the best characteristics of the circuit.

Filter Design

Filtering is an essential building block to electronic circuits in any application that involves sound. Bandpass frequency filtering is an easy and effective way of greatly reducing noises and other types of interferences that might affect the quality of the sound. While filtering has some desirable advantages, it also comes with some drawbacks. Most advantages are specific to the decay in magnitude of "unwanted" frequencies outside of the spectrum that can be played by the guitar. Disadvantages, on the other hand, are multiple. First off, filtering, more specifically, bandpass filtering certainly affects the magnitude of the signal throughout the spectrum of frequencies played by any string. Filtering also requires the addition of many components to the circuit. Even for first order filters, two components have to be used per filter, capacitor and resistor, for simplicity. Nonetheless, filters make the circuit less susceptible to disruptions in the signal and annul undesired DC-biases. When placed in the active bandpass configuration, they reduce the number of components by providing the necessary gain and take advantage of the buffer properties of the op-amp.

Filtering was uniquely designed on a string to string basis. The thought process was to reduce as much as possible the spectrum without interfering in the lowest or highest frequency

attainable in each string. For that, a coefficient, between 0 and 1, was selected that corresponds to the magnitude of the transfer function. For the highpass filter, which affects the lower frequencies of the string, 0.8 was selected, and for the lowpass, which affects the higher frequencies of the spectrum, 0.75. For instance, the lowest frequency for the D-string in a guitar (the 4th string from the bottom up) is 146.83Hz. Thus, the magnitude of the transfer function at that frequency is 0.8. This means that the cutoff frequency is 110.12Hz. Whereas the highest frequency on a 22-fret guitar is 523.25Hz. The magnitude of the transfer function at that point is 0.75, consequently, the cutoff frequency is 593.31Hz. All of these are represented on Table 6.

Table 6: Highpass and lowpass frequency cutoffs (22-fret guitar)

String	Highpass [Hz]	Natural Low [Hz]	Natural High [Hz]	Lowpass [Hz]
E - 6th	61.8075	82.41	293.66	332.979
A - 5th	82.5	110	392	444.486
D - 4th	110.1225	146.83	523.25	593.310
G - 3rd	147	196	698.46	791.979
B - 2nd	185.205	246.94	880	997.826
e - 1st	247.2225	329.63	1174.66	1331.939
All Bands	61.8075			5000
Highpass Coeff	0.8			
Lowpass Coeff	0.75			

There are primarily two reasons for the choice of these coefficients. First, lower frequencies in each string are more commonly played than the higher frequencies. In other words, the first half of frets (from the 0th fret to the 12th fret) is used more regularly. Hence, the disparity in coefficients. Also, many guitarists decide to tune down or tune up their guitarists. This affects the frequency range of each individual string. Thus, a higher magnitude for the transfer function provides some room for other types of guitar tuning.

Amplification and Signal Summation

Another very important feature of circuit design is amplification. Due to the sensitivity of these sensors and their small output signal, amplification at an early stage of the circuit is indispensable. Figure 96 depicts the circuit schematic that was used in this project. Notice that one single op-amp is used for two signals: the first signal coming from UD, which is the Hall Effect sensor for the D-string, and the second one for UG, the sensor for the G-string. The OPA1652 is a low-noise op-amp used in musical applications. It also contains two op-amp circuits inside the package, which reduces the number of components on the board.

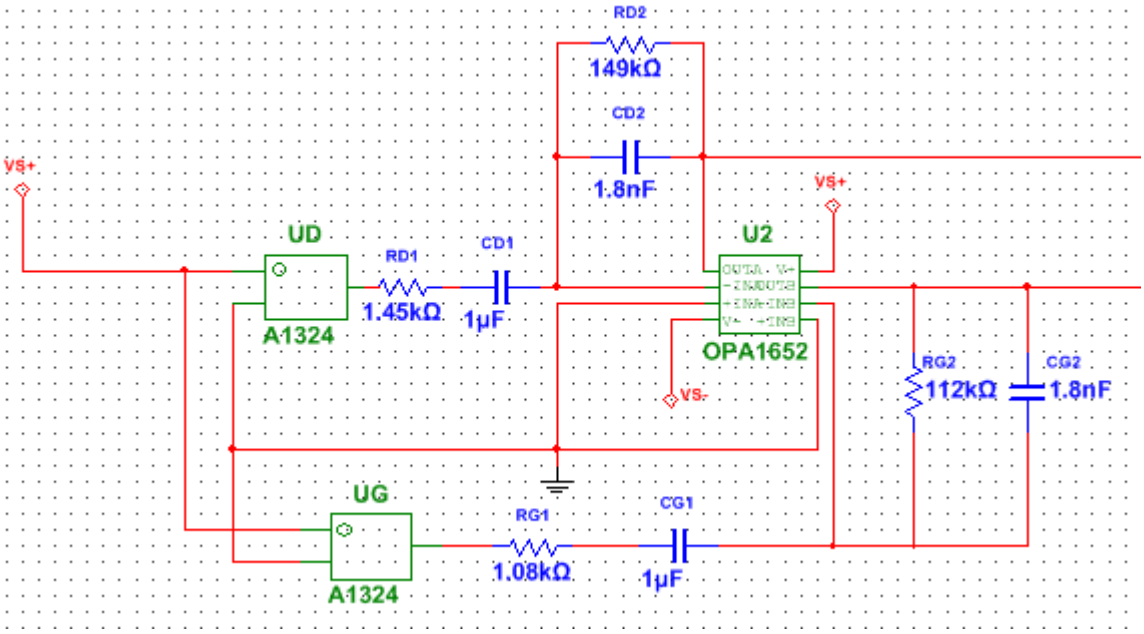

Figure 96: Schematic for two sensors: filtering and amplification

From the active bandpass filters in Figure 96, the gain from each string can be approximated to 100 (149kΩ/1.45kΩ = 102.76 and 112kΩ/1.08kΩ = 103.70). This relatively high gain is necessary in order amplify the signal to a level that is comparable to that of inductive pickups – in the order of hundreds of millivolts. It is necessary to maintain this condition similar to inductive pickups, because guitar amplifiers are fabricated for inductive pickups. Thus,

adjusting the output range prevents issues with the volume of the guitar amplifier. High gain, however, imposes another risk – clipping of signal. In order to compensate the high gain and level all of the signals out, a summing amplifier was utilized in order to connect all of the signals and level out all of the gains by the same factor, $\frac{R_S}{R_i}$. Here, R_S corresponds to the feedback resistor between the summing amplifier and the inverting input of the op-amp and R_i refers to the parallel resistors to the summing amplifier. Since all parallel resistors have the same value, 5kΩ, this multiplication factor, $\frac{R_S}{R_i}$, is always the same. Due to clipping issues, R_S was adjusted to be 2.55kΩ, roughly half of the designed value, reducing the total gain by a factor of 2 due to the inverting feedback configuration of the summing amplifier. A portion of the summing amplifier can be seen in Figure 97. Notice that all of the signals connect at the same node 2 of the chip, which represents the inverting input.

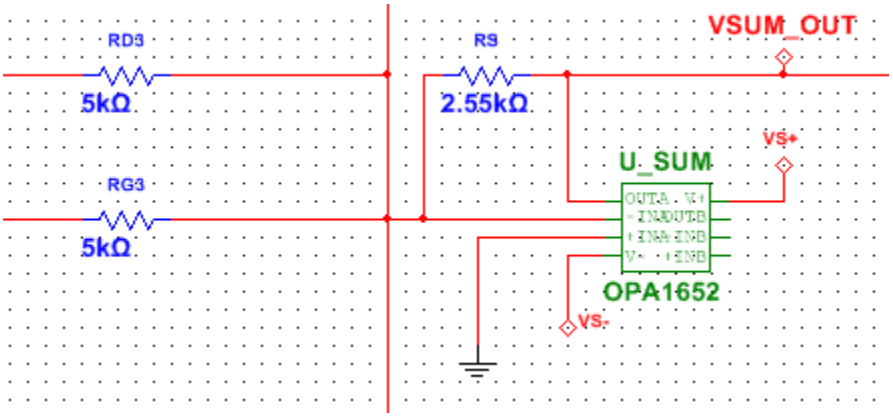

Figure 97: Summing Amplifier Configuration

Power Supply

One of the most important characteristics of any circuit is how power is supplied to all of the resistors, IC's, etc. Since this project concerns a consumer product whose focus is not the supply of power itself, the intent was to design something easily attainable by any guitar player.

AA, AAA, button cell battery or the 9-Volt batteries are all easily accessible to the public. Also, they last long for many consumer electronic applications.

Typical AA, AAA and button cell batteries last longer than 9-Volt batteries that makes it more desirable for this application. According to Battery Savers, AA batteries can power an average flashlight for 24 hours, AAA, 1 hour, a 6-volt lantern, 11 hours, but a 9-Volt will only be able to power a flashlight for 50 minutes. 9-Volt batteries often have 500mAh of charge, whereas other batteries, such as the D battery, can have up to 12,000mAh. This disparity in capacity is a deriding characteristic about this battery.

However, there are two qualities about the 9-Volt battery: the PPE size and the voltage output. The size is compact and it easily fits the hole in the guitar, where the original guitar circuitry was placed. Another convenience about the 9-Volt battery is that it operates by itself. Many applications require a number of AA, AAA or button cell batteries, which clutters up the space available for the circuit. Yet, the most important aspect of the 9-Volt battery is the 9-Volt output. This desired voltage range is capable of powering many circuit components, from op-amps to sensors.

The configuration in Figure 98 is the circuit that is used to power this guitar pickup. This circuit is used to create two rails at +4.5V and -4.5V relative to ground. The voltage divider creates proportional potential differences between the neutral, ground, junction and the rails. The op-amp is used as buffer from the general ground the junction node.

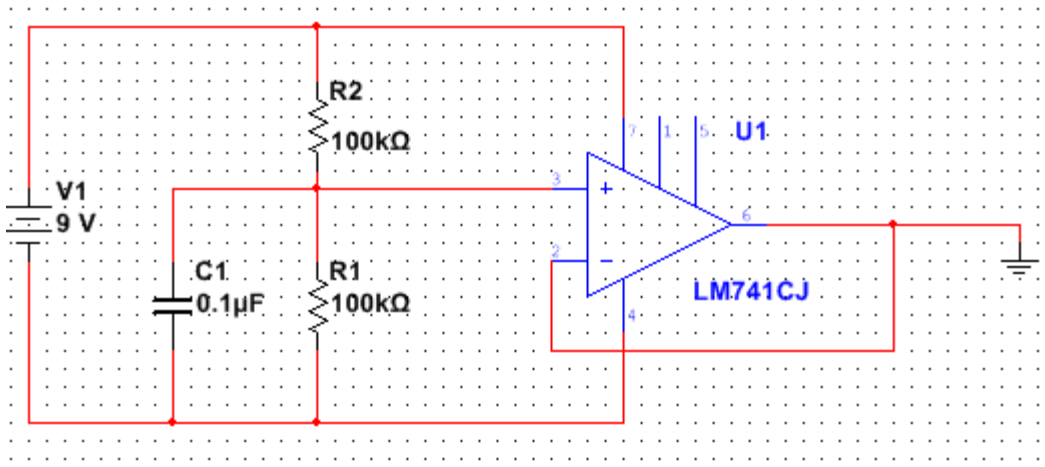

Figure 98: Power Supply Circuit Schematic

PCB Design

The PCB for the Hall Effect pickup needed to be constrained around several geometric constraints. These constraints included the pocket in the purchased guitar body, the distance required under the string, the spacing of the Hall Effect sensors, and others. The first step in designing the PCB was to layout the Hall Effect sensors using a uniform spacing. The space between strings was measured as .437" at the intended location of the pickup. The footprints for the Hall Effect sensors (SOT-23W package) were placed on the top side of the PCB to be on the string side of the board. Figure 99 below shows the top side of the PCB. The figure shows the equal spacing of the Hall Effect sensors.

Next, the RC components for the active filtering were laid out just above the Hall Effect sensors for greater organization and clarity. These components, as shown below, are grouped by string for consistency and to decrease distance between sensor and filter.

Each filter was continued onto the bottom of the PCB by placing the footprint for the OPA1652 audio Op-Amp on the bottom of the board as shown in Figure 100. Since each OPA1652 package contains two amplifiers, the footprint was placed between sets of filter components such

as E and A, D and G, and B and _E. This spacing was done in order to greatly reduce area and distance between components.

The summing amplifier portion of the layout is continued above the RC components for the active filter. Each summing resistor is placed directly above C2 for each string to decrease trace length between components. The traces are then brought through to the bottom of the board where they connect to the summing amplifier U_SUM, which was placed on the bottom for consistency with the other Op-Amp packages.

Lastly for circuit components, the footprints for the notch filter were laid out in a manner to minimize the area of the board. Henceforth, the RC component footprints of the notch filter are on the bottom side of the board while the Op-Amp footprint is on the top side. This allowed for all connections to be made successfully and cleanly.

The final footprint was for the 1x5 connector that will be used to connect the PCB to the external circuitry. The five connections that are made to this connector are V+, V-, GND and V_{out}. However, V_{out} has two pins; one for the output before the notch filter and one for after the notch filter. Two output were used so that the notch filter could be implemented or not implemented during testing and for the final pickup.

Overall, the board measures 76.200mm long by 31.750mm wide by 1.6mm thick (plus components), which is a suitable size for the geometric constraints by the guitar body. For the Hall pickup orientation, the area of the board is not as great of an issue as it is with the GMR pickup because the board will lay flat underneath of the strings, therefore the thickness is the important dimension to keep in consideration. Lastly, the board has 3.175mm (⅛”) holes in each corner for mounting purposes on a fixture.

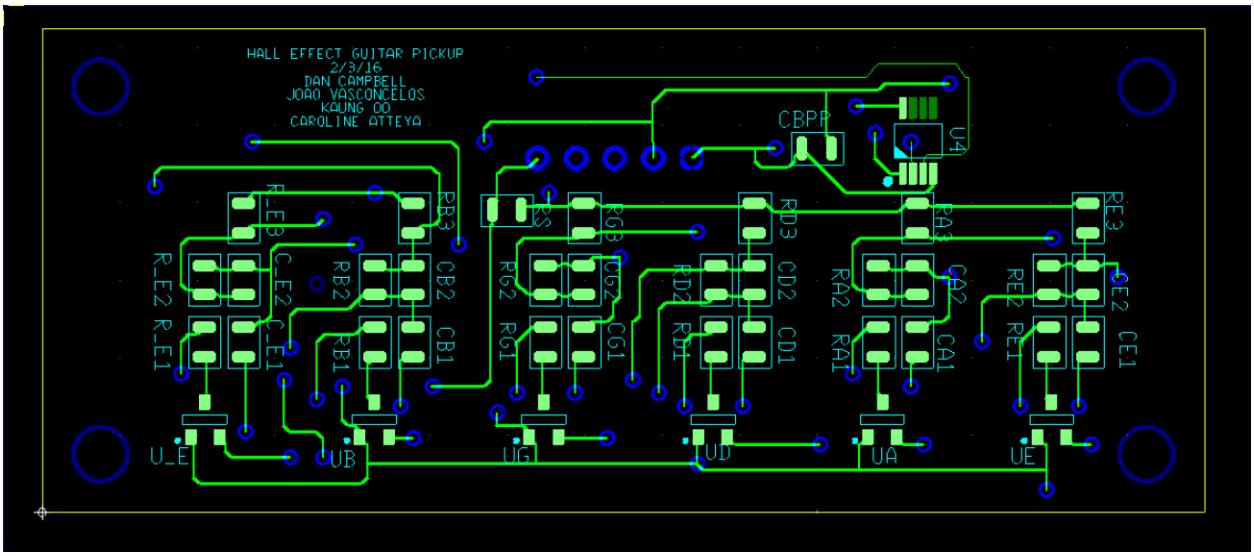

Figure 99: Hall Effect Pickup PCB Top

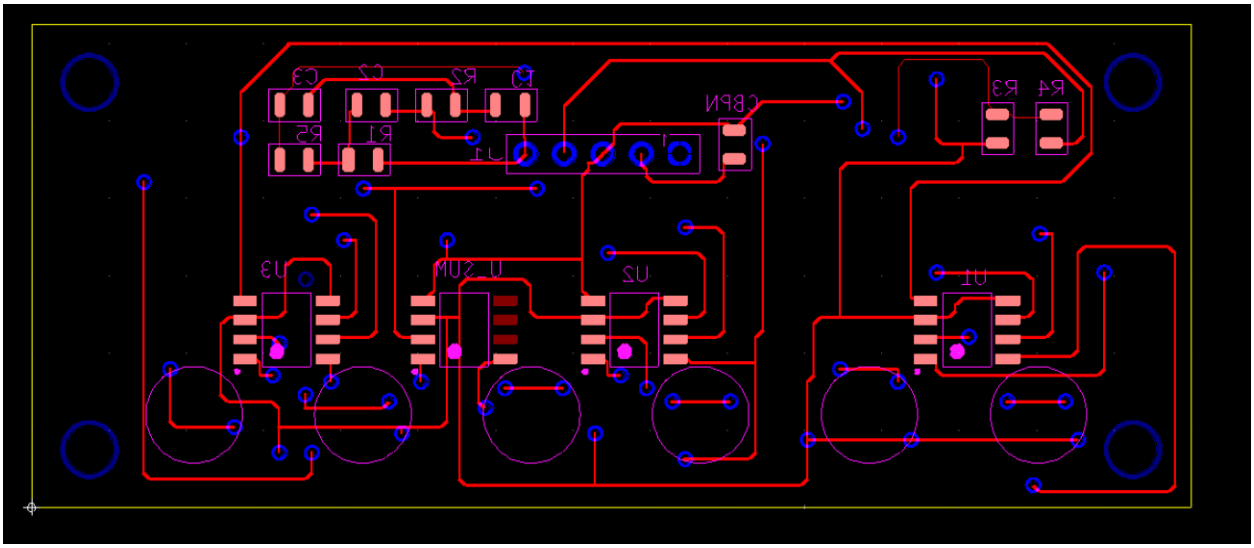

Figure 100: Hall Effect Pickup PCB Bottom

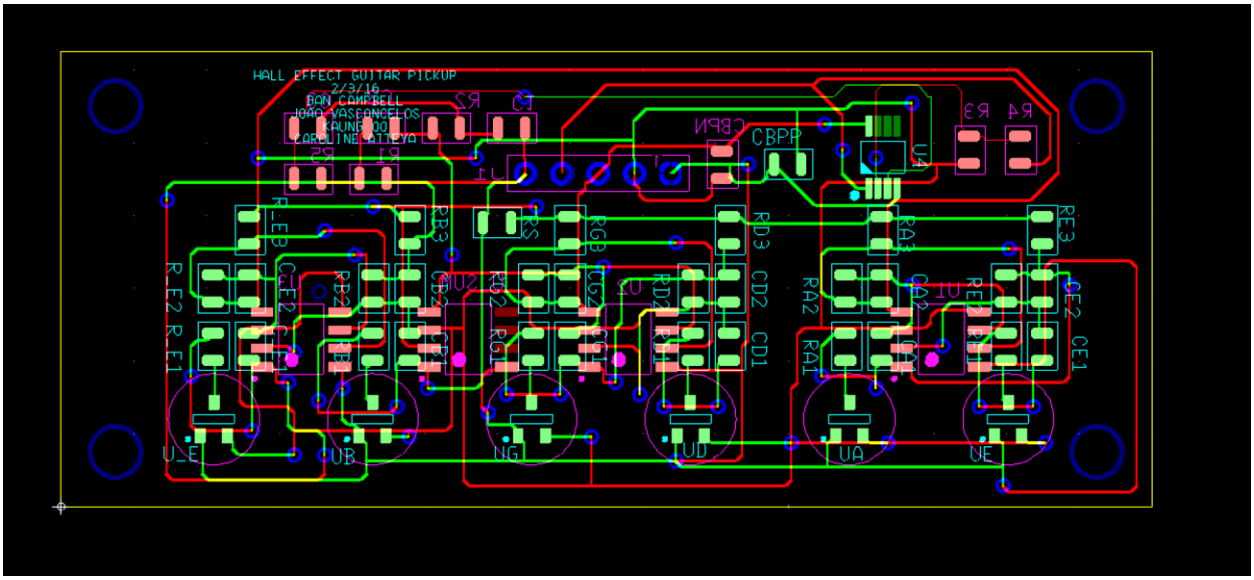

Figure 101: Hall Effect Pickup PCB Full

Testing

There are many technical aspects of this project that have to be examined in order to determine whether it is a good application for a guitar pickup. Most importantly, there are aspects that need to be deeply evaluated, such as sensor sensitivity, in order to compare the Hall Effect technology to the GMR technology. General aspects that have to be evaluated are current drawn from supply, output voltage range, possible DC-bias, signal clipping and voltage output of noise. More profound research aspects include signal-to-noise ratio, FFT analysis, and presence of harmonics in signal output. Soft technical aspects such as sound quality should also be taken into account for comparison purposes, after all the purpose is to understand which sensor can accurately reproduce the mechanical signal.

The general testing of the sensor characteristics can be performed using an oscilloscope and a multimeter. These will determine aspects of the project that are crucial to the performance of the circuit, such as battery life. In order to determine the minor aspects of the project, a more

complete analysis has to be done. Electromagnetic noise is the most common type of interference in sound circuits such as this one. There are a few ways to evaluate how significant it is. First, a fast Fourier transform can be used to visualize the spectrum of frequencies in the output. Plugging the output of the circuit to the guitar amplifier will allow one to audibly understand how significant that noise is to someone who is playing the guitar and how it will affect the notes being played and how it may cause discomfort to the guitar player.

For a better comparison between the GMR and Hall Effect sensors, it is desirable to test the circuit with a laboratory equipment that will output the same sound at precise frequencies. Hooking up the function generator, set to produce a sine-wave with a known frequency, to guitar amplifier helps understand how much noise is generated by mini amp itself. Next, connecting the output of the function generator to the input of the circuit, i.e. where the sensor gets connected, helps understand how much noise is produced by the circuit. Finally, connecting the sensor to the circuit will demonstrate the exact amount of noise that is captured by the sensor.

Hall Effect Pickup Testing Results

The goal of testing the Hall Effect pickup was to serve as a comparison to the GMR pickup on the basis of power consumption, signal strength and quality, and the amount of noise the circuit picks up. Due to the random nature of playing a guitar, the tests outlined serve as typical measurements and or waveforms that were seen throughout the testing. The equipment used in this testing included:

- Tektronix TDS 2004B Oscilloscope
- Tektronix AFG 3021 Function Generator
- GW INSTEK GPS-3303 Power Supply
- Agilent 34405A DMM

Power Consumption

From the datasheet for the A1324 Hall Effect sensor from Allegro, a typical supply current of 6.9mA was expected to be drawn by the sensor itself. In measuring the PCB as a unit, a total current of 14mA was drawn. Excluding the sensor, this left 7.1mA unaccounted for on the PCB. From the datasheets for the various components, the OPA1652 Op-Amp typically draws 2mA of current. With one Op-Amp used for the active filter and one for the summing amplifier, this brings the power budget up to approximately 10.9mA. For the remaining 3.1mA, the current draw could possibly be coming from the RC elements in the filter and amplifier circuits although, more exhaustive testing would need to be done in order to determine this and this testing is difficult on a soldered PCB. The other possibility for the current draw comes from the dual Op-Amp packaging of the OPA1652. The OPA1652 package contains two Op-Amps each and there would be a slight current draw while it is connected to the supply rails despite no inputs being connected.

Signal Size and Quality

The key factor in creating a well-functioning guitar pickup is its ability to recreate the signal generated by the vibrating string. In an inductive pickup, this recreation is effectively perfect due to the passive nature of its circuitry. In the Hall Effect application, with its active filtering and summing amplifier, there are biases and nonlinearities that generate slight variations in the signal. The result of these variations is a different sound output.

To test these qualities, a typical signal was captured and then the amplitude, frequency, and shape was analyzed. First, the amplitude of a typical waveform from the Hall pickup was measured as 516mV peak to peak with roughly 300mV below the bias point and 200mV above the bias point. The signal used for these measurements, which is also a typical waveform from the Hall Effect

pickup, is shown below in Figure 102. Perhaps jumping ahead a bit, this distribution of signal above and below the bias point mimics that of the inductive pickup. With the gain of our system set around 50, these measurements at the output of the pickup indicate that the signal produced by the Hall Effect sensor are approximately 10mV peak to peak.

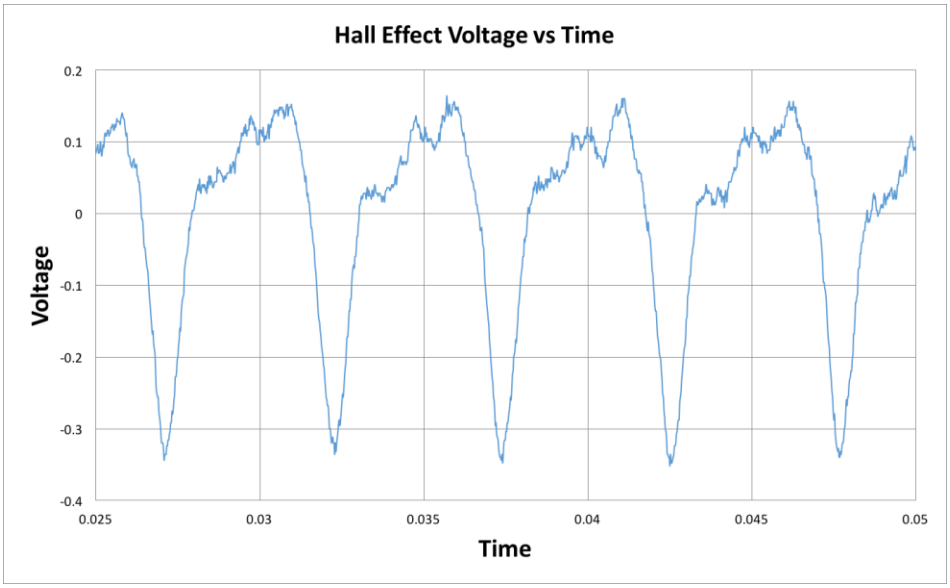

Figure 102: Typical Waveform from Hall Effect Pickup Showing Amplitude

Next, the measured frequency of the G string used for testing was measured at 196.1Hz which is what the tuned frequency should be allowing for a very slight measurement discrepancy. While the confirmation of the correct frequency is important, the most important factor from the figure below, is the very periodic and repetitive nature of the signal.

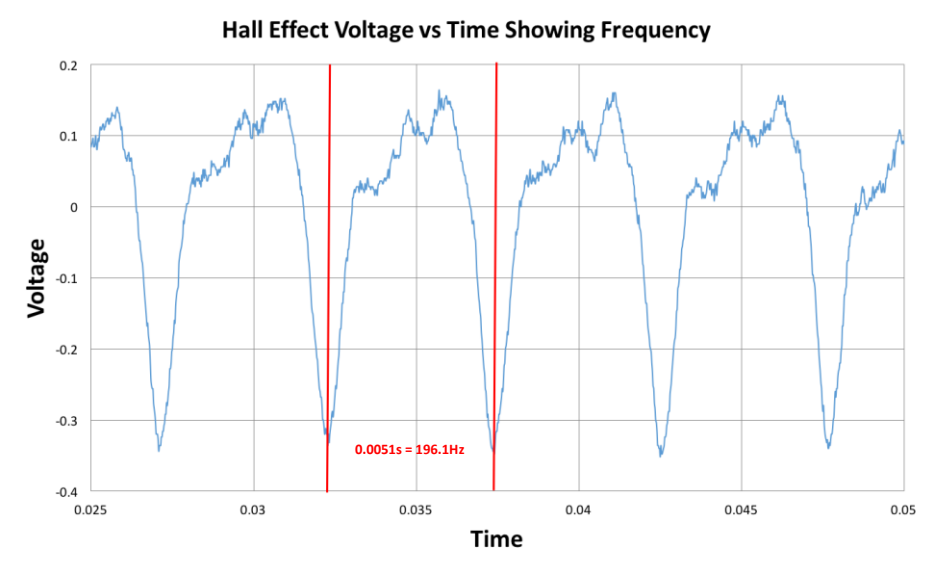

Figure 103: Typical Waveform from Hall Effect Pickup Showing Frequency

Noise

The noise picked up by the Hall Effect sensor was considerable when listening to through the guitar amplifier. This noise was analyzed by connecting the PCB with the Hall Effect sensor to the oscilloscope and allowing the sensor the pickup the ambient electromagnetic noise. This noise was recorded to a CSV file to be analyzed. From Figure 104 below, the noise was measured with amplitudes typically around +/- 0.03V. The noise was then further analyzed using a MATLAB script to understand the spectral components of the noise. The results from this analysis is discussed in detail in the comparison between Hall Effect and GMR pickup.

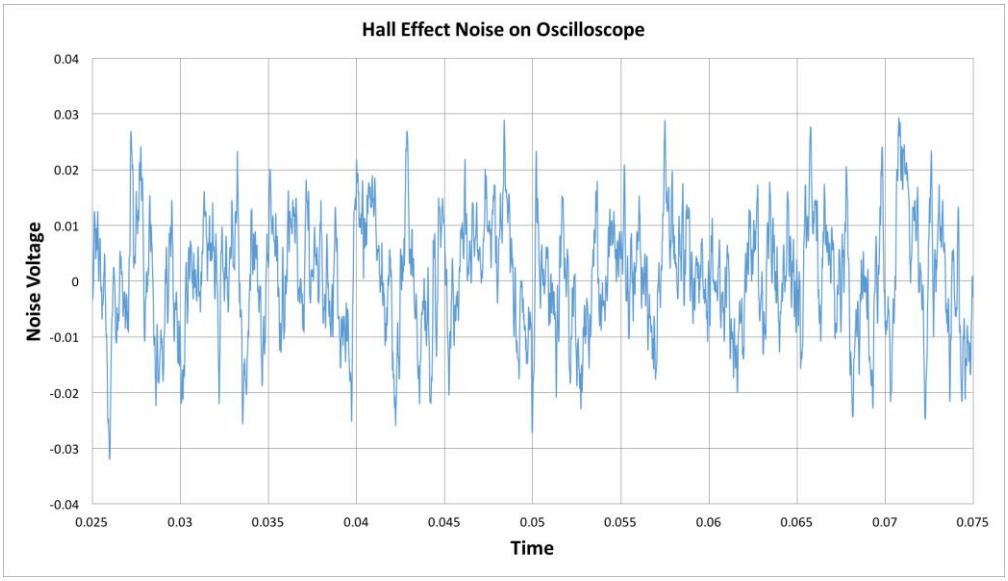

Figure 104: Typical Noise at Hall Effect Pickup Output

Comparing GMR, Hall, and Inductive Pickups

For the final comparison tests, the G string was chosen as the standard string to be plucked across all three pickups. In terms of the gain between the sensor output and final pickup output, GMR pickup uses a gain of 1000, Hall pickup uses a gain of 50, and Inductive pickup (Epiphone 650R & 720T Humbucker) has a gain of 1.

Magnetic Orientations

The magnetic orientation used for the GMR pickup circuit was shown in Figure 105. The magnetic north pole of the magnet is pointed perpendicularly away from the sensor's axis of sensitivity for back-biasing. The magnetic orientation for the Hall pickup is also shown in Figure 106. The magnetic north pole of the cylindrical magnet is pointed in the same direction as the Hall sensor's axis of sensitivity. The distances between the sensors and magnets for both GMR and Hall pickups were adjusted for achieving the biggest output signal.

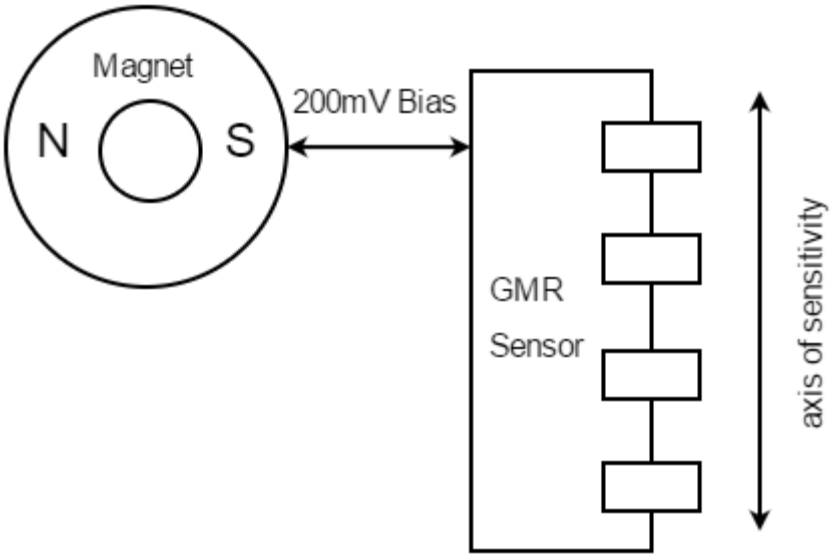

Figure 105: Diagram Showing Magnetic Orientation of GMR Sensor

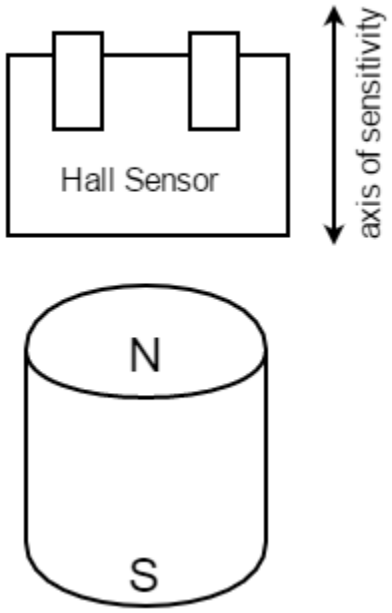

Figure 106: Diagram Showing Magnetic Orientation of Hall Effect Sensor

Sensor Sensitivity, Output Signal Size and Noise

The following figures show the resulting signal and noise waveforms from GMR, Hall, and Inductive pickups. The RMS noise measurements are labelled with σ and the DC offsets are labelled with μ in the MATLAB figures.

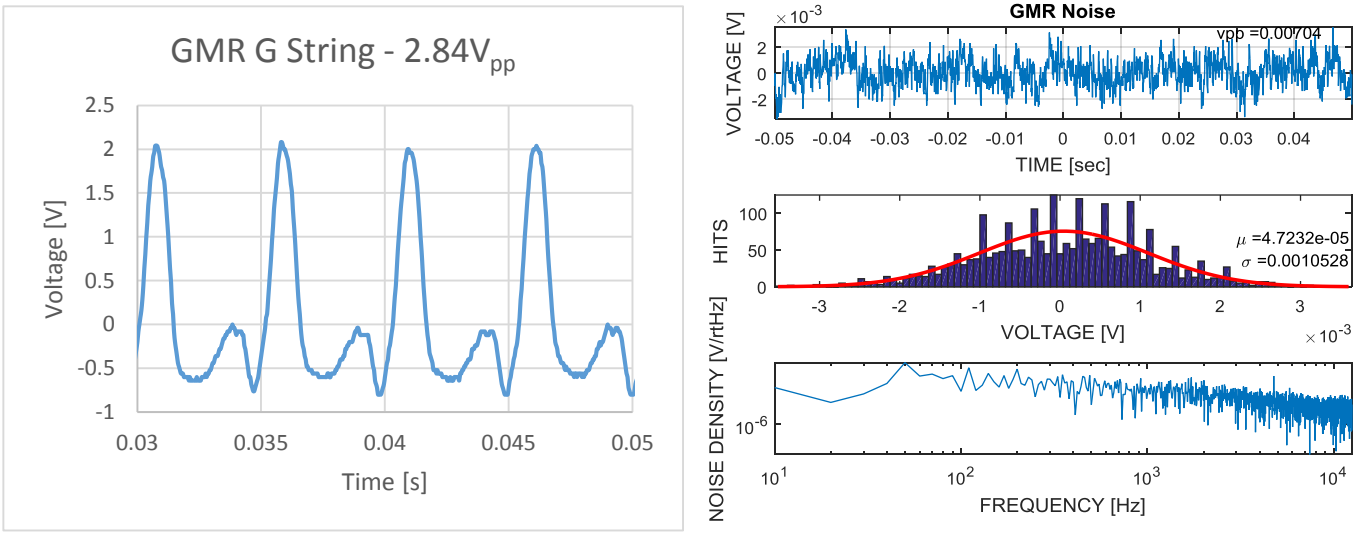

Figure 107: Open G string note signal and noise captured using GMR pickup

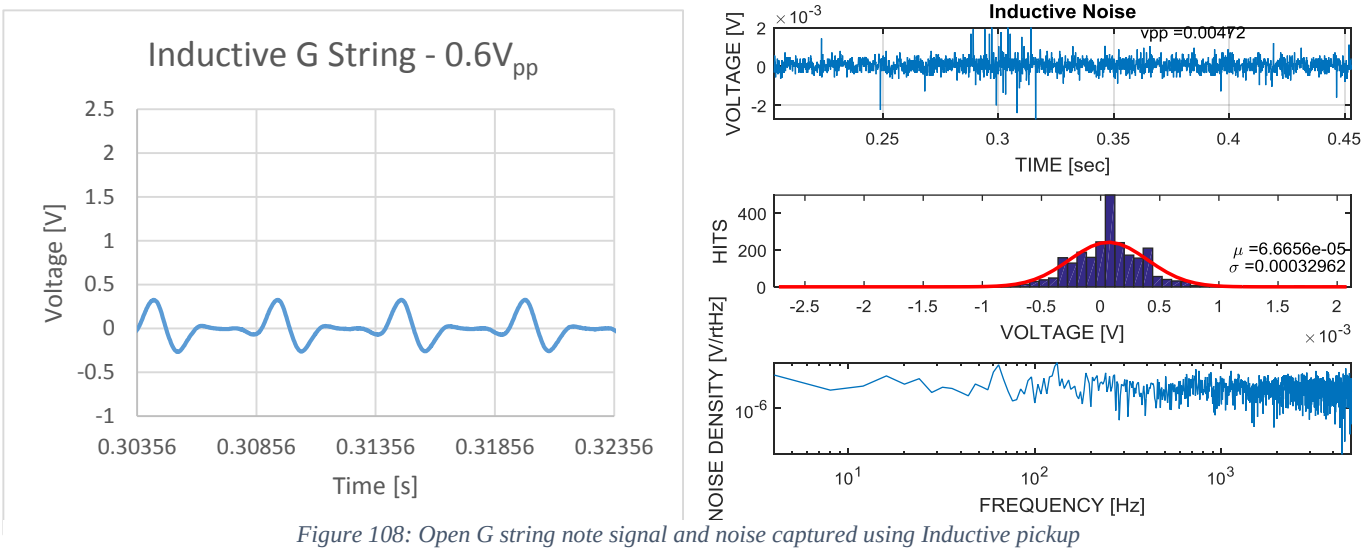

Figure 108: Open G string note signal and noise captured using Inductive pickup

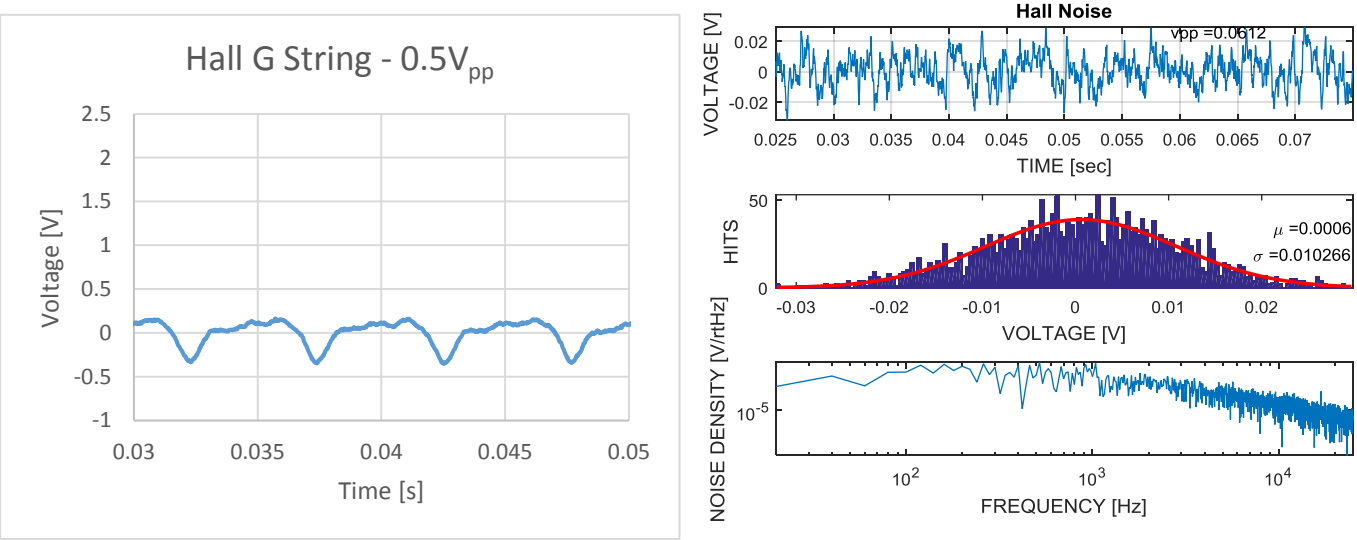

Figure 109: Open G string note signal and noise captured using Hall pickup

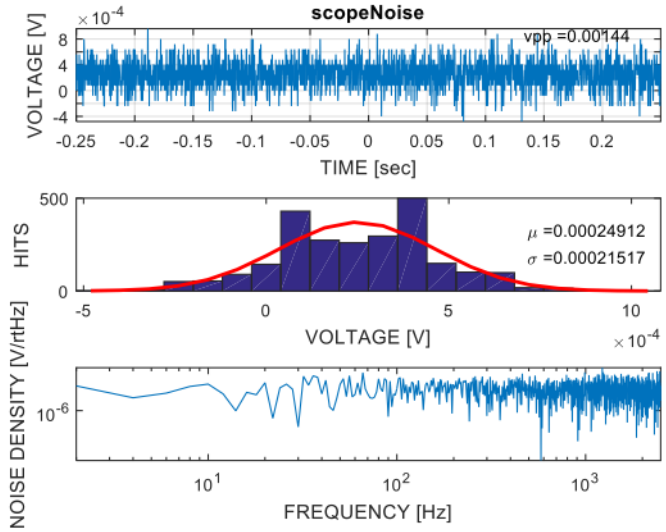

Figure 110: Typical Oscilloscope Noise

Having the highest gain, the GMR pickup produced the largest output signal with a signal size of 2.84Vpp. Hall Effect pickup, on the other hand, produced a signal size of 0.5V with a gain of only 50V/V. It was therefore concluded that the Hall sensor has a higher sensitivity than the GMR sensor. However, even with a gain of 50V/V, Hall Effect pickup showed significantly higher

RMS noise than the GMR pickup, which makes the GMR pickup a better and less noisy pickup than the Hall Effect pickup. Accounting for the typical scope noise, the effective noise of each pickup was calculated by subtracting the scope noise from the output noise. Then, SNR for each pickup was calculated using the effective noise. The results are shown in Table 7.

Table 7: Signal and Noise Comparison Table

	GMR (AA005)	Inductive Epiphone 650R & 720T Humbucker	Hall (A1324)	Unit
Gain	1000	1	50	V/V
Output Signal Size	2.84	0.6	0.5	Vpp
Output Noise	1.0528	0.32962	10.266	mVrms
Scope Noise	0.21517	0.21517	0.21517	mVrms
Effective Noise	0.83763	0.11445	10.05083	mVrms
SNR	61.57311	65.3585	24.90315	dB

As seen from Table 7, the inductive pickup produces the highest SNR value of 65dB while the SNR of Hall Effect pickup was only 25dB. The GMR pickup also showed a remarkable SNR vale of 61.5dB, right below the highest SNR value of the traditional inductive pickup.

Sensor Bandwidth

As discussed in the Signal Size Section of the GMR Pickup Testing Results, the AA005 GMR sensor showed a sharp low pass filter response with a cutoff frequency at about 100Hz. This unexpected feature of the sensor resulted in amplifying different guitar notes at different amplitudes. As seen from Figure 111, the amplitude difference between the 82Hz low E note and the 330Hz high E note is immense and this behavior is not acceptable for the guitar pickup

application since it is desired that all the audible guitar notes have approximately same amplitude. However, for the Hall Effect pickup, it was observed that all the guitar notes show approximately the same amplitude unlike the GMR pickup. Therefore, for future work regarding this project, one starting point would be to further investigate the sharpe low pass filter response of this GMR sensor, AA005, with the help of the sensor manufacturer, NVE Corporation.

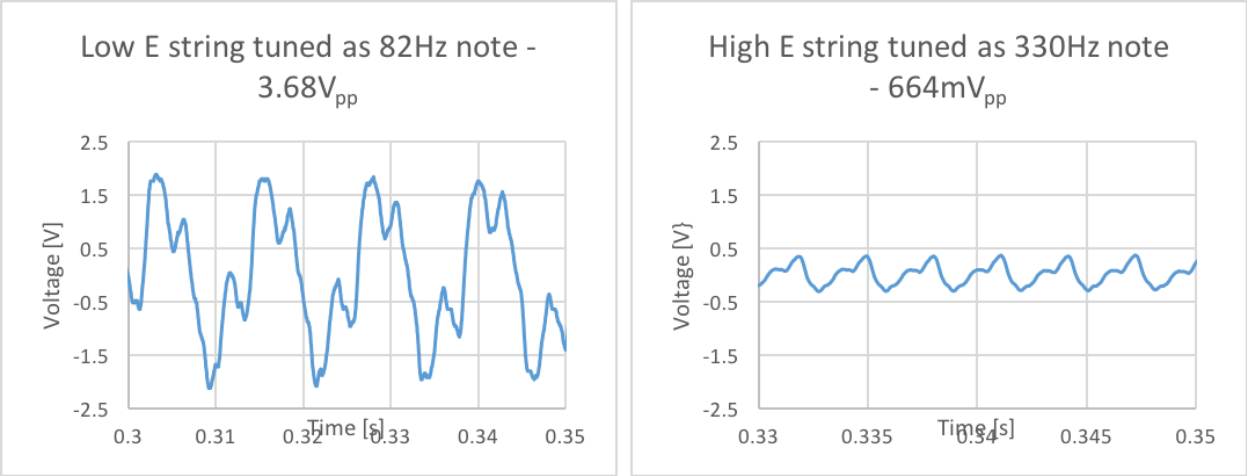

Figure 111: Typical Amplitudes for 82Hz and 330Hz Notes

Power Consumption

Table 8: Pickup comparis

	GMR (AA-005)	Inductive	Hall (A1324)	Unit
Supply Current @5V - Sensor	0.5	0	7	mA
Supply Current @5V - Per String	4.23	0	10.5	mA

It was also observed that the Hall sensor itself consumes 14x times more current than the GMR sensor while the Hall pickup circuit draws only 2x times more current than the GMR pickup circuit. Here, again, it was concluded that the GMR sensor can make a better guitar pickup than the Hall Effect sensor due to its low power consumption, which is critical for battery-operated applications such as an active guitar pickup.

Conclusion

After thorough testing of the Hall Effect and GMR sensors, it was determined that the GMR sensor outperformed the Hall Effect sensor in the guitar pickup application and compares favorably to the existing inductive pickup. The pickups were compared based on their qualities of signal size, bandwidth, noise and current draw. These were important factors in the guitar pickup application that would affect a musician's satisfaction with a pickup and influence how their instrument sounds.

The main drawback of the Hall Effect sensor in this application was its tendency to pick up a large amount of ambient noise that made the signal highly distorted when compared to inductive and GMR pickups. In an audio application, like this, the SNR measurement of 24.9dB for the Hall Effect pickup is unusable due to the noise.

The main goal of this project was to understand GMR sensors through a guitar pickup application while comparing it to an existing Hall Effect sensor. The chosen GMR sensor from NVE performed admirably, beating the Hall Effect sensor by a factor of more than 10 in terms of current draw (7mA vs 0.5mA), and offering similar SNR to the existing inductive pickup (61.57dB for GMR and 65.36 for the inductive).

Recommendations for Future Projects

There were a few areas within this project that need to be explored in more detail. These recommendations are spread across the areas of understanding the magnetic fields at a deeper level, to refining the circuit design process to create a better pickup.

The first recommendation would be to begin the project by understanding the magnetic fields being worked at the beginning of the project. With our lack of understanding of magnetic fields, it made the process of understanding the sensor behavior more difficult later in the project. This process could be done by creating a fixture to hold the sensor early in the process as a means to standardize experiments that will give rise to a greater understanding of the magnetic fields.

Next, GMR sensor being used showed a sharp low pass filter response in the range of roughly 300Hz. This filtering caused the lower frequency notes on the guitar to be produced with much greater amplitude than the notes of higher frequency. One possible cause of this may be an inherent property of a vibrating guitar string; the thinner, higher frequency strings may just natrually create smaller perterbations in the magnetic field and thus the pickup outputs a smaller signal. However, this is conjecture and the frequency response of the GMR sensor should be looked into more deeply for future work.

The other recommendation is on the circuit design side of the project. The first recommendation is to find ways to reduce the power consumption for the GMR pickup signal conditioning circuit. In this work, the signal conditioning circuitry consumed roughly 90% of the power for each string including the sensor. Methods to reduce this value would greatly increase battery life for the pickup.

References

Errede, S. (2005). Electronic Transducers for Musical Instruments.

Jordan, E., & Balmain, K. (1968). Electromagnetic Waves and Radiating Systems: Prentice Hall.

Lenssen, K.-M. H., Somers, G. H. J., & van Zon, J. B. A. D. (2002). Magentoresistive sensors for string instruments.

Nelson, G. A. (2001). Transducer and musical instrument employing the same.

R, P., & P, D. (2002). Bridging The Gap Between AMR, GMR, And Hall Magnetic Sensors. Paper presented at the 23rd INTERNATIONAL CONFERENCE ON MICROELECTRONICS.

Reig, C., Cardoso de Freitas, S., & Mukhopadhyay, S. C. (2013). Giant Magnetoresistance (GMR) Sensors (Vol. 6). New Zealand.

Reig, C., Cubells-Beltran, M.-D., & Muñoz, D. R. (2009). Magnetic Field Sensors Based on Giant Magnetoresistance (GMR) Technology: Applications in Electrical Current Sensing. Sensors (Basel), 9(10), 7919-7942. doi:10.3390/s91007919

Ullaby, F. (2006). Fundamentals of Applied Electromagnetics (5th ed.): Prentice Hall.

White, R. L. (1992). Giant Magnetoresistance: A Primer28. Retrieved from IEEEXplore website: http://ieeexplore.ieee.org.ezproxy.wpi.edu/stamp/stamp.jsp?tp=&arnumber=179533

NVE, C. (2016a). AA and AB-Series Analog Sensors. Retrieved from http://www.nve.com/Downloads/analog_catalog.pdf

NVE, C. (2016b). Application Notes for GMR Sensors. Retrieved from http://www.nve.com/Downloads/apps.pdf

Appendices

Appendix A: Notch Filter

Although the notch filter was not used in the final design, it was included on the PCB, should it be desired to be added at some point in the future. The notch filter was implemented in the Hall Effect pickup circuit with the goal of attenuating the 60Hz noise that is picked up by the Hall Effect sensors. The filter design is based around the LTC6078 amplifier from Linear Technology. It was chosen based on its low power consumption along with its capability of working within the +/- 4.5V dual supplies set by the 9V battery chosen to power the pickup. The notch frequency is determined by the components R1, R2, R5, C1, C2, and C3. These components from a high pass filter (C1, C3, R2) and a low pass filter (R1, R5, C2), where the cutoff frequencies are determined by the basic $1/2\pi RC$ equation. In the circuit shown in Figure 112, the cutoff for the high pass filter is 117.89Hz while the cutoff frequency for the low pass 29.47Hz. However, the important value for a notch filter is the notch frequency. This notch frequency is determined by the resistor value of the low pass filter (R1=R5) and the capacitor value of the high pass filter (C1=C3). Again this frequency is calculated with the same equation, yielding 58.94Hz, close to the desired 60Hz. This value will also fluctuate with the tolerances of any given component.

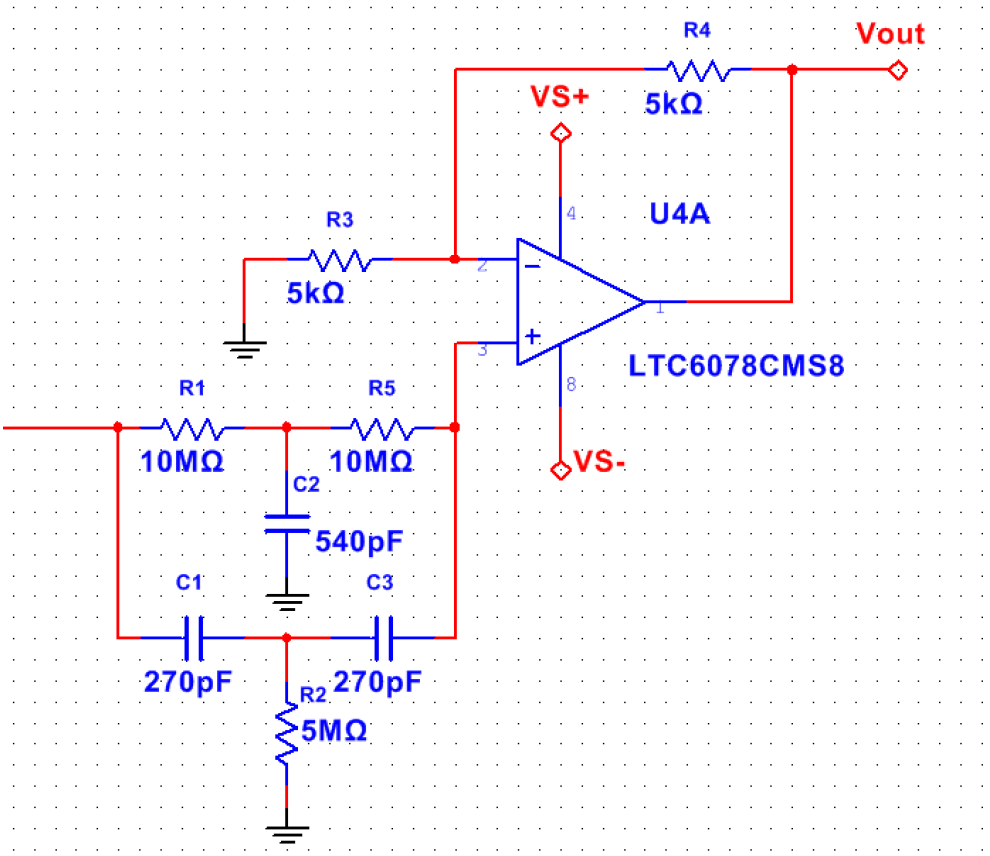

Figure 112: Notch Filter Circuit Schematic

The circuit was simulated in LTSpice to understand the performance of the filter. With the given component values, the simulation indicated an attenuation of approximately -73dB at the target frequency of 60Hz. The bode plot for this circuit is shown below in Figure 113.

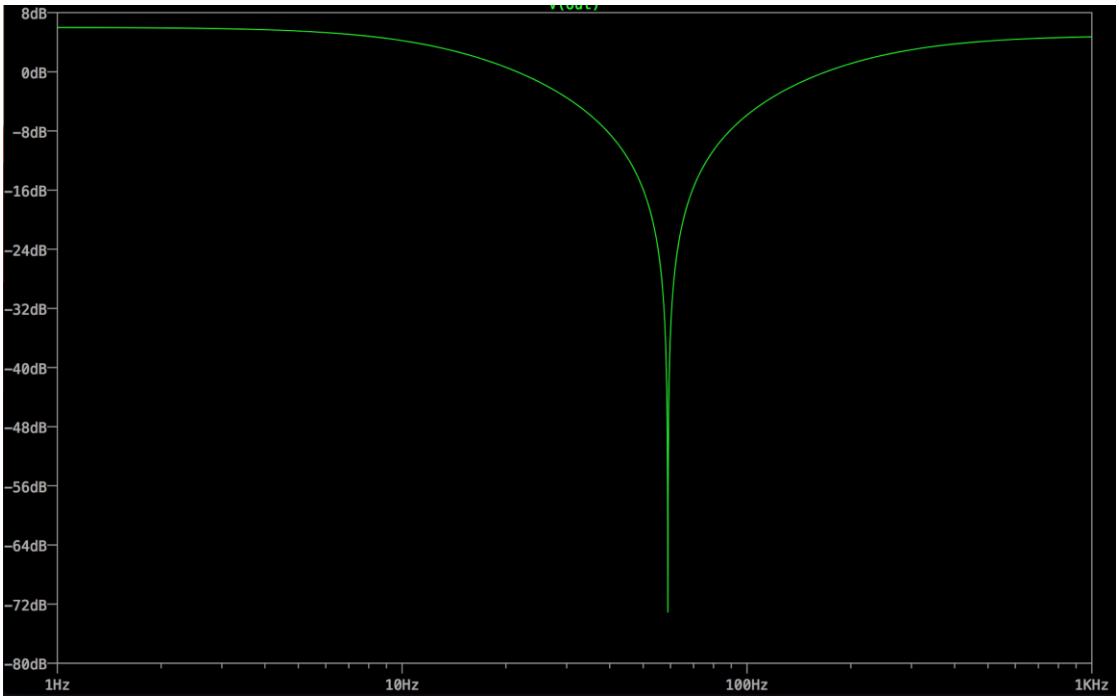

Figure 113: Notch Filter Spice Simulation

Appendix B: GMR Final PCB Circuit Schematics

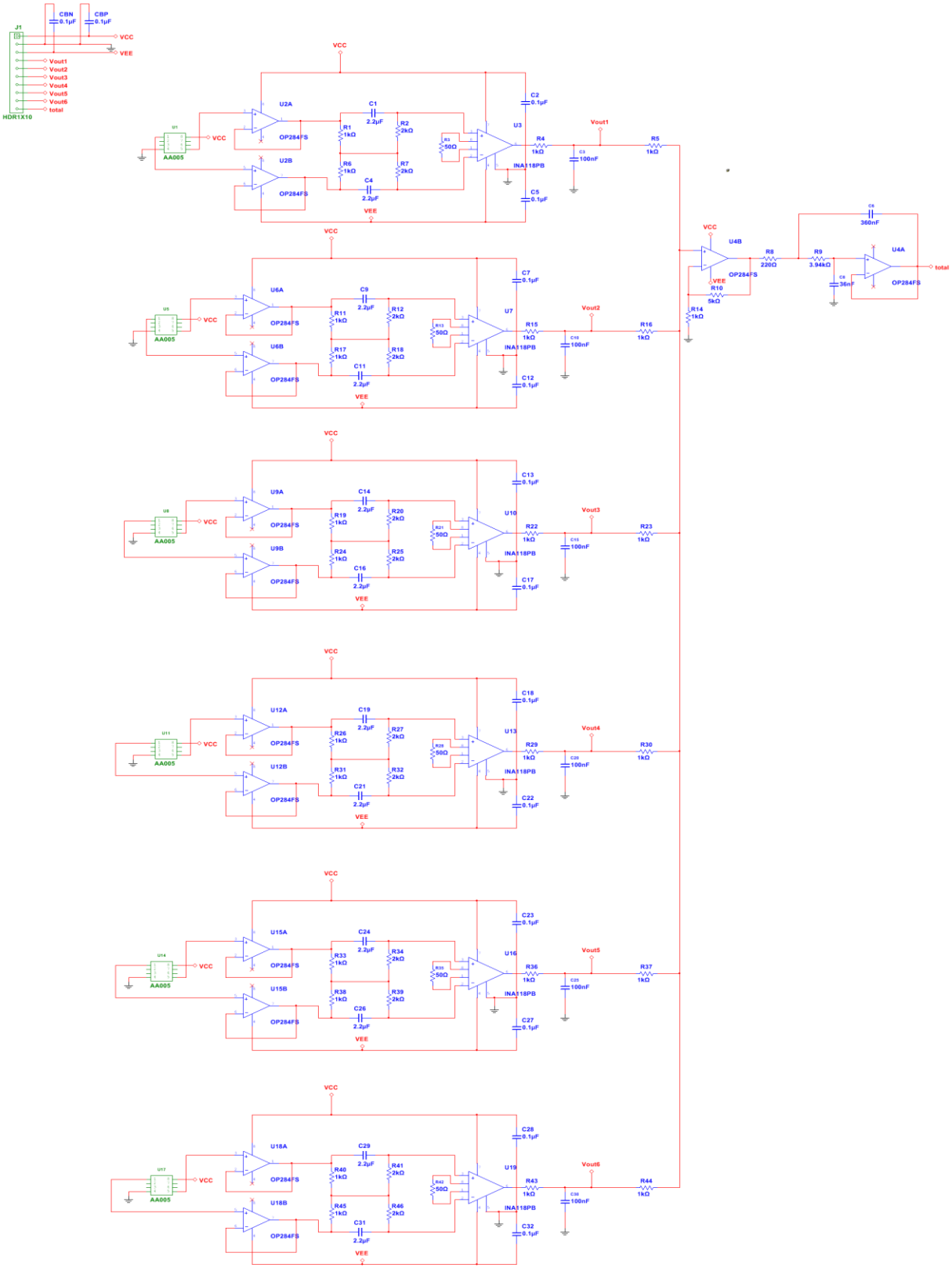

Appendix C: MATLAB Script for Analyzing the Noise Waveforms

```
% scopenoise2
% Courtesy of Prof. McNeill, WPI

% reads .csv file of data from scope
M=csvread('AD4084BufNoise.csv',0,3);
% Time is in first column; voltages in second
t=M(:,1);
v=M(:,2);


% Read volts per division from data file
v_per_div=csvread('AD4084BufNoise.csv',8,1,'B9..B9');
t_per_div=t(2)-t(1);

% number of points
npts=length(v);

% Determine mean and standard deviation for fitting normal PDF
mu=mean(v);
sig=std(v);
vpp = max(v) - min(v);

% will plot histogram; vector of bin centers based on ADC which has
% LSB equal to
lsb=v_per_div/25;
% min and max voltage for histogram
v_min=min(v);v_max=max(v);
% min, max bin centers
bin_min=lsb*floor(v_min/lsb);
bin_max=lsb*(1+floor(v_max/lsb));
bin_ctrs=(bin_min:lsb:bin_max);

% plot scope waveform
figure(1)
subplot(3,1,1)
plot(t,v)
axis tight
grid on
text(0.9*max(t),0.9*max(v),['vpp =' num2str(vpp)], ...
    'HorizontalAlignment','Right')
xlabel('TIME [sec]')
ylabel('VOLTAGE [V]')

%>>>>>>>>>>>>>>>>>> change this
title('AD4084BufNoise')

% plot histogram
subplot(3,1,2)
hold off
hist(v,bin_ctrs)
hold on
gaussian1=npts*lsb*(1/sig)*normpdf((bin_ctrs-mu)/sig);
```

```
plot(bin_ctrs,gaussian1,'color',[1 0 0],'linewidth',2)
% Show mean, stdev on plot
text(max(bin_ctrs),0.9*max(gaussian1),['\mu =' num2str(mu)], ...
    'HorizontalAlignment','Right')
text(max(bin_ctrs),0.5*max(gaussian1),['\sigma =' num2str(sig)], ...
    'HorizontalAlignment','Right')
axis tight
xlabel('VOLTAGE [V]')
ylabel('HITS')

% plot fft
subplot(3,1,3)
% Remove DC from FFT (don't include offset error)
Y=fft(v-mu);
% FFT magnitude
fft_mag=Y.*conj(Y);

% FFT is dimensionless - need to massage numbers to make meaningful
% power spectral density
% We sampled at fS = 1/t_per_div and took  npts  number of samples
% So frequency vector is
f_bin=1/(t_per_div*npts);
f=(0:npts)*f_bin;
% to convert FFT magnitude to psd in V^2/Hz, need to scale by npts^2
% and then divide by width of frequency bin
% Factor of 2 covers single-sided double-sided conversion
freq_spect=fft_mag/(f_bin*(npts^2));
loglog(f(2:1250),sqrt(2*freq_spect(2:1250)))
axis tight
xlabel('FREQUENCY [Hz]')
ylabel('NOISE DENSITY [V/rtHz]')
```